Aus der Klinik für Allgemeine, Viszerale und

Transplantationschirurgie

Klinikum der Ludwig-Maximilians-Universität München

Tumor-immune-interaction in a pancreatic cancer organoid co-culture model

Dissertation

zum Erwerb des Doktorgrades der Medizin

an der Medizinischen Fakultät der

Ludwig-Maximilians-Universität München

vorgelegt von

Tianmiao Ma

aus

Liaoning, Volksrepublik China

Jahr

2022

Mit Genehmigung der Medizinischen Fakultät der

Ludwig-Maximilians-Universität zu München

Erster Gutachter:	PD Dr. Bernhard W. Renz
Zweiter Gutachter:	Prof. Dr. Jens Neumann
Dritter Gutachter:	Priv. Doz. Dr. Georg Beyer
ggf. weitere Gutachter:	
Dekan:	Prof. Dr. med. Thomas Gudermann

Tag der mündlichen Prüfung: 16.12.2022

Affidavit

Ma, Tianmiao

Surname, first name

I hereby declare, that the submitted thesis entitled

Tumor-immune-interaction in a pancreatic cancer organoid co-culture model

is my own work. I have only used the sources indicated and have not made unauthorised use of services of a third party. Where the work of others has been quoted or reproduced, the source is always given.

I further declare that the dissertation presented here has not been submitted in the same or similar form to any other institution for the purpose of obtaining an academic degree.

Shenyang, China, 22.12.2022

Place, Date

Tianmiao Ma

Signature doctoral candidate

Table of Contents

Zusammenfassung (Deutsch)

Zweck: In Anbetracht der immer noch sehr schlechten Prognose und weiter steigenden Inzidenz des duktalen Adenokarzinoms des Pankreas (PDAC) sind klinische translationale Studien zur Früherkennung, Behandlung und Prognose von entscheidender Bedeutung. In dieser Studie untersuchten wir die Wechselwirkungen von Tumor- und Immunzellen, indem wir ein Kokulturmodell primärer menschlicher PDAC-Organoide und peripherer mononukleärer Blutzellen (PBMCs) etablierten, die von denselben Patienten stammten.

Methoden: Wir haben eine Kokulturmethode für von Patienten stammende Organoide und passende PBMCs bestimmt, um die Differenzierung von Gedächtnis-T-Zell-Subtypen und regulatorischen T-Zellen (Tregs) durch Fluoreszenz-aktivierten Zellsortierer (FACS) zu testen.

Ergebnisse: Die Ergebnisse waren bei 4 Patienten-Co-Kulturen unterschiedlich, wobei die Co-Kultur eines Patienten einen Anstieg der $CD4^+$ Tcm- und Tnaiv-, $CD8^+$ Tcm- und Tnaiv-Zellpopulationen und einen Rückgang der $CD4^+$ Tem- und Teff-, $CD8^+$ Tem-Zellen, verglichen mit denen in der Gruppe der allein kultivierten PBMCs; und mit einer Kokultur eines anderen Patienten, die eine erhöhte Anzahl von $CD4^+$ Tnaiv- und $CD8^+$ Tcm-Zellen zeigt, während eine verringerte Anzahl von $CD4^+$ Tem- und $CD8^+$ Tem-Zellen. Abgesehen davon war die Population von Treg-Zellen in allen Co-Kulturen der PDAC-Patienten höher als in ihren gematchten Kontrollen.

Schlussfolgerung: Hier wurde ein autologes Kokulturmodell mit von Patienten stammenden Organoiden und PBMCs etabliert, um die Wechselwirkung zwischen Krebszellen und verschiedenen Immunzellen bei einzelnen PDAC-Patienten zu untersuchen. Mit diesem Modell steht uns ein Werkzeug zur Verfügung, mit dem wir die Wirksamkeit von Immuntherapien

vorhersagen könnten und so dazu beitragen können, das Outcome unserer Patienten zu verbessern.

Abstract (English)

Purpose: Considering the rising incidence and dismal prognosis of pancreatic ductal adenocarcinoma (PDAC), clinical translational studies for early diagnosis, treatment, and prognosis are of crucial importance. In this project, we studied interactions of tumor and immune cells by establishing a co-culture model of primary human PDAC organoids and peripheral blood mononuclear cells (PBMCs) derived from the same patients.

Methods: We determined a co-culture method for patient-derived organoids and matched PBMCs to test the differentiation of Memory T cell subtypes and Regulatory T cells (Tregs) by Fluorescence Activated Cell Sorter (FACS).

Results: The results were variable in 4 patient co-cultures, with one patient's co-culture showing an increase in $CD4^+$ Tcm- and Tnaiv-, $CD8^+$ Tcm- and Tnaiv cell populations, and a decrease in $CD4^+$ Tem- and Teff-, $CD8^+$ Tem cells, compared to those in PBMCs cultured alone group; and with the co-culture from another patient displaying elevated numbers of $CD4^+$ Tnaiv- and $CD8^+$ Tcm cells, whereas reduced numbers of $CD4^+$ Tem- and $CD8^+$ Tem cells. Besides that, the population of Treg cells in all co-cultures of the PDAC patients was higher than in their matched controls.

Conclusion: Here an autologous co-culture model with patient-derived organoids and PBMCs was established to study the crosstalk between cancerous cells and various immune cells in individual PDAC patients. Having this model available we have a tool at hand which might predict the effectiveness of immune therapies thereby helping to improve the outcome of our patients.

List of figures

List of Tables

List of Abbreviations

%	Percentage
2D	Two-dimensional
3D	three-dimensional
ACK	Ammonium-Chloride-Potassium
APC	Antigen-presenting cells
BME	Cultrex Basement Membrane Extract
BSA	Bovine serum albumin
℃	Degree Celsius
CASY	Cell Counter and Analyzer
CCL/CXCL	C-C Motif Chemokine Ligand/C-X-C Motif Chemokine Ligand
CM	Conditioned medium
cm	centimeter

CON	Control
CpG ODN	CpG-containing oligodeoxynucleotides
CTLA	Cytotoxic T-lymphocyte-associated protein 4
DCs	Dendritic cells
DMEM	Dulbecco's Modified Eagle Medium
DMSO	Dimethyl sulfoxide
EGF	Epidermal growth factor
EXP	Experiment
FACS	Fluorescence Activated Cell Sorter
FBS	Fetal bovine serum
FGF	Fibroblast growth factors
FMO	Fluorescence Minus One
g	gram
GITR	Glucocorticoid-induced tumor necrosis factor receptor
h	Hour/hours
HBV	Hepatitis B virus
HCV	Hepatitis C virus
HD	Healthy donors
HEPES	4-(2-hydroxyethyl)-1-piperazineethanesulfonic acid
IFN-γ	Interferon-gamma
IL	Interleukin
LAC	Leukocyte activation cocktail
MAZR	Myc-associated zinc finger-related factor
MDSCs	Myeloid-derived suppressor cells
mg	Milligram
min	Minute
ml	Milliliter
M-MDSCs	monocytic MDSCs
MMP9	Matrix metallopeptidase 9

NAC	N-Acetyl-L-Cystein
NaN3	Natriumazid
NK cells	Natural Killer cells
NO	nitrogen oxide
NTR	Neurotensin receptors
Org	Organoid
P	Patient
P/S	Penicillin/Streptomycin
PBMC	Peripheral Blood Mononuclear Cell
PBS	Phosphate-buffered saline
PD-1	Programmed death protein 1
PDAC	Pancreatic ductal adenocarcinoma
PMN-MDSCs	polymorphonuclear MDSCs
rcf	Relative centrifugal force
RNA	Ribonucleic acid
Rock Inhibitor	Rho-associated, coiled-coil-containing protein kinase Inhibitor
ROS	reactive oxygen species
rpm	Revolutions per minute
RPMI1640	Roswell Park Memorial Institute 1640
RT	Room temperature
Runx3	Runt-related transcription factor 3
stim	Stimulation
TAMs	Tumor-associated Macrophages
Tcm cells	Central Memory T cells
Teff cells	Effector T cells
Tem cells	Effector Memory T cells
TGF-β	Transforming growth factor Beta
Th cells	T Helper cells
TME	Tumor microenvironment

Tnaiv cells	Naïve T cells
TNF	Tumor necrosis factor
Tregs	Regulatory T cells
unstim	Unstimulation
VEGF	Vascular endothelial growth factor
µg	Microgram
µl	Microliter
µm	Micrometer

1.Introduction

Pancreatic ductal adenocarcinoma (PDAC) is the most frequent malignant tumor of the pancreas with median survival of 6 months and by 2030, PDAC is predicted to be the second leading cause of cancer-related death in the United States [1, 2]. The compromised immune system hijacked by tumor cells leading to immune escape is critical for PDAC progression and metastasis, as well as poor outcomes for patients [3]. Considering the rising incidence of PDAC [4], clinical translational studies are needed to gain immune-therapeutically advancement for these patients [5]. An important step to achieve this goal was the introduction of three-dimensional (3D) *in vitro* organoids generated from primary tumors that are long-term stable, and more representative of tumor heterogeneity, cell-to-cell contact, structure, and genetic expression than conventional 2D cell cultures [6, 7]. The attempts to establish a complex co-culture with tumor-derived organoids and immune cellular components can provide a preclinical model to investigate interactions between tumor cells and immune cells, as well as the possibility to evaluate immunotherapies. In this section, I will introduce the background and research purpose of our project.

1.1 The background of PDAC

The occurrence of PDAC is relatively insidious, and the clinical manifestations are not obvious or present late [8]. Therefore, most patients are detected in advanced metastatic stages, causing a low 5-year survival rate (below 10%) [9]. According to the online data from the Global Cancer Observatory (GCO) website (gco.iarc.fr), there were almost as many deaths (466,003) as new cases (495,773) worldwide in 2020, attributed to the dismal prognosis. Nowadays, PDAC is the fourth cause of cancer death in Europe, and the number of death cases is estimated to grow over the years [10].

Surgical resection is the most effective treatment of PDAC at present [8].

However, only a small proportion of patients (15%-20%) diagnosed at early and locally restricted stages can undergo upfront surgery [11].

In a multimodal therapeutic strategy with neoadjuvant chemotherapy approximately 30% of locally advanced PDAC patients can be downgraded to a resectable stage [12] thereby improving overall survival for patients after surgery [13]. Regarding patients with unresectable disease with or without metastatic lesions, precision medicine and radiation therapy have also shown certain effects [14, 15]. Despite that, the expense of considerable toxicity and the terrible physical status of the patients when receiving these treatments cannot be ignored.

In recent years, immunotherapy is one of the fastest growing research areas in cancer research. The rationale of this method is to rebuild and maintain the tumor-immune cycle, then take advantage of the own normal anti-tumor immune responses to control and eliminate the tumor cells with distinct individual differences [16]. The efforts targeting immunotherapeutic strategies in cancers are extensive, including immune checkpoint inhibitors, adoptive cell transfer, cancer vaccines, small molecule inhibitors, immune system modulators, and the combination of these therapies [17-19]. Although these schemes have shown excellent efficacy and innovation in some refractory cancers [20-24], the benefit in PDAC is still limited owing to the profound immunosuppression of tumor microenvironment (TME) in this cancer [25, 26]. Therefore, an in-depth understanding on the complex roles of different components in the PDAC microenvironment should be given high priority to help guiding therapeutic decisions of individualized treatment regimens for patients in the near future.

1.2 Organoid models establishment

For decades, animal models and conventional two-dimensional (2D) cell lines have been employed in cancer research. However, the complex immunobiology of native human tumors cannot be sufficiently modeled in mice,

and cell lines are limited by the loss of genetic heterogeneity of the original tumor after multiple passages and their inability to mimic cell-cell and cell-extracellular interactions [27-29].

Organoid technology has emerged as an independent research tool. Compared to 2D cell lines, this heterogeneous 3D structure better reflects the genome, morphology, and physiological characteristics of the original tumor [30, 31]. The advantages and disadvantages of conventional 2D cell lines and 3D patient-derived organoids were concluded in Table 1.

Table 1 Comparison of cell lines and organoid models

Types	2D cancer cell line	3D patient-derived organoid
Advantages	Simple cultural conditions and low cost	Resemble the parent organ in vivo of morphology and physiological characteristics
	Easy to expand *in vitro*	Genetic stability after several passages
Disadvantages	Loss of genetic heterogeneity after several passages	Sophisticated culture conditions
	Inability in simulating TME	Time consumption

1.2.1 The application of the organoid model in cancer research

This developed *in vitro* 3D culture technology avoids many of the shortcomings of 2D cell lines and has great potential for cancer research and clinical applications, involved in cancer modeling, RNA and exome sequencing, proteomic analysis, drug efficacy and safety evaluation, and personalized medicine implementation [32-34].

During organoid culture, we can observe and analyze tumor dynamic processes in real-time that faithfully recapitulate many steps of tumor progression [35, 36]. A variety of cancer-related infection models were established by organoids to illustrate the carcinogenic formation, such as

Hepatitis-B-Virus (HBV) [37] or Hepatitis-C-Virus (HCV) [38] to liver cancers, Helicobacter pylori to gastric cancers [39], and pathogenic Escherichia coli to intestinal cancers [40]. In another study, the CRISPR-Cas9 genome-editing system was used to introduce numerous gene mutations in normal intestinal organoids to drive colorectal cancer development [41].

Utilizing organoids, Gao et al. [42] summarized the molecular diversity of prostate cancer subtypes in 7 patients, comprising TMPRSS2-ERG fusion, PTEN and CHD1 depletion, CDKN2A and SPINK1 overexpression, as well as TP53, SPOP, FOXA1 and PIK3R1 mutation, describing the common features in this cancer.

The organoid models also help to test the safety and efficacy of drugs and extend the therapeutic options for more cancer patients. Zumwalde et al. [43] revealed that $V\delta2^+$ γδ T cells in breast cancer organoids could produce the anti-tumor cytokine IFN-γ to kill tumor cells responded to an aminobisphosphonate drug, proposing a non-invasive approach to treat ductal carcinoma in situ. Della Corte et al. [44] demonstrated through organoids derived from non-small cell lung cancer patients that the combination of MEK inhibitors and anti-PD-1 (Programmed death protein 1) treatment can be useful for KRAS mutated patients, with a high clinical value. Wensink et al. [45] reviewed 17 studies to evaluate the feasibility of using organoids to select drugs and predict clinical response. This innovation of organoid drug screening was validated to reflect the patient susceptibility to therapeutic drugs that significantly improve the cost-effectiveness of individualized treatment.

To date, the organoid models have been successfully established for diverse cancers, including breast cancer [46, 47], colon and gastrointestinal cancer [48-51], liver cancer [52, 53] pancreatic cancer [54, 55], prostate cancer [42, 56], bladder cancer [57] and many more, which are applied in imitating human tumors *in vitro* and tremendously support the translation from basic cancer research to clinical practice.

1.2.2 The co-culture model with PDAC organoids and immune cellular components establishment

As the organoid model is now being implemented in research on a broader scale, more complicated organotypic platforms using organoids in multi-cellular co-cultures with immune cellular components ((i.e. Peripheral Blood Mononuclear Cell (PBMCs)) are applied to form a more complete model of the disease and its described TME [29, 58, 59]. For example, Dijkstra et al. indicated that the co-culture of autologous tumor organoids and PBMCs could be used to enrich tumor-reactive T cells from peripheral blood of patients with colorectal and non-small-cell lung cancer [60]. This *ex vivo* model may help us to explore the interaction between tumor cells and immune cells, supporting the development of T cell-based immunotherapies.

While studying the tumor and immune system in PDAC patients, Holokai et al. [61] established a pre-clinical model with human PDAC organoids, cytotoxic T lymphocytes, and myeloid-derived suppressor cells (MDSCs), affirming the inhibitory effect of elevated MDSCs on T cell effector function, and the restoration of T cell proliferation and cancer cell clearance capacity after depleting MDSCs with cabozantinib.

Marcon et al. [62] found the downregulation of CD16, CD57, CD226, and NKG2D expression on Natural Killer (NK) cells after co-culturing with PDAC organoids and autologous PBMCs, which revealed the differential features of NK cells in patients with PDAC and offered more insights into NK cell-based immunity treatments.

It is known that the growth and metastatic spread of PDAC are influenced by cancer-associated fibroblasts (CAFs) promoting the secretion of growth factors, cytokines, and immune-mediators in TME [63, 64]. Tsai et al. [58] identified CAFs activation and tumor-dependent lymphocyte infiltration when co-cultured with pancreatic cancer organoids, resulting in a novel, complex, anddisease-relevant 3D model, amenable to the study of drug response testing

and individualized treatments.

The addition of exogenous immune components, particularly specific cell types, provides viability for prolonged tumor organoid culture, helps to investigate the interaction between tumor cells and immune cells, and facilitates improvements in immunotherapy research.

1.3 Immune cells involved in the anti-cancer immune responses

Immune system imbalance is a critical hallmark of cancers, with the exclusion of immune effector cells and the enrichment of immunosuppressive cells [65].

1.3.1 T cells

The T lymphocytes play a central role in cell-mediated immunity, which are originated from hematopoietic stem cells in the bone marrow, and are transported to the thymus for final maturation, and then distributed to immune organs and tissues of the body through the lymphatic and blood circulatory system, exerting potent tumor-killing capability [66].

Conventional adaptive T cells can be divided into Helper $CD4^+$ T cells, Cytotoxic $CD8^+$ T cells, Memory T cells, and Regulatory T cells (Tregs) according to their functions and surface markers [67].

Helper $CD4^+$ T cells make up about 50-60% of the total number of T cells, assisting in the cellular and humoral immunity of other lymphocytes, and modulating the overall immune response [68]. Cytotoxic $CD8^+$ T cells are supported by $CD4^+$ T cells, responsible for distinguishing between normal cells and abnormal cells that should be killed, as well as influencing immune functions of macrophages and NK cells [69].

Before an antigen invades, mature $CD4^+$ and $CD8^+$ T cells are released peripherally, defined as Naive T (Tnaiv) cells with the lack of CD45RO expression, and are usually functionally quiescent [70]. Upon exposure to the

specific antigen in the context of antigen-presenting cells and co-stimulatory signals, these cells will be activated and differentiated into short-lived Effector T (Teff) cells, unleashing cellular immune effects via two aspects: 1) specifically bind to target cells, releasing perforin and granzyme to destroy the target cell membrane and directly kill the target cell; 2) secrete immunocompetent lymphokines, such as Interleukin (IL)-2, Interferon (IFN)-γ, Tumor necrosis factor (TNF)-α, etc., ultimately expand and enhance immune activities [71].

After that, a portion of the primed T cells persist as long-lived Memory T cells, maintaining the immune response converting into large numbers of Teff cells when attacked again by the cognate antigen [66, 72]. Various Memory T cell subtypes have made different contributions to immune protection. Historically, Memory T cells are divided into Effector Memory T (Tem) cells, signified as $CD45RO^{+}/CCR7^{-}$; and Central Memory T (Tcm) cells, expressed as $CD45RO^{+}/CCR7^{+}$ [73, 74]. Tem cells are considered as the first line of defense against pathogen re-exposure, capable of trans-locating to multiple peripheral tissue sites and rapidly exerting cytotoxic action [72, 75]; while Tcm populations are commonly found in lymph nodes and peripheral circulation [76], have stronger proliferative potential and provide long-term anti-tumor reactivity [77]. Subsequently, other subpopulations of Memory T cells have been discovered, including Tissue Resident Memory T cells [78], Virtual Memory T cells [79, 80], and Stem Memory T cells [81], exhibiting distinctive properties in the immune response.

Effective immunity depends on the long-term survival of Memory T cells, mobilizing the killing patterns in memory to eliminate the target cells in the next infection [82]. However, this differentiation program changes dramatically under constant stimulation by chronic infectious pathogens or tumor antigens, which poses an obstacle to mediate cancer cell clearance and the novel immunotherapeutic fields [83]. Henning et al. [83] showed that the epigenetic modifiers could regulate the differentiation and function of Memory T cells, and

impact the effectiveness of drugs for tumor interventions, which has the potential to improve current immunotherapies.

Understanding the mechanisms behind the maintenance of Memory T cells and the lineage relationship may have important implications for designing of future cancer treatments, inducing more effector cells from memory cells to reinforce the immune efficacy of therapies [84].

1.3.2 Tregs

Tregs are thought to suppress tumor immunity, promoting immune escape of tumor cells, thus hindering the body's innate ability to control cancer development [85]. Their numbers increase markedly as disease progresses, correlating with undesirable outcomes and poor prognosis [86-88].

In mice, Tregs can be effectively characterized on basis of $CD4^+$ $CD25^+$ and FoxP3 expression. However, FoxP3 cannot be equally applied to fully purified human Tregs, because of the absence of this marker in some actual human diseases [89]. A few studies have proved that $CD127^-$ could serve as a surrogate for Treg detection in clinical practice [90-92].

As a principal member of the immune system, Tregs contribute mainly to the suppressive function by secreting inhibitory factors, such as granzymes, Interleukin (IL)-10, tumor growth factor-beta (TGF-β), cytotoxic T-lymphocyte-associated protein (CTLA)-4, etc.; by supporting the accessory cells in tumors and regulating other immune cells; and also by the competition with antigen-presenting cells (APC) for co-stimulatory molecules [93-95]. Given their intratumoral or circulating presence severely impairing the immune homeostasis, current studies targeting tumor-associated Tregs can open up extra opportunities for immunotherapy options. Several factors including CTLA-4 [96, 97], PD-1 [98], C-C-chemokine-receptor Type (CCR)-4 [99], Glucocorticoid-induced tumor necrosis factor receptor (GITR) [100], OX-40 [101] and CD25 [102, 103] that relatively specific to Tregs are suggested as good markers for modulating their depletion and suppressive function in

therapeutic strategies of various cancers [85, 94, 104].

1.3.3 B cells

Mature B cells in the bone marrow migrate to peripheral lymphoid organs through the blood, become activated B cells after being stimulated by corresponding antigens, and then proliferate and differentiate into plasma cells that synthesize and secrete antibodies, thereby mainly performing the body's humoral immunity [105, 106]. It has been confirmed that the existence of B cells is associated with a favorable outcome in cancer patients [107, 108]. Therefore, future studies of cancer immunotherapies should also contain the B cell-mediated antibody responses [109]. Kemp et al. [110] demonstrated that CpG-containing oligodeoxynucleotides (CpG ODN) could trigger B cells to kill tumor cells in a TRAIL/Apo-2L-dependent manner. Conversely, the elimination of the immunosuppressive B cell subtype could enhance chemotherapy-induced tumor regression [111].

1.3.4 NK cells

NK cells are a type of cytotoxic lymphocytes critical to the innate and adaptive immune system, with the ability of immediate activating immune defenses and rapidly killing diseased and cancerous cells without prior exposure to pathogens [112]. Activated NK cells produce several toxic molecules (perforins and granzyme), pro-inflammatory cytokines (such as IFN-γ, TNF-α, IL-10, and Granulocyte-macrophage colony-stimulating factor (GM-CSF)), and some chemokines (C-C Motif Chemokine Ligand (CCL)-3, 4, 5, CXCL8) to modulate immune and inflammatory responses [113]. Besides, the NK cell-mediated cytotoxicity and cytokine production also regulates the functions of T cells, B cells, dendritic cells, macrophages, and neutrophils [112].

As an important effector in cancer immunity, NK cells have been widely studied in cancer immunotherapies. The Latest NK cell-based therapeutic approaches focus on the cytokine supplement [114, 115], monoclonal antibody

[116], adoptive transfer [117], and genetic engineering of NK cells [113, 118]. With the rapid progress in the knowledge of anti-tumor immune control, NK cells are undoubtedly the most expected immune targets for cancer treatments.

1.3.5 Neutrophils

Neutrophils are the most common subtype of granulocytes and can take the anti-tumorigenic (N1) or the pro-tumorigenic (N2) phenotype [119]. On one hand, N1 neutrophils may kill cancer cells via antibody-dependent cell cytotoxicity (ADCC) [120], or induce T-cell proliferation and IFN-γ production to display anti-tumor ability [121, 122]. On the other hand, N2 neutrophils facilitate tumor progression by producing high levels of the pro-angiogenic factors (like Vascular endothelial growth factor (VEGF) and Matrix metallopeptidase (MMP)-9) [123, 124] and dampening the anti-tumor immunity of T cells [125]. Inhibiting the T-cell suppressive functions or promoting the anti-tumor reaction of neutrophils provides the possibility for highly effective Immunotherapy [126].

1.3.6 Dendritic cells (DCs)

DCs are specialized antigen-processing and presenting cells that initiate Naive T cell priming into Effector T cells and control the immune process [127, 128]. In the settings of chronic infection and cancers, DCs can differentiate into regulatory DC subsets, contributing to the formation of the immunosuppressive TME and leading to the tumor immune escape [129]. The DC-based immunotherapy can restore self-antigen-presenting function to stimulate specific T cell and NK cell immunity so that generates resistance to cancer cells [130]. This enhanced immune response can powerfully fight cancers while improving the efficiency of chemotherapy, radiotherapy, and other conventional oncology therapies, as well as minimizing the side effects of other cancer treatments [131, 132].

1.3.7 Macrophages

Macrophages are strategically distributed throughout the body, and involved in diverse aspects of immune surveillance and homeostasis, including phagocytosis, antigen presentation, and immune regulation [133, 134]. Classically activated macrophages (M1 macrophages) can mediate anti-tumor immunity, whereas, under the conditions of tumor establishment, these cells differentiate into tumor-associated macrophages (TAMs), inhibiting immune properties [130, 135], commonly recognized as a barrier to many forms of cancer therapy [136]. Current clinical trials with therapeutic agents altering the proliferation, trafficking, and polarization of TAMs may offer more treatment opportunities for cancer patients in the future [137, 138].

1.3.8 MDSCs

MDSCs are classed as one of the main suppressive cell populations of the immune system [139], which can restrain T cells and NK cells immune activity by releasing reactive oxygen species (ROS), nitrogen oxide (NO), arginase-1, etc., and also foster Tregs expansion and differentiation [140]. MDSCs can be divided into two subsets: polymorphonuclear MDSCs (PMN-MDSCs), shared morphological and phenotypic features with N2 neutrophils; and monocytic MDSCs (M-MDSCs), similar to TAMs [71, 141].

Recently, the clinical significance of MDSCs in solid tumors receives increasing attention. They can appear during cancer progression and correlate with poor prognosis and metastasis [142-144]. Some treatment strategies targeting MDSCs have achieved promising results in mice [145-147], however, the safety and efficacy of these methods in humans use are still not well-proven.

In summary, TME is a complex ecosystem with a wide range of immune components changing during initiation and progression of cancer [148]. Therefore, the relationship between immune cells and tumor cells should be fully understood in order to bring more immunotherapeutic alternatives for cancer patients in clinical applications.

1.4 Objectives of this project

A multi-cellular co-culture model established with tumor organoids and PBMCs will hopefully serve as a preclinical model belonging to an individual patient, helping to study the complexity of tumor cell-immune cell interaction in TME and to develop new immunotherapeutic strategies to address difficulties in PDAC tretament. For that purpose, the following aspects will be explored in this project:

a. Obtaining PDAC patient-derived organoids from surgical material.

b. Establishing a co-culture model with PBMCs and organoids.

c. Analyzing the differentiation properties of PBMCs in co-culture established with tumor organoids and PBMCs from the same PDAC patient.

2. Materials and Methods

2.1 Materials

2.1.1 Apparatus

Autoclave	Unisteri, Germany
BD LSRFortessa™ Cell Analyzer	BD Biosciences, US
Cell Counter and Analyzer (CASY)	OMNI Life Sciences, Germany
Cell culture incubator	Binder, Germany
Centrifuge	Heraeus, Germany
Fridge (4°C, -20°C, -80°C)	Siemens, Germany
GentleMACS dissociators	Miltenyi Biotec, Germany
Ice machine	KBS, Germany
Lamina flow	Heraeus flow laboratories, Germany
Liquid nitrogen tank	MVE, US
Micro weigh	Chyo, Germany
Microscope	Olympus, Germany
Pipette controller	Eppendorf, Germany
Pipettes	Sigma-Aldrich, US
Vortexer	Labnet, Germany
Water bath	Memmert, Germany

2.1.2 Experimental consumables

Blot paper	Bio-Rad, Germany
Cell flasks (T75)	Thermo Fisher Scientific, US
Cell strainer (100µm)	BD Bioscience, US
Cryotubes (1.0ml, 1.8ml)	Thermo Fisher Scientific, US
Disposable safety scalpels #22	Thermo Fisher Scientific, US

FACS tube	
Falcon tube (15ml, 50ml)	Corning, Mexico
Filters (0.20µm)	Sartorius, Germany
GentleMACS™ C Tubes	Miltenyi Biotec, Germany
Needle and Cannula	SARSTEDT, Germany
Orange gloves	SHIELD Scientific, Netherlands
Petri plate (10cm)	Thermo Fisher Scientific, US
Pipette (5ml, 10ml, 25ml, 50ml)	Costar, US
Plates (6-, 24-well)	Thermo Fisher Scientific, US
S-Monovette	SARSTEDT, Germany
Tips (10µl, 100µl, 1ml)	Eppendorf, Germany

2.1.3 Reagents, chemicals, and buffer

1x Phosphate-buffered saline (PBS)	PAN BioTECH, Germany
A83-01	Tocris Bioscience, England
ACK Lysing buffer	Gibco Life Technologies, Germany
Advanced DMEM/F-12	Gibco Life Technologies, Germany
B27 supplement	Gibco Life Technologies, Germany
Biocoll	Biocell Technology, US
Bovine serum albumin (BSA)	Biomol, Germany
CASY Ton	OMNI Life Science, Germany
Collagenase Type II	Thermofischer, US
Dimethylsulfoxide (DMSO)	ROTH, Germany
EGF recombinant human protein	Gibco Life Technologies, Germany
Fetal Bovine Serum (FBS)	Thermo Fisher Scientific, US
FGF-10 recombinant human protein	Peprotech, Germany
Fixation buffer	Invivogen, US
GlutaMAX supplement	Gibco Life Technologies, Germany
BD Golgistop	BD Biosciences, US

HEPES buffer solution (1M)	Sigma Aldrich, US
Leucocyte activation cocktail (LAC)	BD Golgiplug, US
Matrigel (growth factor reduced)	Corning, US
N-Acetyl-L-Cysteine (NAC)	
Natriumazid (NaN3)	Thermo Fisher Scientific, US
Nicotinamide	Sigma Aldrich, US
Noggin recombinant human protein	Peprotech, Germany
Penicillin/Streptomycin (P/S)	PAN BioTECH, Germany
Perm buffer	Invivogen, US
Primocin	Invivogen, US
Protein Transport Inhibitor	BD Golgistop, US
Recombinant Human R-Spondin 1 protein	R&D systems, US
Recovery cell culture freezing medium	Thermo Fischer Scientific, US
ROCK inhibitor (Y-27632)	Sigma Aldrich, US
RPMI1640	Gibco Life Technologies, Germany
TrypLE express enzyme (1X)	Gibco Life Technologies, Germany
Wnt3a recombinant human protein	R&D Systems, US

2.1.4 Antibodies

CD45 BUV650	BD Bioscience, US
CD3 PerCP-Cy5.5	Biolegend, US
CD4 BUV395	BD Bioscience, US
CD8 APC-H7	BD Bioscience, US
CD25 PE	BD Bioscience, US
CD127 BV421	BD Bioscience, US
CD197 BV421	BD Bioscience, US
CD45RO PE-Cy7	BD Bioscience, US
IFN-γ FITC	Biolegend, US

2.1.5 Software

Endnote X7	Thomson Scientific, US
GraphPad Prism 9	Graphstats, US
BD FACS Diva 8.0.1	BD Bioscience, US
CASY 2.5	OMNI Life Sciences, Germany
Flowjo 10	BD Bioscience, US

2.2 Methods

2.2.1 PBMCs preparation

2.2.1.1 Blood samples from HD and PDAC patients

In this study, we continuously collected blood and tissue from PDAC patients that underwent surgery from 2020 to 2021 in Klinikum Grossharden. Meanwhile, 10 healthy people were also enrolled for blood donation. None of them had HBV, HCV, or other infectious diseases. The blood collection and processing of all the patients were taken by professionals blinded to the information of the patients in strict accordance with local safety regulations before surgery, and the same goes for healthy donors. Institutional review board approval was obtained.

2.2.1.2 PBMC isolation

Firstly, 2 falcon tubes (50ml) were prepared before PBMC isolation: one was filled with 20ml of Biocoll, and the other was used for containing the whole fresh blood and PBS mixture diluted in a proportion of 1:1. Next, the Biocoll was carefully overlaid by blood/PBS mixture without destroying its surface. The different components of peripheral blood were separated into different layers after centrifugation with no brake at 20min/1200rcf/room temperature (RT). Then the intermediate phase (PBMCs) was carefully transferred to a new falcon tube and washed with PBS in proportion 1:4. Afterward, PBMCs were

resuspended in the washing buffer and centrifuged at 10min/300rcf/RT. The supernatant discarded was followed by centrifugation, and the PBMC pellets were thoroughly washed again with 20ml of PBS later. The falcon tubes contained with PBMCs were then centrifuged at 10min/200rcf/RT, and the supernatant was rejected after that. Finally, the loose pellets of PBMCs through adequate vortexing were dissolved in the desired culture medium (RPMI1640+10%FBS+1%P/S) and ready for cell counting.

2.2.1.3 Cell counting

20μl of the cell suspension was collected for cell counting by the CASY machine. A template for calculating the numbers of PBMCs had already been set up on the software. Typically, 10ml of whole blood could extract $1x10^7$ PBMCs.

2.2.1.4 Freezing and thawing of PBMCs

PBMCs were cryopreserved in the prepared freezing medium (95%RPMI1640+5%DMSO) until later use.

2.2.2 Organoid establishment

2.2.2.1 Surgical specimens collected from PDAC patients

The tumor tissues from PDAC patients were collected after surgical resection and identification by the pathologists. All the information about these patients was unclear except the surgery date and the pathological results.

2.2.2.2 The process of organoid isolation and culture

All reagents and media involved in organoid isolation and culture were listed in Table 2 and Table 3.

Table 2 Reagents preparation in organoid isolation and culture

Reagents	Chemicals/Medium	Dose
NAC solution	Deionized water (DIW)	10ml
	NAC	82mg
Wnt3a	PBS (1X)	0.5ml

	BSA	50mg
	Wnt3a	50µg
Noggin	PBS (1X)	1ml
	BSA	100mg
	Noggin	100µg
EGF	DIW	500µl
	EGF	50µg
Gastrin	5% NH_4OH	1ml
	Gastrin	50µg
FGF-10	Sodium Phosphate	500µl
	FGF-10	50µg
Nicotinamide	DIW	10ml
	Nicotinamide	1.22g
A83-01	DMSO	1ml
	A83-01	2.1mg
R-Spondin	PBS (1X)	250µl
	BSA	25mg
	H R-Spondin	25µg
Rock Inhibitor	DIW	1.56ml
	Rock Inhibitor	5mg

Table 3 Medium preparation for organoid isolation and culture

Medium	Reagents	Volume
Splitting Medium	Advanced DMEM/F12	500ml
	HEPES (1M)	5ml
	GlutaMAX Supplement	5ml
	Primocin	1ml
Digestion buffer	Splitting medium	10ml
	Collagenase II	60mg

	Rock inhibitor	5μl
Feeding medium	Splitting medium	50ml
	B27	1ml
	Noggin	50μl
	EGF	50μl
	Gastrin	10μl
	FGF-10	50μl
	A83-01	5μl
	R-Spondin	250μl
	NAC	125μl
	Nicotinamide	500μl
Complete medium	Feeding medium	50ml
	Wnt3a	50μl
	Rock Inhibitor	50μl

Fresh tissue derived from surgical resection was placed in a 50ml falcon tube with 10ml of PBS on ice. The isolation procedure should start as soon as possible to ensure that the tissue and the resulting pellet containing the dissociated cells remain viable, thereby increasing the chance of isolating organoids.

The tissue was transferred to a 10cm Petri plate, carefully minced into small fragments by two scalpels, and added to a GentleMACS C tube with 10ml of prepared digestion buffer. This tube was then fixed on GentleMACS and incubated for 2h at RT with gentle shaking (the program was pre-set in the software). Subsequently, this sample was filtered through the cell strainer (100μm) to a new falcon tube, added with the required volume of ice-cold PBS+0.1%BSA to 15ml, and centrifuged at 5min/1000rpm/4 ℃. After discarding the supernatant, the pellets were washed with 3ml of ACK buffer and incubated at RT for at least 3min until the red blood cells were invisible,

then washed with 5ml of ice-cold PBS+0.1%BSA to stop lysis, and centrifuged at 5min/1000rpm/4℃ before the supernatant was carefully discarded. Next, 3ml of TrypLE was added to dissociate the cell clusters into single ones and incubated for 5min in a 37℃ water bath. Later, the sample was washed with 5ml of ice-cold PBS+0.1% BSA and centrifuged at 5min/1000rpm/4℃ again to obtain qualified cells for culture. The cell pellets collected after the supernatant discarded were re-suspended in the required amount of matrigel (50μl/well) and immediately placed on ice. Normally, organoids were cultured in the 24-well culture plate, and enough cells isolated from one tissue (0.1-0.2g) can be accommodated into 2-4 wells. 50μl of matrigel mixture was pipetted into the certain wells of the plate to form a dome and ensure no air bubbles. This plate was then placed carefully in the incubator for 10-15min until the gel was stable. Finally, each dome of matrigel mixture was covered by 500μl of pre-warmed complete medium for long-time culture in the incubator. This procedure can be seen in Figure 1 (created with *BioRender.com*). The medium should be refreshed every 3 to 4 days during organoid culture.

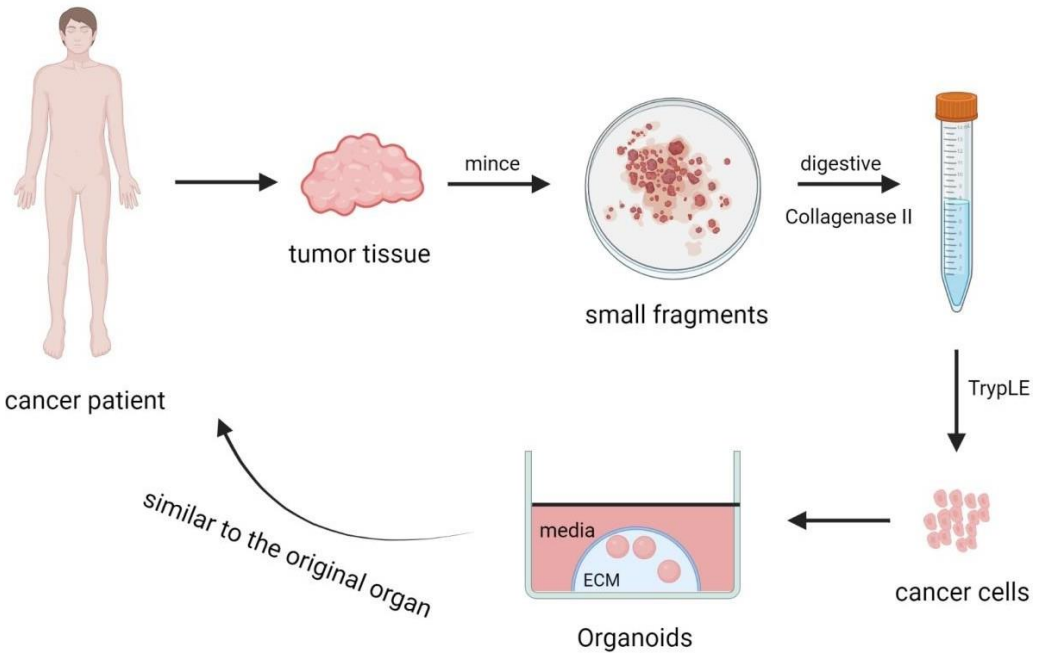

Figure 1: The process of PDAC organoid isolation.

2.2.2.3 Organoid passaging

Organoids should be split into more wells every 5-10 days, usually in a ratio of 1:2, giving them more space to grow. The matrigel-organoid mixture was collected in a new falcon tube until fully washed with cold cell recovery solution and cold PBS (10ml in total), respectively. Those remaining organoids in the wells also needed to be scraped off with a pipette tip, and then transferred into the same falcon tube. The cell pellets were acquired after centrifugation at 5min/1000rpm/4°C and the supernatant was carefully discarded. The desired amount of matrigel (50μl/well) was added to the dissociated cells and mixed completely on ice. 50μl of the new matrigel-organoid mixture was pipetted in the particular wells of the 24-well plate without air bubbles, and when the liquid mixture turns into a gel, each of them was replenished with 500 μl of pre-warmed complete medium. The plate was then returned to the incubator for further culturing.

2.2.2.4 Organoid freezing and thawing

At passage 2 and/or more, the organoids should be cryopreserved with the recovery cell culture freezing medium for later use.

When needed, organoid cryovials were taken out from liquid nitrogen and thawed in a 37°C water bath for 5min. The contents in the cryovials were then transferred into a new falcon tube with 9ml pre-warmed DMEM and centrifuged at 5min/1000rpm/4℃. Following discarding the supernatant, the cell pellets left in the tube were washed with 10ml of cold PBS+0.1%BSA and centrifuged again. The cells collected after supernatant removal were dissolved in the required amount of matrigel (50μl/well) and placed on ice. 50μl of the matrigel-organoid mixture was pipetted in the given wells of the 24-well plate, and each mixture was covered with 500μl pre-warmed complete medium when the liquid turned into gel.

Organoids that still grow normally after freezing and thawing were considered successful cultures.

2.2.3 Co-culture model establishment

2.2.3.1 Culture PBMCs with conditioned medium (CM) derived from human pancreatic cancer cell lines

Human pancreatic cancer cell lines (Panc1 and Miapaca2) were received from the biobank of our lab, which were originally from American Type Culture Collection. These cell lines were separately cultivated in a T-75 flask with 15ml of RPMI1640+10%FBS+1%P/S, detached with 5ml 0.025% Trypsin/EDTA solution, and passaged every 3-4 days depending on cell growth. The CM samples from the supernatant of Panc1 and Miapaca2 after culturing for 72h were gathered in a new falcon tube and filtered through a 0.20μm filter to remove cell debris, then frozen at -20℃, respectively.

The culture experiment was carried out on a 6-well plate. In the upper 3 wells of the plate, the prepared PBMCs from HD were cultured only with RPMI1640+10%FBS+1%P/S, as a control group; while in the lower 3 wells, the PBMCs were cultured with 50% of RPMI1640+10%FBS+1%P/S and 50% of Panc1/Miapaca2-derived CM, as an experimental group. 48h later, PBMCs from the top and bottom wells were collected separately and stained for FACS analysis.

2.2.3.2 Co-cultured PBMCs with human pancreatic cancer cell lines

Panc1/Miapaca2 cells were seeded in the bottom 3 wells of the 6-well plate at the desired numbers one day before being co-cultured with PBMCs so that these cells were stably attached to the wells. The next day, one or two vials of frozen PBMCs were thawed in a 37℃ water bath, transferred to a falcon tube, and washed with 9ml of PBS. After centrifuging at 5min/500rcf/RT and discarding the supernatant, the PBMCs were resuspended in the normal culture medium (RPMI1640+10%FBS+1%P/S). The same amount of prepared PBMCs were added to each of the upper 3 wells, as well as the bottom 3 wells at a ratio of 25:1 with Panc1/Miapaca2 cells. Waiting for 48h, the PBMCs in the upper 3 wells (control group) and the mixture of PBMCs and Panc1/Miapaca2

in the bottom 3 wells (experimental group) were collected respectively and then stained for FACS analysis.

2.2.3.3 Co-cultured PBMCs with organoid lines from PDAC patients

The co-culture of PBMCs and organoids was established on the basis that 60 to 100 well-growing organoids can be counted in each well of the 24-well plate from one complete and clear view taken under the microscope. Then, the qualified PBMCs were resuspended in the organoid complete medium, added to the certain wells with organoids-matrigel mixtures, and cultured in the incubator for 48h, which served as an experimental group (co-culture). In the control group, the same numbers of PBMCs were cultured alone in the same medium and matrigel for 48h. The staining of PBMCs for FACS was performed after cell collecting in the control group and co-culture group respectively.

The PBMCs from one HD and different organoid lines were employed to determine the co-culture methods. Afterward, four autologous co-cultures were established with PDAC patient-derived organoid lines and their matched PBMCs to analyze the differentiation characterization of the immune cells in the TME.

2.2.4 Fluorescence-Activated Cell Sorting (FACS)

2.2.4.1 Definition of T cell subsets and cytokines in FACS

T cells can be divided into different subpopulations. In this study, we focused on the differentiation of Memory T cell subsets and Tregs as well as the production of IFN-γ during the establishment of the co-culture model.

The definitions for the cell subsets and IFN-γ production are listed in Table 4.

Table 4 Definition of measured immune cell subsets and cytokines

Cell type or cytokine	Markers
T cells, % of Lymphocytes	$CD3^+$, % of $CD45^+$
Helper T cells, % of T cells	$CD4^+/CD8^-$, % of $CD45^+/CD3^+$
Cytotoxic T cells, % of T cells	$CD8^+/CD4^-$, % of $CD45^+/CD3^+$

Tem cells, % of $CD4^+$ T cells	$CD197^-/CD45RO^+$, % of $CD45^+/CD3^+/CD4^+$
Tcm cells, % of $CD4^+$ T cells	$CD197^+/CD45RO^+$, % of $CD45^+/CD3^+/CD4^+$
Teff cells, % of $CD4^+$ T cells	$CD197^-/CD45RO^-$, % of $CD45^+/CD3^+/CD4^+$
Tnaiv cells, % of $CD4^+$ T cells	$CD197^+/CD45RO^-$, % of $CD45^+/CD3^+/CD4^+$
Tem cells, % of $CD8^+$ T cells	$CD197^-/CD45RO^+$, % of $CD45^+/CD3^+/CD8^+$
Tcm cells, % of $CD8^+$ T cells	$CD197^+/CD45RO^+$, % of $CD45^+/CD3^+/CD8^+$
Teff cells, % of $CD8^+$ T cells	$CD197^-/CD45RO^-$, % of $CD45^+/CD3^+/CD8^+$
Tnaiv cells, % of $CD8^+$ T cells	$CD197^+/CD45RO^-$, % of $CD45^+/CD3^+/CD8^+$
Tregs, % of $CD4^+$ T cells	$CD25^+/CD127^-$, % of $CD45^+/CD3^+/CD4^+$
IFN-γ, % of $CD45^+$ T cells	IFN-γ, % of $CD45^+$
IFN-γ, % of $CD4^+$ T cells	IFN-γ, % of $CD45^+/CD3^+/CD4^+$
IFN-γ, % of $CD8^+$ T cells	IFN-γ, % of $CD45^+/CD3^+/CD8^+$

2.2.4.2 Immunophenotyping staining of PBMCs for FACS analysis

Panel 1 and Panel 2 were designed for examining Memory T cells and Tregs, respectively, including the markers to be measured, an unstained tube as blank control, two Fluorescence Minus One (FMO) control tubes, and a test tube of the sample. According to the extracellular staining protocol, the PBMCs were re-suspended in the desired medium at $1x10^6$cells/ml and transferred to the FACS tubes (200µl/tube). The certain tubes in both control and experimental group were added with 1µl of each antibody (see Panels), vortexed, and incubated in a dark chamber for 15-30min/RT. Then the samples were washed with 2ml of FACS buffer (PBS+2%NaN3+5%BSA) completely and centrifuged at 5min/500rcf/RT. After discarding the supernatant and adding another 500µl of FACS buffer in each tube, the samples were ready for FACS analysis of T cell differentiation with or without being influenced by the tumor cells.

Panel 1 Memory T cells

Tube	BUV395	BV650	PerCP-Cy5.5	APC-H7	BV421	PE-Cy7
unstained	--	--	--	--	--	--
FMO 1	CD4	CD45	CD3	CD8	--	CD45RO
FMO 2	CD4	CD45	CD3	CD8	CD197	--
sample	CD4	CD45	CD3	CD8	CD197	CD45RO

Panel 2 Regulatory T cells

Tube	BUV395	BV650	PerCP-Cy5.5	APC-H7	PE	BV421
unstained	--	--	--	--	--	--
FMO 1	CD4	CD45	CD3	CD8	--	CD127
FMO 2	CD4	CD45	CD3	CD8	CD25	--
sample	CD4	CD45	CD3	CD8	CD25	CD127

Sample preparation for IFN-γ production detection by FACS was based on intracellular staining protocol. The test cells required to be stimulated and fixed for permeabilization, thus the additional LAC (with monensin to support the accumulation of intracellular proteins and/or cytokines in the Golgi complex and increase their detectability by FACS) was involved to induce IFN-γ production in the experimental group, and Golgistop (a protein transport inhibitor-containing monensin) was supplemented to the control groups. Panel 3 was designed for IFN-γ detection and comprised of the specified markers, an unstained tube, an FMO tube, an un-stimulated control tube (unstim), and a stimulated experimental tube (stim).

Both the samples in the control and experimental groups were further divided equally into two sub-groups: the cells in the “unstim” group were pre-processed with Golgistop (0.7µl for $1x10^6$ cells) and those in the “stim” group were treated with LAC (2µl for $1x10^6$ cells). The cells were incubated for 3h. Later, each FACS tube was filled with $5x10^4$ to $1x10^6$ of PBMCs

suspension and 1μl of each extracellular antibody (see Panel 3), then fully vortexed and incubated for 15-30min/RT/dark. Following that, 100μl of IC Fixation buffer was supplied in each group for fixing cells, which is necessary for intracellular staining of antigens located in the cytoplasm or secretory pathway. After two washes with Perm buffer, 1μl of IFN-γ antibody was added to the test tubes, then vortexed and incubated for another 30-60min/RT/dark. All the samples were washed with 2ml of Perm buffer and 2ml of FACS buffer and finally stabilized in 500μl of FACS buffer for detection.

Panel 3 IFN-γ

Tube	BUV395	BV650	PerCP Cy5.5	APC-H7	FITC
unstained	--	--	--	--	--
FMO 1	CD4	CD45	CD3	CD8	--
sample (unstim)	CD4	CD45	CD3	CD8	IFN-γ
sample (stim)	CD4	CD45	CD3	CD8	IFN-γ

2.2.5 Gating strategy to get FACS data

The population of certain immune cells and cytokines in all the samples was examined by BD LSRFortessaTM Cell Analyzer. The data was recorded and downloaded from BD FACS Diva 8.0.1 software, and imported to Flowjo10 for further analysis.

The gating strategies of Memory T cells, Tregs, and IFN-γ production on the FACS plots were shown in Figure 2, 3, and 4.

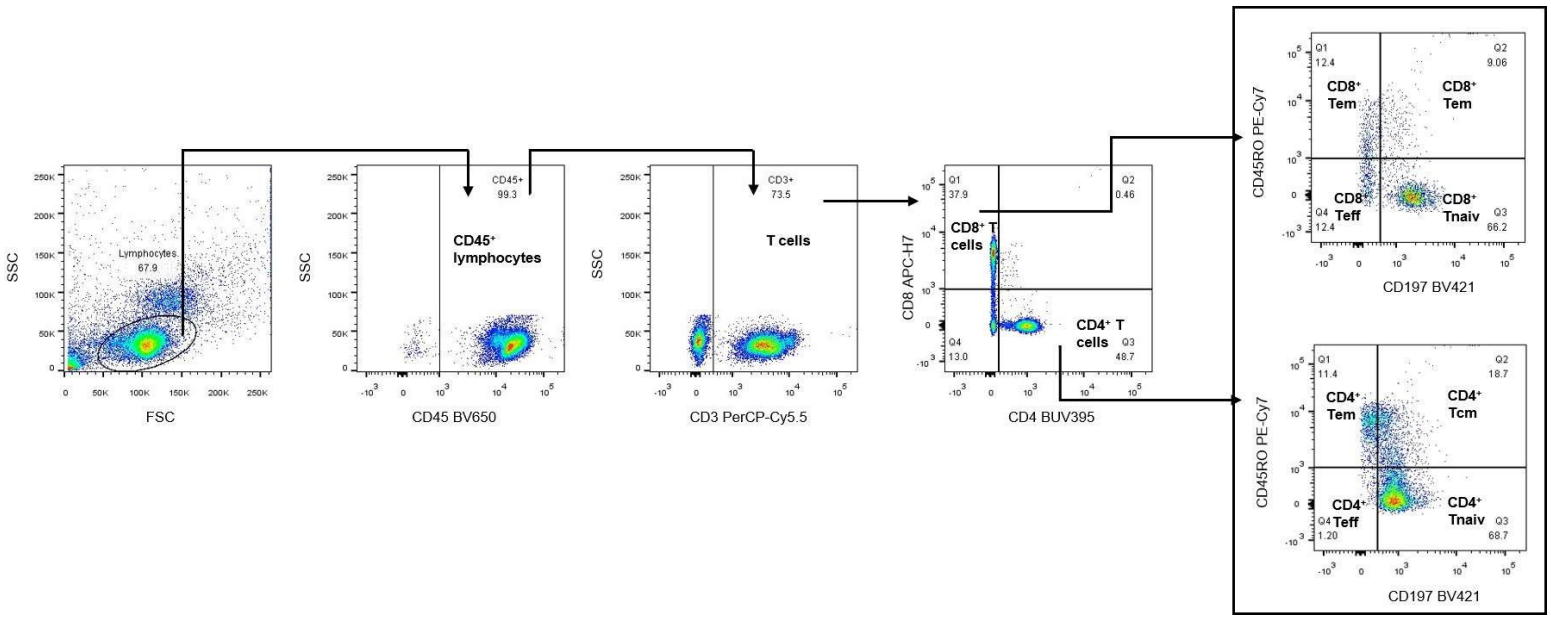

Figure 2: Gating strategy of Memory T cells in FACS plot (Lymphocytes display low FSC and low SSC physical parameters and are also defined by $CD45^+$. T cells are identified by $CD3^+$, and then further classified into $CD8^+$ T cells and $CD4^+$ T cells by the same gating strategy. Both $CD8^+$ and $CD4^+$ T cell populations can be divided into 4 subsets: Tem was gated as $CD197^-/CD45RO^+$ in the Q1 quadrant, Tcm was $CD197^+/CD45RO^+$ in the Q2 quadrant, Teff was $CD197^-/CD45RO^-$ in the Q4 quadrant, and Tnaiv was $CD197^+/CD45RO^-$ in the Q3 quadrant).

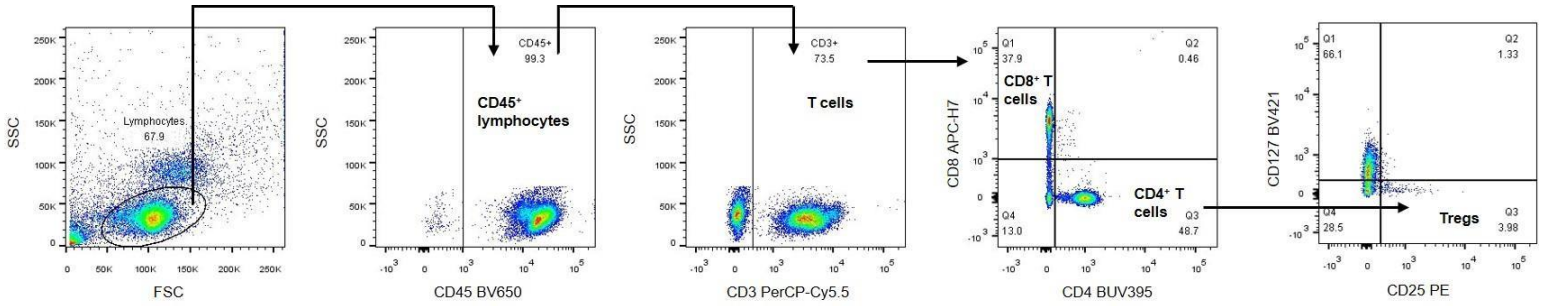

Figure 3: Gating strategy of Tregs in FACS plot (Lymphocytes, T cell populations, $CD4^+$ and $CD8^+$ T cells were defined as described in Figure 2. Tregs were isolated from $CD4^+$ T cells, and identified by $CD25^+/CD127^-$ in the Q3 quadrant).

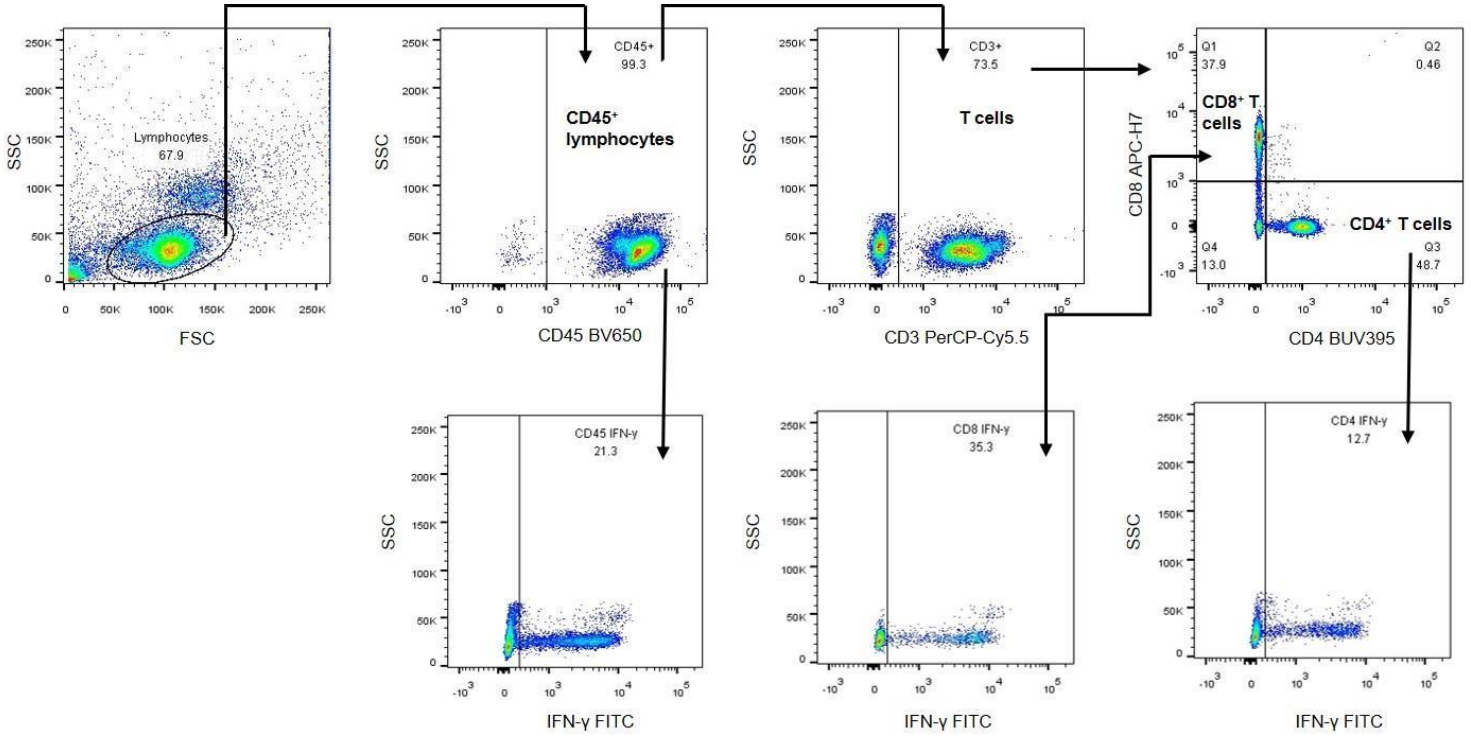

Figure 4: Gating strategy of IFN-γ production in FACS plot (Lymphocytes, T cells, $CD4^+$ and $CD8^+$ T cells were defined as introduced in Figure 2. IFN-γ production of $CD45^+$, $CD4^+$, and $CD8^+$ T cells was all gated by the same strategy).

2.2.6 Statistical Analysis

The student's t-test was applied in all statistical analyses to evaluate the differences between control and experimental groups by GraphPad Prism 9 based on the population of immune cells and the $P < 0.05$ was considered to be statistical significance.

3. Results

3.1 Obtaining PDAC patient-derived organoids from surgical material

Since October 2020, we have started to collect tumor tissues from patients with PDAC after surgical resection and attempt to isolate and culture organoids from these tissue samples, thereby establishing a patient-derived organoid biobank. So far, we have successfully grown 9 organoid lines from 9 PDAC patients (Table 5).

Table 5 Organoid datasheet

Trial no.	Date	Patient	Type	Passage	Comments
1	22.12.2020	A704854	PDAC	P6	grows slowly
2	16.02.2021	A302197	PDAC	P4	grows well
3	05.05.2021	A575633	PDAC	P3	grows well
4	30.06.2021	A891299	PDAC	P2	no matched blood
5	30.07.2021	AN38302	PDAC	P2	grows slowly
6	26.08.2021	A298492	PDAC	P2	grows slowly
7	09.09.2021	A930788	PDAC	P3	grows well
8	15.09.2021	AN88191	PDAC	P2	grows slowly
9	08.10.2021	AN85498	PDAC	P3	grows well

Among them, 4 organoid lines from Patient 2, 3, 7, and 9 were employed in further co-culture model establishment with their autologous PBMCs. Before that, pancreatic cancer cell lines and their derived CM were used to culture PBMCs from HD or PDAC patients as preliminary experiments, and the differentiation of certain T-cell subtypes and the production of IFN-γ were detected and analyzed to investigate the interaction between cancer cells and immune cells.

3.2 Culturing PBMCs with CM derived from pancreatic cancer cell lines

Proteins in the CM secreted by cultured cells are a source that can be utilized to promote the production of cytokines and the growth of other cells [149]. The differentiation of T cell subsets and IFN-γ production in PBMCs (HD) was detected after culturing PBMCs with 50% of normal medium (RPMI1640+10%FBS+1%P/S) and 50% of CM from Panc1/Miapaca2 for 48h (EXP (+CM) group) and made a comparison with those cultured in normal medium only (CON (HD) group). CD197 and CD45RO antibodies were applied to identify the effector and central Memory T cell population in $CD4^+$ and $CD8^+$ T cells in PBMCs.

3.2.1 No effects on the Memory T cell subtype differentiation in PBMCs (HD) after culturing with CM (Panc1/Miapaca2)

The population for $CD4^+$ Tem, Tcm, Teff, and Tnaive cells in the EXP (+CM)-Panc1 group was 13.00%, 16.60%, 2.76%, and 67.60%, respectively, but in the matched CON (HD) group, the population of these four T cell subsets was 14.90%, 15.40%, 4.59%, and 65.10%, respectively. No significant changes were found between these two groups ($P>0.05$, Figure 5 A, B).

In the EXP (+CM)-Miapaca2 group, the population of $CD4^+$ Tem, Tcm, Teff, and Tnaive cells was 18.60%, 21.70%, 2.72%, 57.00%, respectively, and in its control group, these numbers were 17.90%, 20.80%, 2.73%, 58.50%, respectively. There were also no statistical differences between the CON (HD) and EXP (+CM)-Miapaca2 groups ($P>0.05$, Figure 5 A, C).

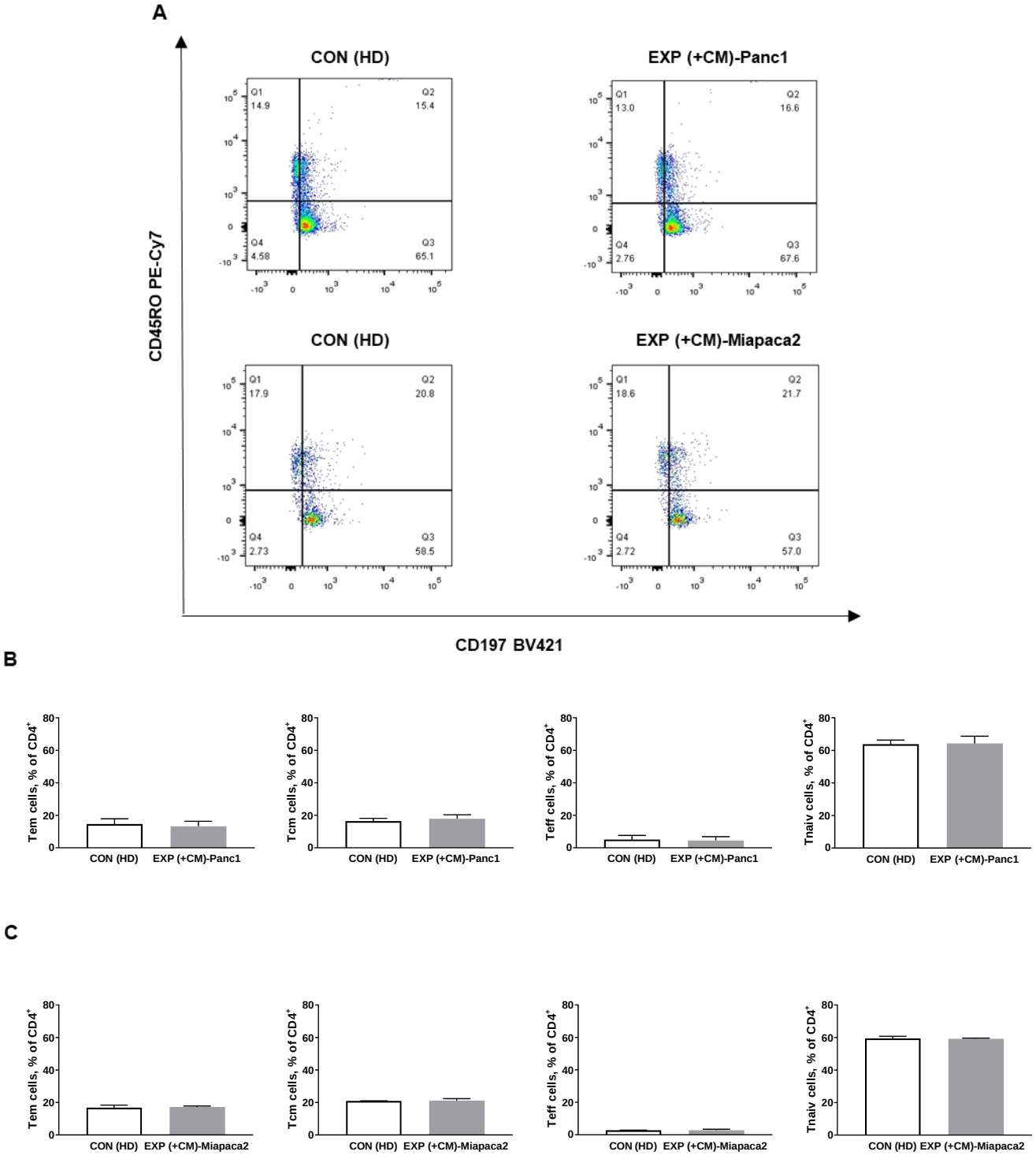

Figure 5: (A): Representative FACS plot of Memory $CD4^+$ T cell subset in the CON (HD) and EXP (+CM)-Panc1/Miapaca2 groups. (B)(C): The population of $CD4^+$ Tem, $CD4^+$ Tcm, $CD4^+$ Teff, and $CD4^+$ Tnaiv between CON (HD) and EXP (+CM)-Panc1/Miapaca2 group has no statistical significances (P>0.05).

For $CD8^+$ Memory T cells, the population of Tem, Tcm, Teff, and Tnaive cells in the EXP (+CM)-Panc1 group were 14.60%, 8.80%, 12.30%, and 64.30%, respectively, which still has no obvious differences compared to that in the CON (HD) group with the corresponding numbers of 12.00%, 9.94%, 13.30%, and 64.80%, respectively ($P>0.05$, Figure 6 A, B).

Similarly, the population of $CD8^+$ Tem cells in the CON (HD) and EXP (+CM)-Miapaca2 group was 12.20% and 14.00%, of $CD8^+$ Tcm cells was 6.95% and 6.87%, of $CD8^+$ Teff cells was 5.92% and 5.98%, and of $CD8^+$ Tnaive cells was 75.00% and 73.10%, respectively, showing no statistical alterations between these two groups ($P>0.05$, Figure 6 A, C).

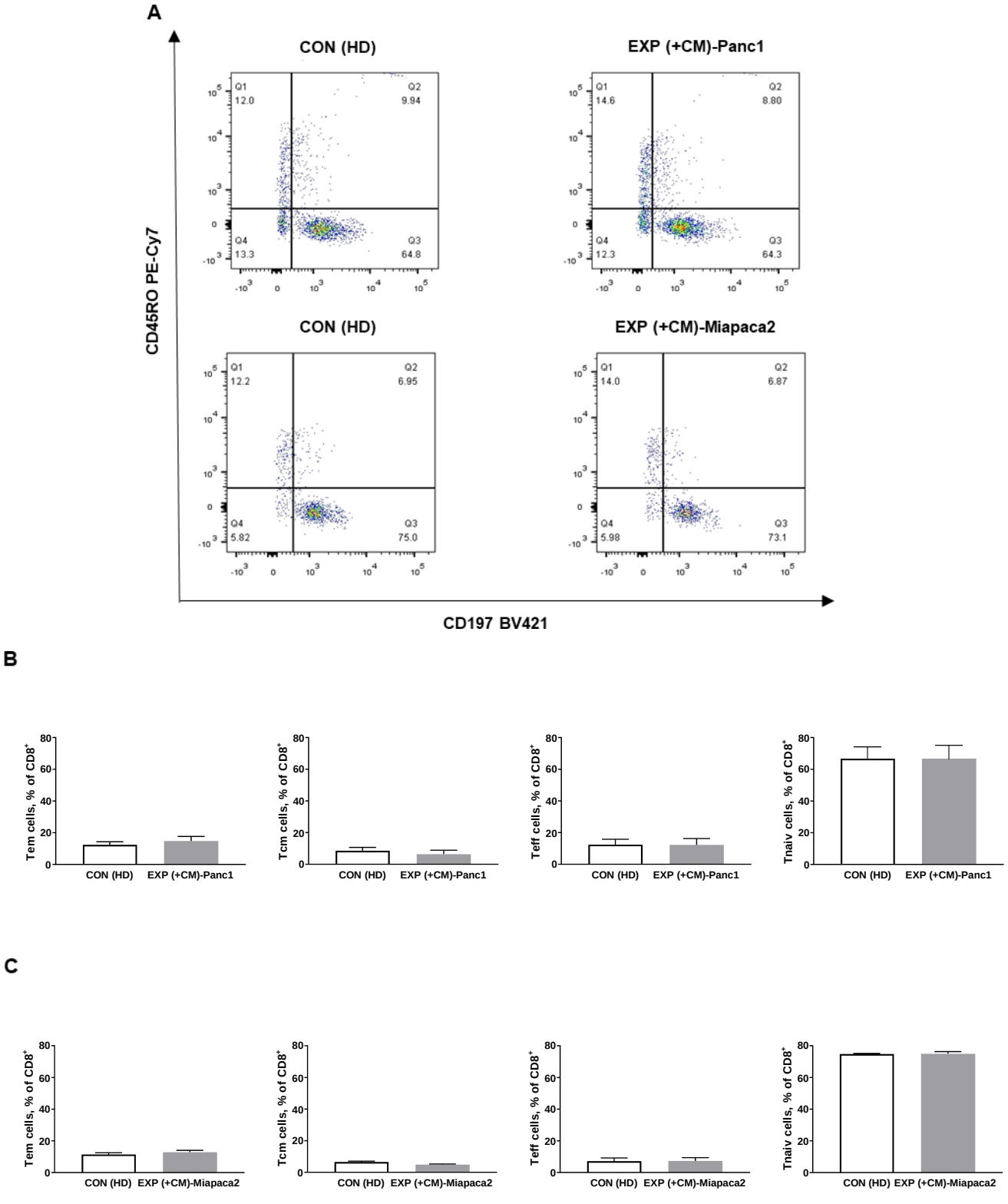

Figure 6: (A): Representative FACS plot of Memory $CD8^+$ T cell subsets in the CON (HD) and EXP (+CM)-Panc1/Miapca2 groups. (B)(C): The population of $CD8^+$ Tem, $CD8^+$ Tcm, $CD8^+$ Teff, and $CD8^+$ Tnaiv between CON (HD) and EXP (+CM)-Panc1/Miapaca2 group has no statistical significances (P>0.05).

3.2.2 No effects on the differentiation of Tregs in PBMCs (HD) after culturing with CM (Panc1/Miapaca2)

The PBMCs in the CON (HD) groups were only cultured with the normal medium (RPMI1640+10%FBS+1%P/S) for 48h, while in the EXP (+CM) of Panc1/Miapaca2 groups, the cells were cultured with half normal medium and half CM from Panc1/Miapaca2 cell lines. CD25 and CD127 antibodies were used for classifying Tregs of $CD4^+$ T cells.

The population of Tregs in $CD4^+$ T cells detected by FACS was 3.50% in the CON (HD) group and 3.88% in the EXP (+CM)-Panc1 group. The numbers in the CON (HD) and EXP (+CM)-Miapca2 groups were 4.09% and 4.35%, respectively. The differences between the control and experimental groups were not statically significant (P>0.05, Figure 7).

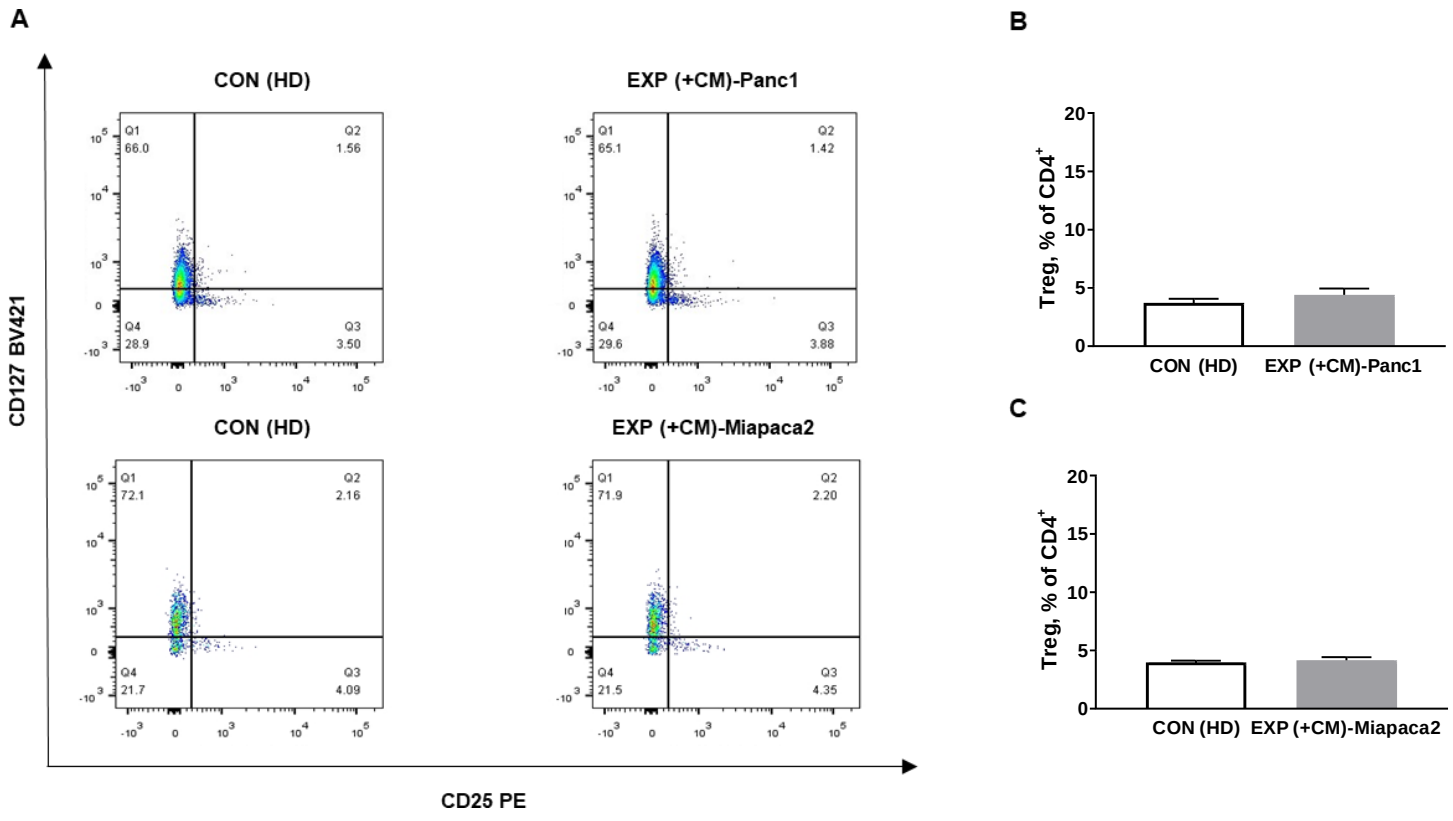

Figure 7: (A): Representative FACS plot of Tregs in the CON (HD) and EXP (+CM)-Panc1/Miapaca2 groups. (B)(C): The differentiation of $CD4^+$ Tregs between control and experimental groups has no statistical significance (P>0.05).

3.2.3 No effects on IFN-γ expression in PBMCs (HD) after culturing with CM (Panc1/Miapaca2)

The CON (HD) group and the EXP (+CM)-Panc1/Miapaca2 group were set as above. The production of $CD45^+$, $CD4^+$, and $CD8^+$ IFN-γ were almost unobservable in FACS plots of the experimental groups and the matched control groups (Figure 8).

After adding the LAC to the medium of PBMCs and 3h incubation, the production of IFN-γ was increased and could be detected by FACS. The population of $CD45^+$ IFN-γ in the CON (HD) +LAC and EXP (+CM)-Panc1 +LAC groups was 14.90% and 15.50%, of $CD4^+$ IFN-γ was 12.50% and 13.20%, and of $CD8^+$ IFN-γ was 27.30% and 27.90%, respectively. However, statistical changes between these two groups for the IFN-γ production were not significant ($P>0.05$, Figure 8 A, B). This phenomenon was also seen in the CON (HD) +LAC and EXP (+CM)-Miapaca2 +LAC groups. The population of $CD45^+$ IFN-γ in these two groups was 12.00% and 13.60%, of $CD4^+$ IFN-γ was 8.48% and 9.10%, and of $CD8^+$ IFN-γ was 19.80% and 20.00%, respectively ($P>0.05$, Figure 8 C, D).

In summary, the exchange of soluble factors in indirect co-culture of PBMC (HD) and CM from human pancreatic cancer cell lines (Panc1/Miapaca2) failed to promote T cell differentiation and activation in PBMCs (HD).

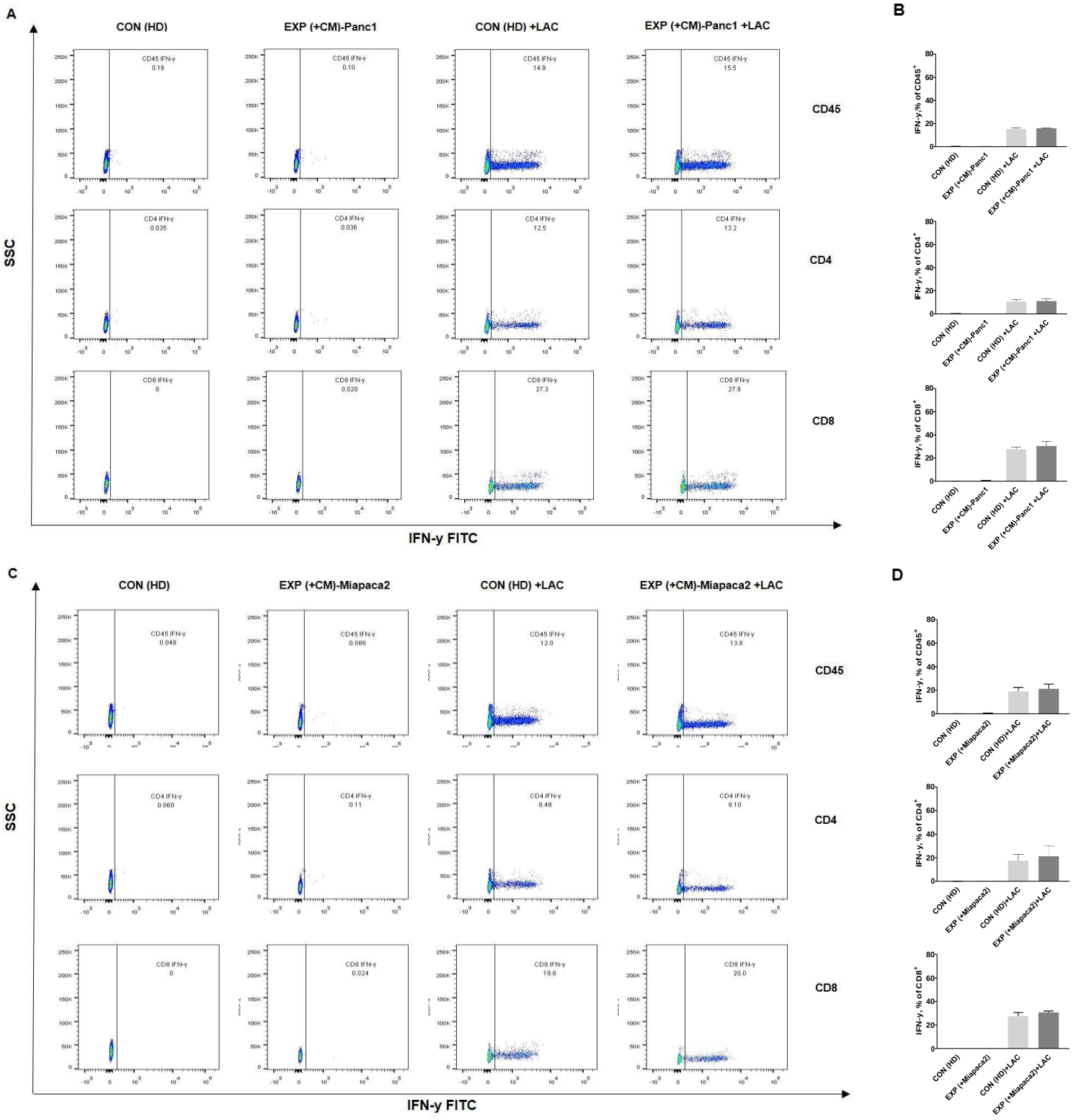

Figure 8: (A)(C): Representative FACS plot of IFN-γ production in the CON (HD), EXP (+CM)-Panc1/Miapaca2, CON (HD) +LAC, and EXP (+CM)-Panc1/Miapca2 +LAC groups; (B)(D): The production of $CD45^+$, $CD4^+$, and $CD8^+$ IFN-γ between the CON (HD) +LAC, and EXP (+CM)-Panc1/Miapca2 +LAC groups has no statistical significances (P>0.05).

3.3 The co-culture model establishment with PBMCs (HD) and pancreatic cancer cell lines

According to the results above, the CM seemed not sufficient to stimulate the differentiation of immune cells. So we decided to directly co-culture PBMCs with Panc1/Miapaca2 cells in the EXP (+Panc1)/(+Miapaca2) groups for 48h, and in the CON (HD) groups PBMCs were cultured only with the normal medium (RPMI1640+10%FBS+1%P/S) as controls. The differentiation characterization of T cell subtypes was recorded in both control and experimental groups.

3.3.1 The population of $CD4^+$Tcm and $CD8^+$Tem cells in PBMCs (HD) was increased after co-culturing with the Panc1 cell line

After co-culturing PBMCs (HD) with Panc1 cells, we observed that the population of $CD4^+$ Tcm cells in the EXP (+Panc1) group was 28.70%, which was higher than that in the CON (HD) group (18.70%), with a P-value of 0.04 (Figure 9); While the population of $CD4^+$ Tem cells in the EXP (+Panc1) and CON (HD) groups was 11.20% and 11.40% and $CD4^+$ Teff cells were detected in 0.70% and 1.20%, respectively, with no significant changes. As for the CD4+ Tnaiv cells, although the population of this cell type was reduced in the co-culture group (59.40%) compared to the control group (68.70%), the statistical analysis between the two groups was also not significant (P>0.05, Fig. 9 A, B).

In the EXP (+Miapaca2) group with co-culture of PBMCs (HD) and Miapaca2, the population of $CD4^+$ Tem, Tcm, Teff and Tnaiv was 16.90%, 19.20%, 2.83% and 61.30%, respectively, and these numbers in the CON (HD) group were 14.00%, 18.30%, 1.77% and 65.90%, respectively. Therefore, Miapaca2 cells had no significant effect on the stimulation of Memory CD4+ T cell differentiation in PBMCs. (P>0.05, Figure 9 A, C).

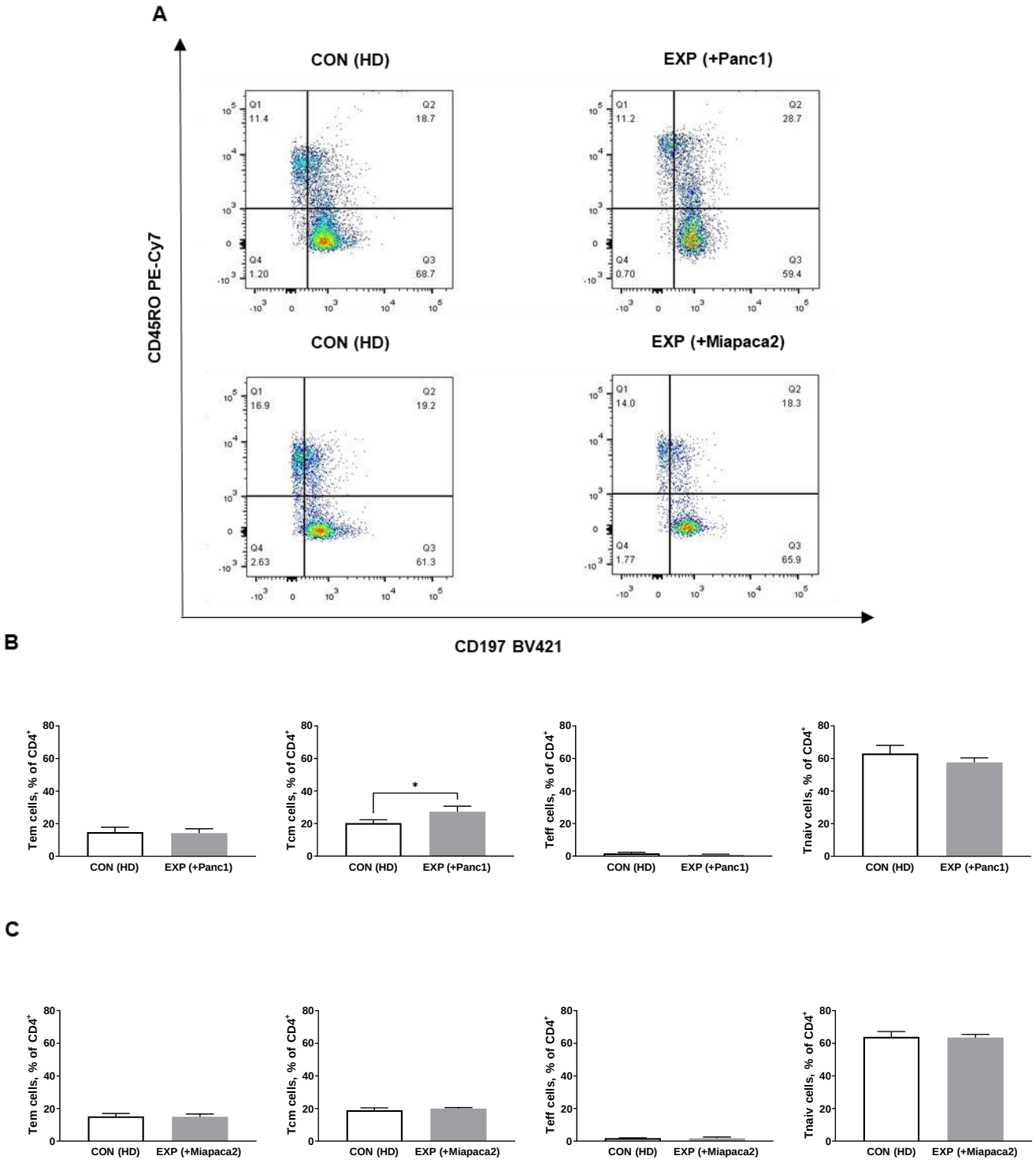

Figure 9: (A): Representative FACS plots of Memory $CD4^+$ T cell subsets in the CON (HD) and EXP (+Panc1)/ (+Miapaca2) groups. (B): There was a statistically significant difference in the population of $CD4^+$ Tcm cells between the CON (HD) and EXP (+Panc1) group (*P<0.05), however, those changes in $CD4^+$ Tem, $CD4^+$ Teff, and $CD4^+$ Tnaiv cells were not statistically significant (P>0.05). (C): There were no statistically significant differences between the CON (HD) and EXP (+Miapca2) groups (P>0.05).

In contrast, we noted that the population of $CD8^+$ Tem cells in the EXP (+Panc1) group was higher than that in the CON (HD) group (18.83% vs.13.83%). This difference was considered to be statistically significant (P = 0.046). For $CD8^+$ Tcm, Teff, and Tnaiv cells, as the numbers in the EXP (+Panc1) group were 6.60%, 10.60%, and 61.70%, respectively, and in the CON (HD) group, were 6.15%, 14.60%, and 64.40%, respectively. There were no significant changes in these three cell populations between the control and experimental groups (P>0.05, Figure 10 A, B).

However, the population of $CD8^+$ Tem, Tcm, Teff, and Tnaiv cells in the EXP (+Miapaca2) group was 14.40%, 5.56%, 14.80%, and 65.20%, respectively, with little differences compared to those in the CON (HD) group of 13.20%, 5.89%, 14.30%, and 66.60%, respectively (P>0.05, Figure 10 A, C).

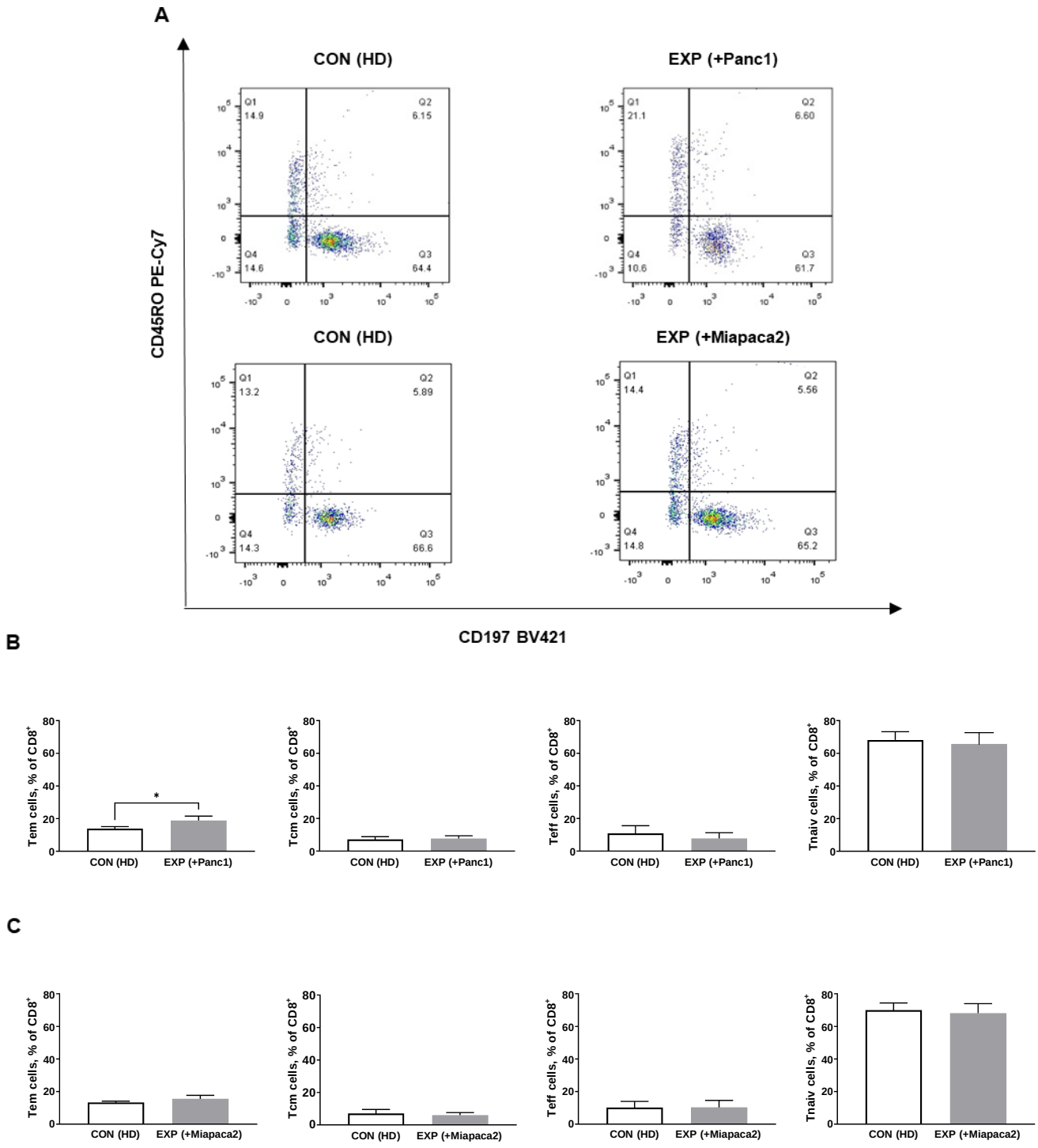

Figure 10: (A): Representative FACS plot of Memory $CD8^+$ T cell subsets in the CON (HD) and EXP (+Panc1)/ (+Miapaca2) groups. (B): There was a statistically significant difference in the population of $CD8^+$ Tem cells between the CON (HD) and EXP (+Panc1) group (*P<0.05), however, those differences of $CD8^+$ Tcm, $CD8^+$ Teff, and $CD8^+$ Tnaiv cells between these two groups were not statistically significant (P>0.05). (C): There were no statistically significant differences between the CON (HD) and EXP (+Miapca2) groups (P>0.05).

3.3.2 The population of Tregs in PBMCs (HD) was increased after co-culturing with Panc1 cell lines

The population of Tregs in the CON (HD) group and EXP (+Panc1) group was 3.28% and 7.40%, respectively. In contrast with the controls, the differentiation of Tregs in the co-culture group was significantly enhanced, with a P-value of 0.01 (Figure 11 A, B).

But the numbers of Tregs in the CON (HD) group and EXP (+Miapaca2) group were 4.04% and 5.07%, respectively. The differences between these two groups were not statistically significant (P>0.05, Figure 11 A, C).

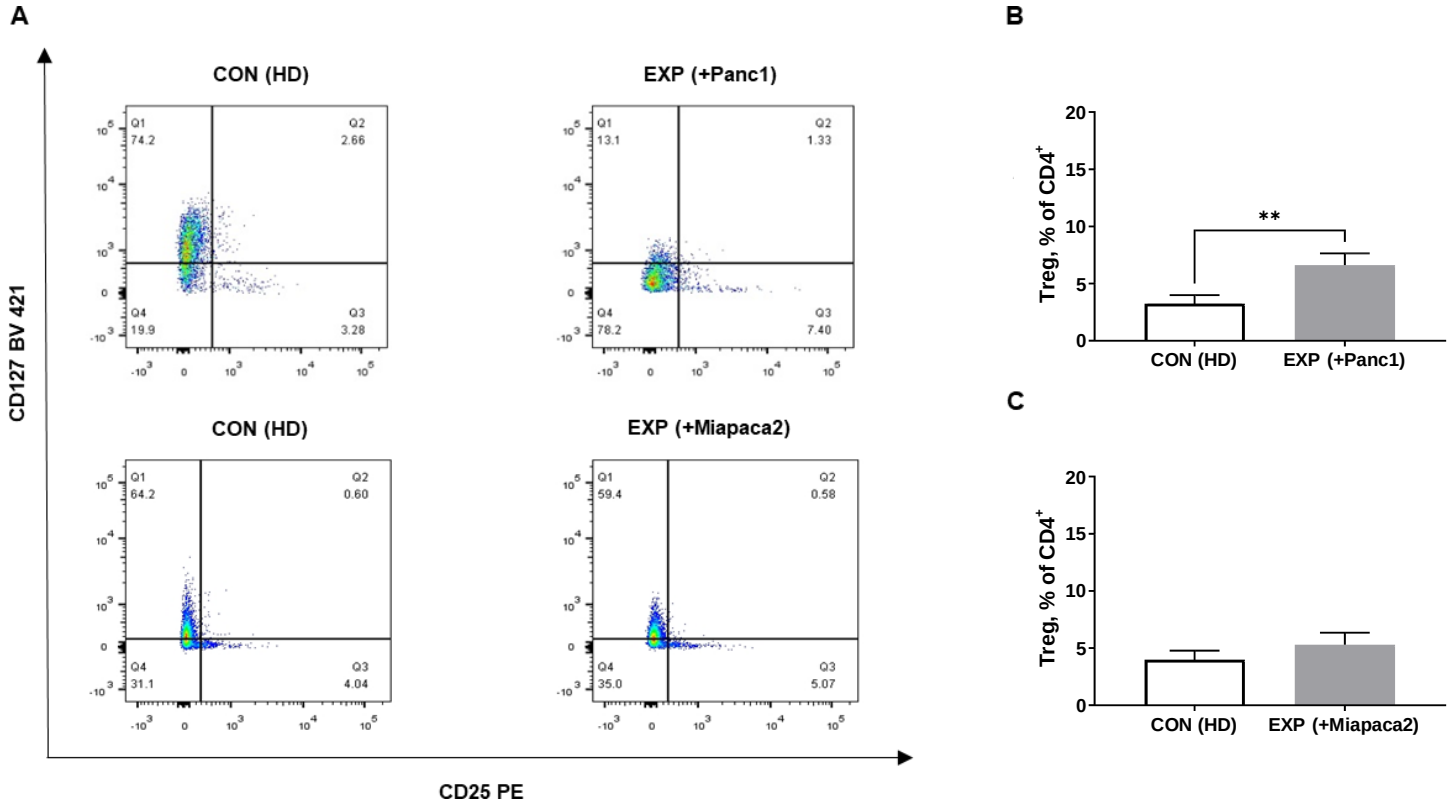

Figure11: (A): Representative FACS plot of Tregs in the CON (HD) and EXP (+Panc1)/ (Miapaca2) groups. (B): The population of $CD4^+$ Tregs in the EXP (+Panc1) group was higher than that in the CON (HD) group (**P<0.01). (C): The difference between $CD4^+$ Tregs in the CON (HD) and EXP (+Miapca2) groups was not statistically significant (P>0.05).

3.3.3 No effects on IFN-γ stimulation in PBMCs (HD) after co-culturing with Panc1/Miapaca2 cell lines

Similar to the results of PBMCs cultured with CM, we still did not see $CD45^+$, $CD4^+$ and $CD8^+$ T cells producing IFN-γ in both CON (HD) and EXP (+Panc1) groups, as well as in the CON (HD) and EXP (+Miapaca2) groups (Figure 12).

LAC was applied for improving IFN-γ production. The numbers of $CD45^+$, $CD4^+$, and $CD8^+$ T cells IFN-γ stimulated by LAC in the CON (HD) group were 22.40%, 18.00%, and 25.80%, respectively. These were not statistically correlated with the results of the EXP (+Panc1) +LAC co-culture group, with the corresponding numbers of 22.80%, 20.10%, and 26.50%, respectively ($P>0.05$, Figure 12 A, B).

After co-culturing PBMCs (HD) with the Miapaca2 cell line and LAC in the EXP (+Miapaca2) +LAC group, the population of IFN-γ of $CD45^+$, $CD4^+$, and $CD8^+$ T cells was 21.30%, 15.00%, and 31.60%, respectively, which had no significant changes to that in the positive control group with populations of 17.70%, 13.40%, and 29.70%, respectively ($P>0.05$, Figure 12 C, D).

In this section, we found that the proportion of $CD4^+$ Tcm, $CD8^+$ Tem, and Treg cells was increased significantly when co-cultured PBMCs (HD) with Panc1 cells, compared to the controls. However, these were not confirmed in the co-culture group with Miapaca2.

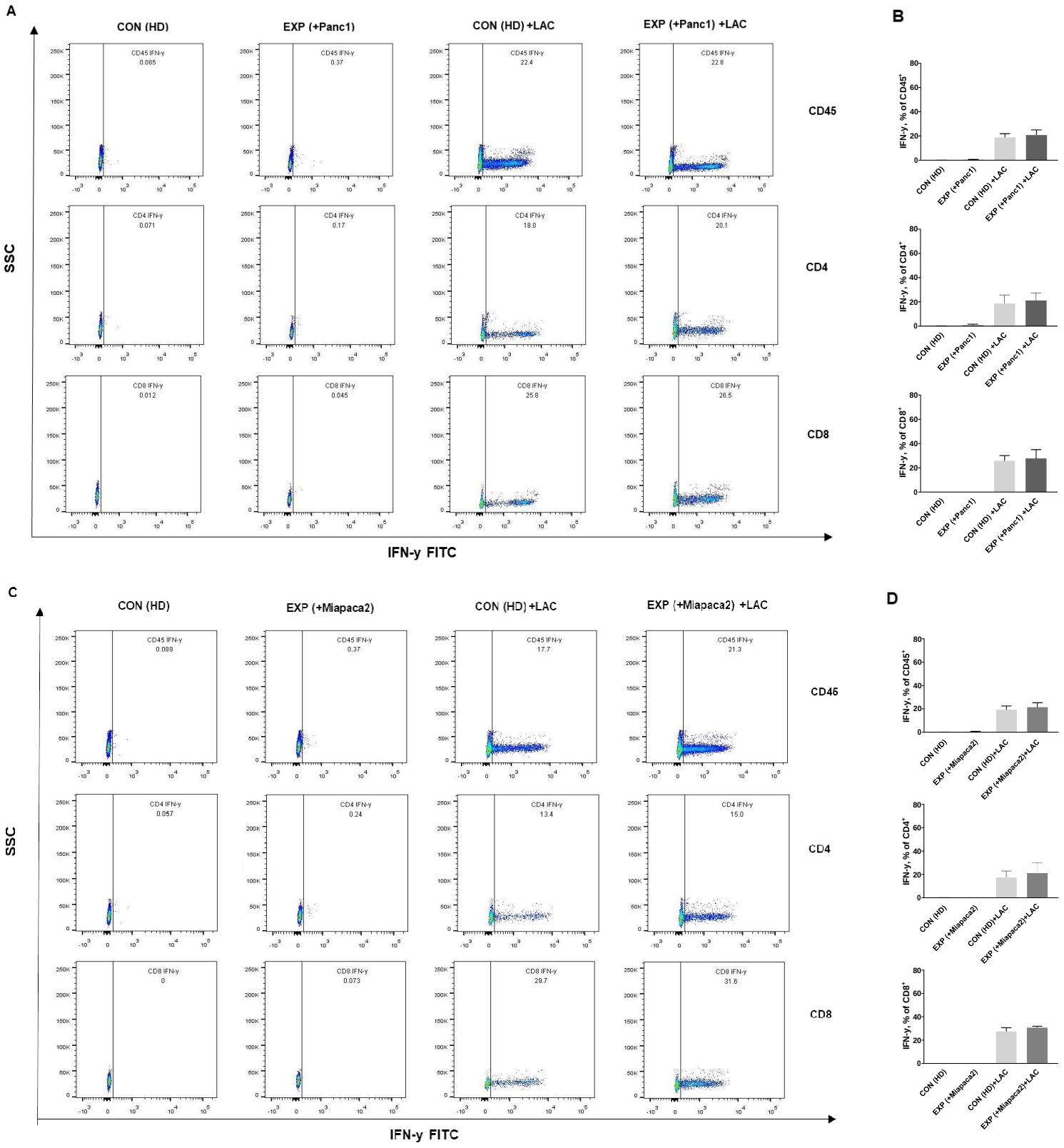

Figure 12: (A)(C): Representative FACS plot of IFN-γ production in the CON (HD), EXP(+Panc1)/(+Miapaca2), CON (HD) +LAC, and EXP (+Panc1)/(+Miapaca2) +LAC groups. (B)(D): The production of $CD45^+$, $CD4^+$, and $CD8^+$ IFN-γ between the CON (HD) +LAC and EXP (+Panc1)/ (+Miapaca2) +LAC groups has no statistical significance (P>0.05).

3.4 The characterization of T cell differentiation and IFN-γ production in PBMCs of HD and PDAC patients.

In contrast to healthy people, the differentiation of various immune cell subpopulations in PBMCs of PDAC patients has been altered during disease progression [3, 18]. Here, we compared T cell differentiation and IFN-γ production in PBMCs of HD (PBMC (HD) group) and PDAC patients (PBMC (P) group).

3.4.1 The differences in the Memory T cell differentiation between the PBMCs of HD and PDAC patients

Of $CD4^+$ Memory T cells, the Tem population raised from 17.90% in the PBMC (HD) group to 33.80% in the PBMC (P) group ($P<0.01$), the Tcm increased from 20.80% to 26.70% ($P<0.01$), and the Teff increased from 2.73% to 14.00% ($P<0.001$), but the Tnaiv population dropped sharply from 58.50% to 25.50% ($P<0.001$). The results were shown in Figure 13.

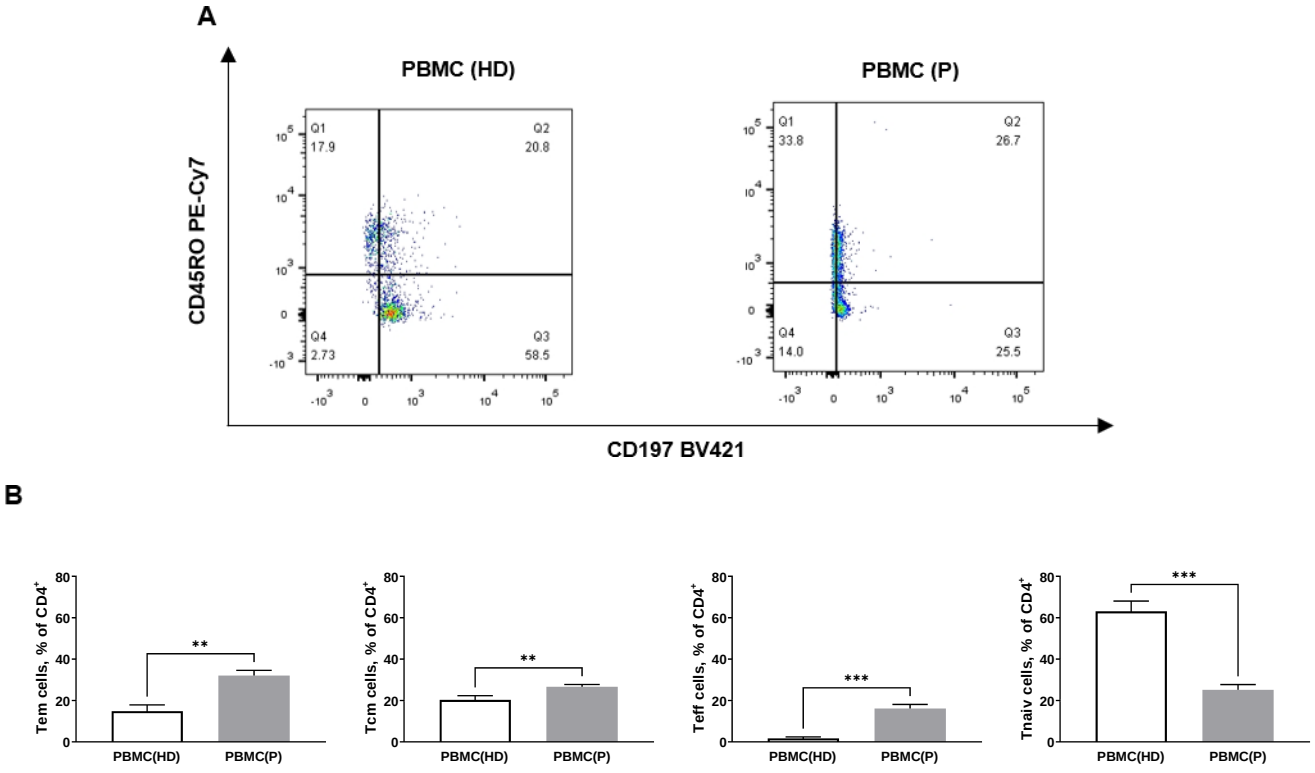

Figure 13: (A): Representative FACS plots of Memory $CD4^+$ T cell subsets in the PBMC (HD) and PBMC (P) groups. (B): Compared to the PBMC (HD) group, the population of $CD4^+$ Tem, Tcm, and Teff cells was increased in the PBMC (P) group (**P<0.01, **P<0.01, and ***P<0.001, respectively), while of $CD4^+$ Tnaiv cells was significantly decreased (***P<0.001),.

Simultaneously, the population of $CD8^+$ Tem, Tcm, and Teff cells in the PBMC (P) group was detected as 23.30%, 11.40%, and 38.60%, respectively, higher than those in the PBMC (HD) group, which were 14.20%, 6.45%, and 5.59%, with the P-values all below 0.05. On the contrary, the population of $CD8^+$ Tnaiv in the experiment group was 26.80%, showing a clear downward trend compared to 73.80% in the control group (P<0.001, Figure 14).

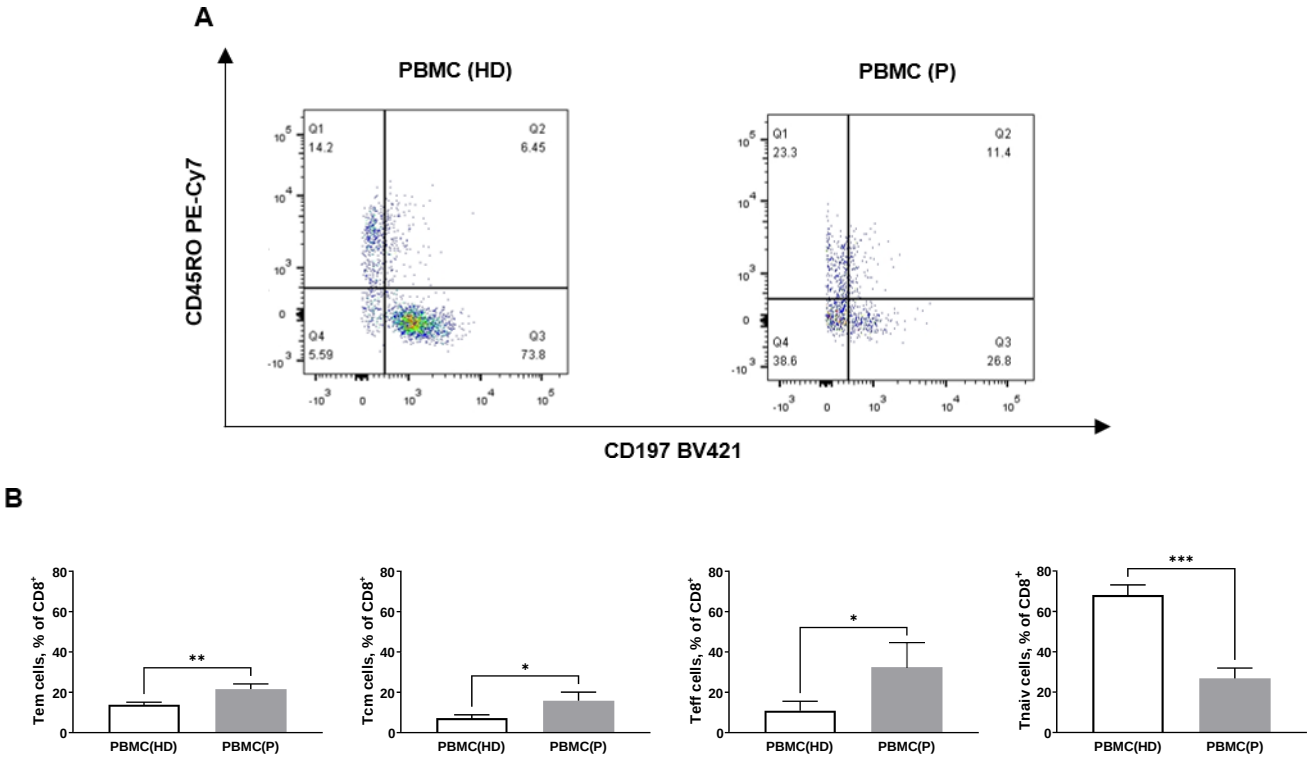

Figure 14: (A): Representative FACS plots of Memory $CD8^+$ T cell subsets in the PBMC (HD) and PBMC (P) groups. (B): Compared to the PBMC (HD) group, the population of $CD8^+$ Tem, Tcm, and Teff cells was increased in patients' PBMCs (**P<0.01, *P<0.05, and *P<0.05, respectively), while $CD8^+$ Tnaiv cells was significantly decreased (***P<0.001).

3.4.2 The Treg population was increased in PBMCs of PDAC patients compare to that in healthy PBMCs

Tregs are immunosuppressive cells. The population of Tregs in PBMCs of PDAC patients was 5.09%, which was higher than 3.50% in healthy PBMCs ($P<0.05$, Figure 15).

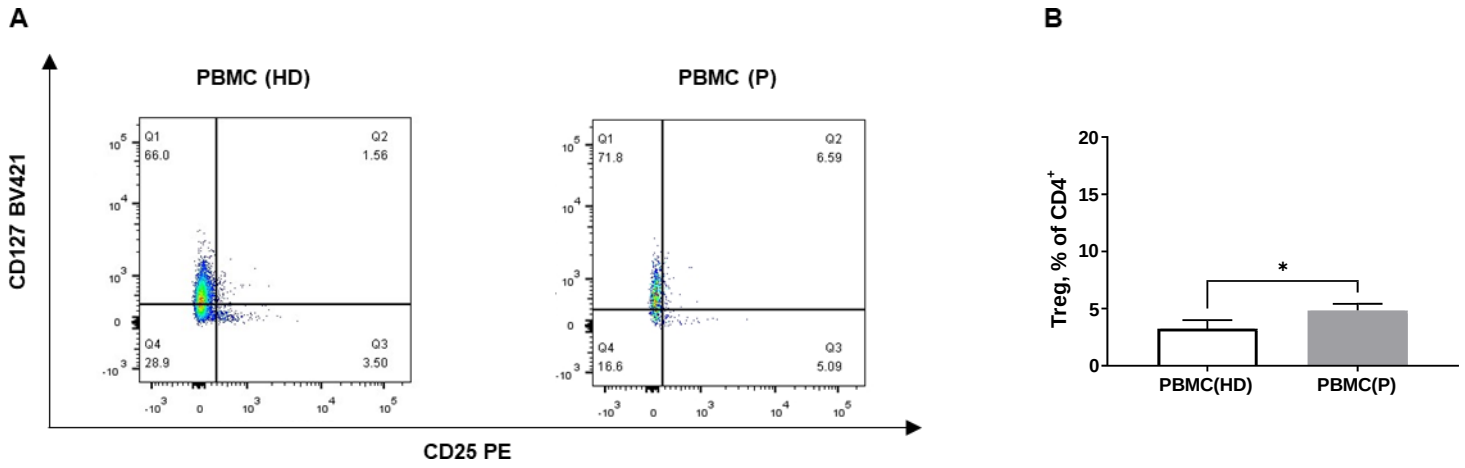

Figure15: (A): Representative FACS plot of Tregs in the PBMC (HD) and PBMC (P) groups. (B): The Treg population of $CD4^+$ T cells in the PBMC (P) group was higher than that in the PBMC (HD) group (*$P<0.05$).

3.4.3 The $CD8^+$ IFN-γ production in PBMCs of PDAC patients was higher than in healthy PBMCs

In both PBMC (HD) and PBMC (P) groups, we could hardly observe the population of IFN-γ from $CD45^+$, $CD4^+$, and $CD8^+$ cells (Figure 16). The addition of LAC in the culture medium of PBMCs stimulated the IFN-γ production. There were no apparent changes in $CD45^+$ and $CD4^+$ IFN-γ production between the PBMC (HD) +LAC group and PBMC (P) +LAC group. However, a noticeable increase was displayed in $CD8^+$ IFN-γ production of the experimental group with a number of 32.40%, compared to 27.40% in the positive control group (*$P<0.05$, Figure 16).

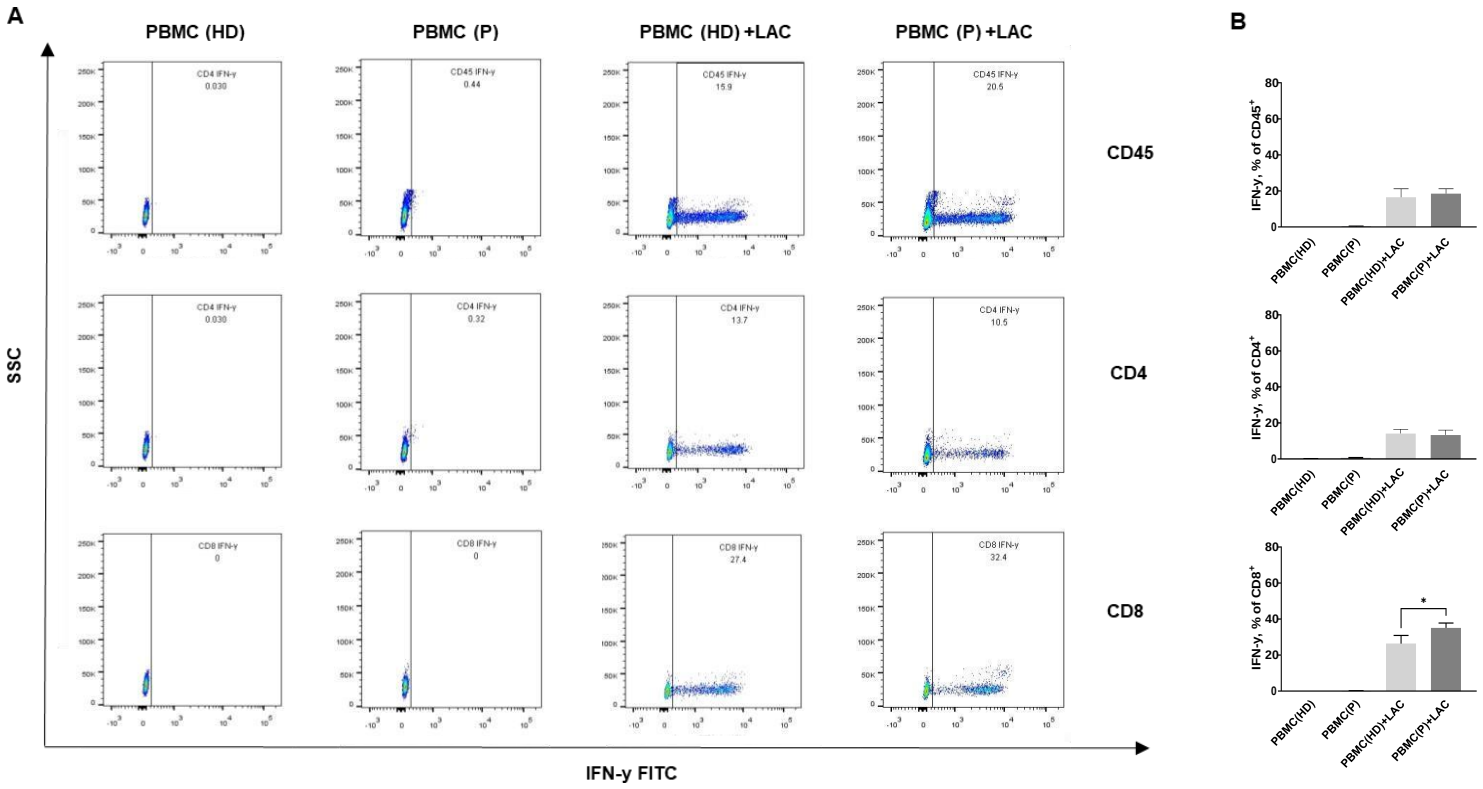

Figure 16: (A): Representative FACS plot of IFN-γ production in the PBMC (HD), PBMC (P), PBMC (HD) +LAC, and PBMC (P) +LAC groups. (B): The production of $CD45^+$, $CD4^+$ IFN-γ between the PBMC (HD) +LAC and PBMC (P) +LAC groups has no statistical significance ($P>0.05$). However, the $CD8^+$ IFN-γ production in the PBMC (P) +LAC group was higher than that in the PBMC (HD) +LAC group ($*P<0.05$).

Generally speaking, the majority of Naïve T cells in PBMCs of PDAC patients had been differentiated into Memory T cells and Effector T cells, and the number of Treg cells was also higher. At the same time, we also detected increased IFN-γ production in $CD8^+$ T cells from these patients.

3.5 The co-culture model establishment with PBMCs from PDAC patients and the Panc1 cell line

From previous results, we discovered that only Panc1 cells induced the variations in Memory T cell subtypes and Tregs, implying that the TME formed by different cell lines could affect the differentiation direction of immune cells.

Hereafter, we co-cultured patients' PBMCs with Panc1 and analyzed the

differentiation of immune cell subtypes, obtaining some interesting results that differ from Section 3.2.1. In the CON (P) group, the PBMCs from patients were cultured alone in the normal medium (RPMI1640+10%FBS+1%P/S), while in the EXP (+Panc1) group, the PBMCs were co-cultured with Panc1.

3.5.1 The population of $CD4^+$/$CD8^+$ Memory T cells in PBMCs from PDAC patients was changed after co-culturing with Panc1

The population of $CD4^+$ Tcm cells in the CON (P) group was 26.70%, but when patients' PBMCs were co-cultured with Panc1, this number increased to 48.80%, with a P-value of 0.013 analyzed from replicated FACS experiments. This action was also found in Section 3.2.1. More importantly, the $CD4^+$ Tem and Teff populations in the EXP (+Panc1) group (16.60% and 6.27%, respectively) were both lower than those in the CON (P) group (33.80% and 14.00%, respectively), with the P-values of 0.001 and 0.016, respectively. However, the population of $CD4^+$ Tnaiv cells in PBMCs cultured with Panc1 showed a number of 28.30%, which was not significantly raised compared to those cultured alone (25.50%). These results can be seen in Figure17.

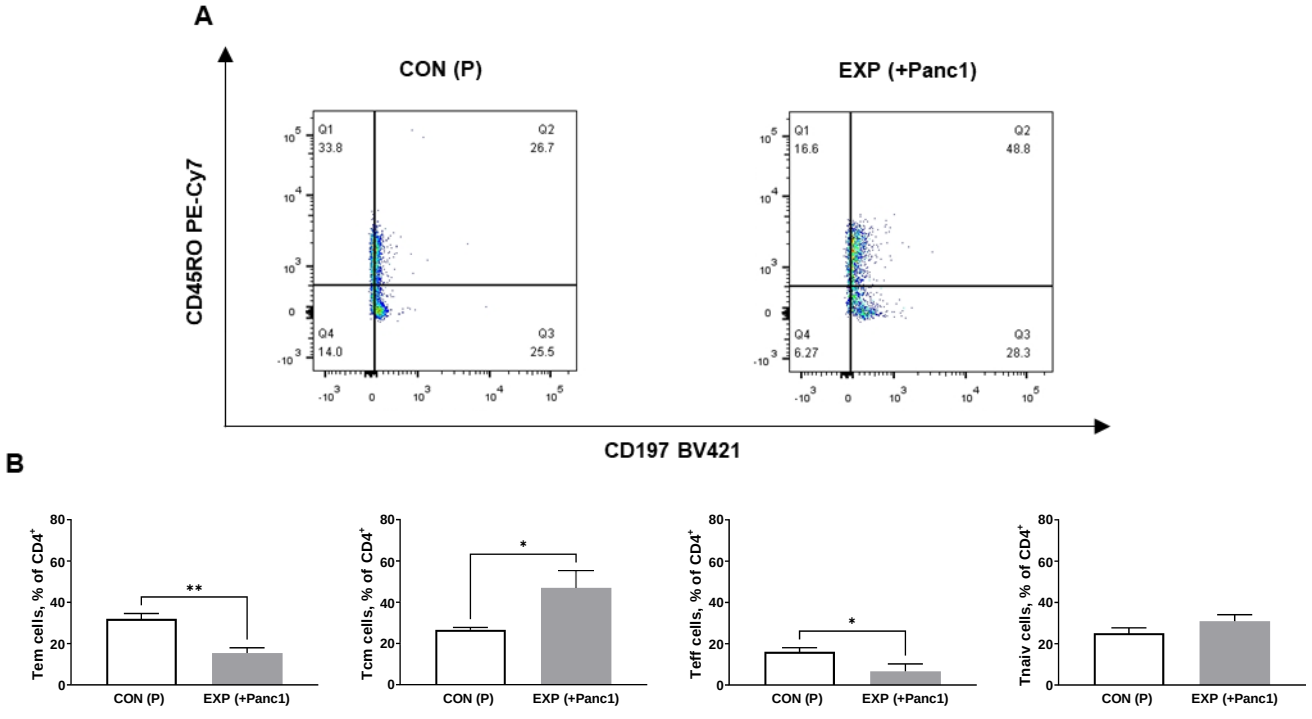

Figure 17: (A): Representative FACS plot of different Memory $CD4^+$ T cell subsets in the CON (P) and EXP (+Panc1) groups. (B): The population of $CD4^+$ Tcm cells was higher, while $CD4^+$ Tem and Teff cells were lower in the EXP (+Panc1) group than that in the CON (P) group (**P<0.01, *P<0.05, and *P<0.05). However, the difference in $CD4^+$ Tnaiv cells between these two groups was considered not statically significant (P=0.07).

Next, we also analyzed the differentiation of $CD8^+$ Memory T cell subtypes in the CON (P) and EXP (+Panc1) groups. The population of $CD8^+$ Tem cells in the co-culture group (8.46%) was significantly lower than that in the control group (23.30%) with a P-value of 0.002. Conversely, the population of $CD8^+$ Tnaiv cells in the EXP (+Panc1) was higher than that in the CON (P) group, with numbers of 48.20% and 26.80%, respectively (P<0.01). Moreover, there was a decline in the $CD8^+$ Teff population and an ascent of the $CD8^+$ Tcm population in the EXP (+Panc1) compared with that in the CON (P) group. But these results were deemed not statistically significant after repeated experiments (Figure 18).

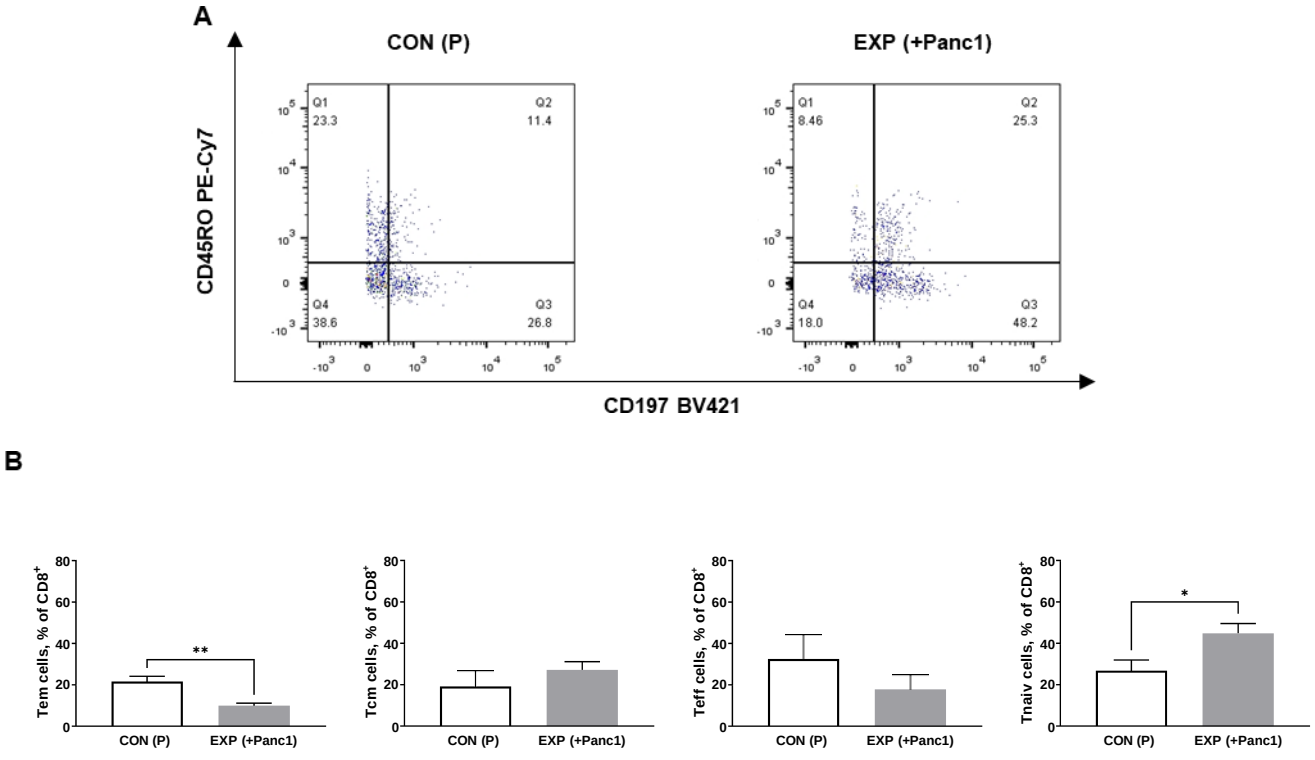

Figure 18: (A): Representative FACS plot of Memory $CD8^+$ T cell subsets in the CON (P) and EXP (+Panc1) groups (B): The population of $CD8^+$ Tem was lower, while Tnaive was higher in the EXP (+Panc1) group than in the CON (P) group (**P<0.01 and*P<0.05). But the difference of $CD8^+$ Tcm and Teff between these two groups was not statistically significant (P>0.05).

3.5.2 No effects on Tregs in PDAC patient PBMCs after co-culturing with Panc1

The population of Tregs in the CON (P) and EXP (+Panc1) groups was 5.09% and 5.59%, respectively, displaying no statistically significant difference (P>0.05, Figure 19).

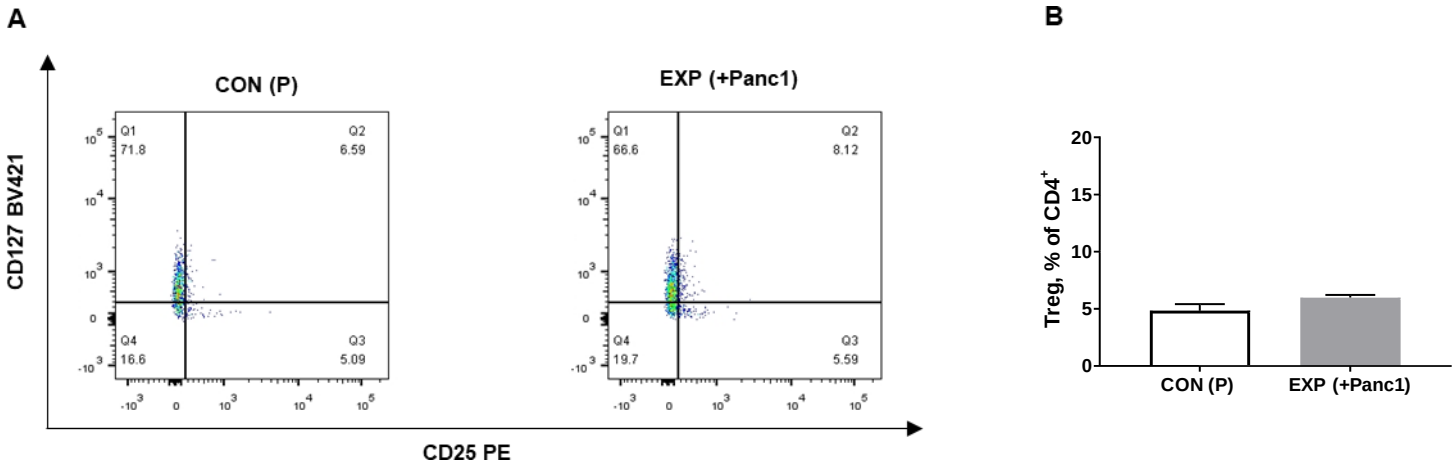

Figure 19: (A): Representative FACS plot of Treg population in the CON (P) and EXP (+Panc1) group. (B): The difference in Treg populations between the two groups was not significant (P>0.05).

3.5.3 No effects on the production of IFN-γ in PBMCs after co-culturing with Panc1

In the CON (P) and EXP (+Panc1) groups, the production of $CD45^+$, $CD4^+$, and $CD8^+$ IFN-γ could not be detected by FACS without adding LAC (Figure 20).

In the CON (P) +LAC and EXP (+Panc1) +LAC groups, the population of $CD45^+$ IFN-γ was 20.50% and 21.30%, of $CD4^+$ IFN-γ was 10.50% and 12.70%, and of $CD8^+$ IFN-γ was 32.40% and 35.30%, respectively. After

statistical analysis, there was no significant difference in IFN-γ production between the control group and the experimental group (P>0.05, Figure 20).

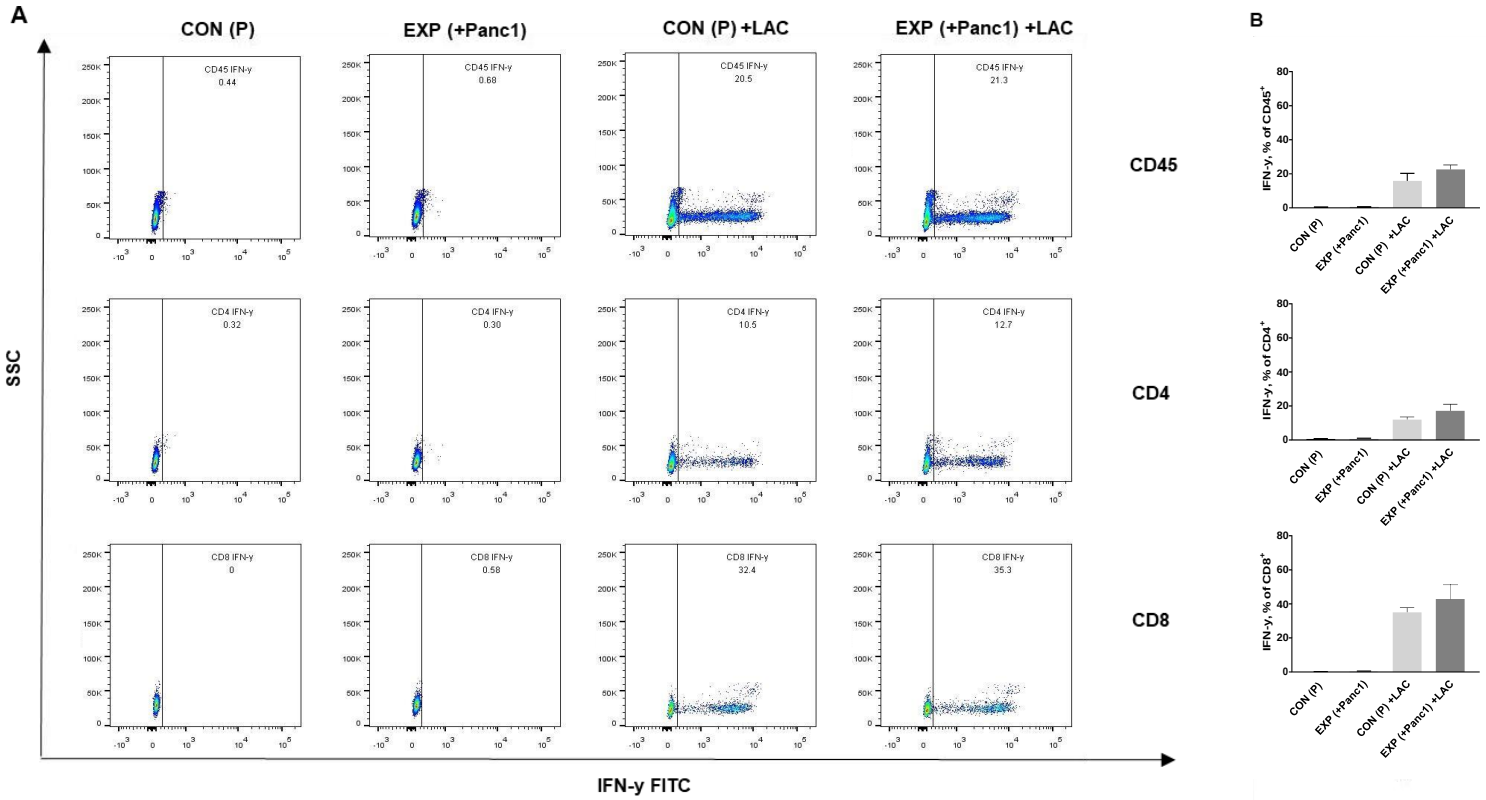

Figure 20: (A): Representative FACS plot of IFN-γ production in the CON (P), EXP (+Panc1), CON (P) +LAC, and EXP (+Panc1) +LAC groups. (B): The production of $CD45^+$, $CD4^+$, and $CD8^+$ IFN-γ between the CON (P) +LAC group and the EXP (+Panc1) +LAC group has no statistical significance (P>0.05).

Anyhow, when co-cultured PBMCs from PDAC patients with Panc1, the proportion of $CD4^+$ Tcm and $CD8^+$ Tnaiv cells were increased, and $CD4^+$ Tem, $CD4^+$ Teff, and $CD8^+$ Tem cells were decreased, but the Treg cell population and IFN-γ production had no significant changes.

3.6 The establishment of co-culture with HD PBMCs and PDAC patient-derived organoid lines

Given the results identified in co-cultures with PBMCs and 2D cell lines, we proceeded to apply this protocol to co-culture with PBMCs and 3D organoids in

direct contact, also examining the alterations of immune cell differentiation and cytokine stimulation. In this part, PBMCs isolated from one HD and three organoid lines from Patient 2, 3, and 7 were employed to determine co-culture conditions. We also investigated differentiation characteristics of Memory T cell subtypes and Tregs, as well as the production of IFN-γ.

The CON (HD) was the control group with PBMCs cultured alone in the organoid complete medium, and the EXP (+Org) was the experimental group in which PBMCs were co-cultured with different organoid lines under the same culture conditions.

3.6.1 The population of $CD4^+/CD8^+$ Memory T cells was changed in PBMCs after co-culturing with organoid lines

The population of $CD4^+$ Tem cells in the CON (HD) and EXP (+Org) groups was 31.10% and 22.90%, respectively, expressing a significant reduction (P=0.03); while the $CD4^+$ Tcm population in the co-culture group was with 34.80% higher than 26.40% in the control group (P=0.04). But the discrepancy of $CD4^+$ Teff and Tnaiv differentiation in these two groups expressed not statistically significant (P>0.05). These results were shown in Figure 21.

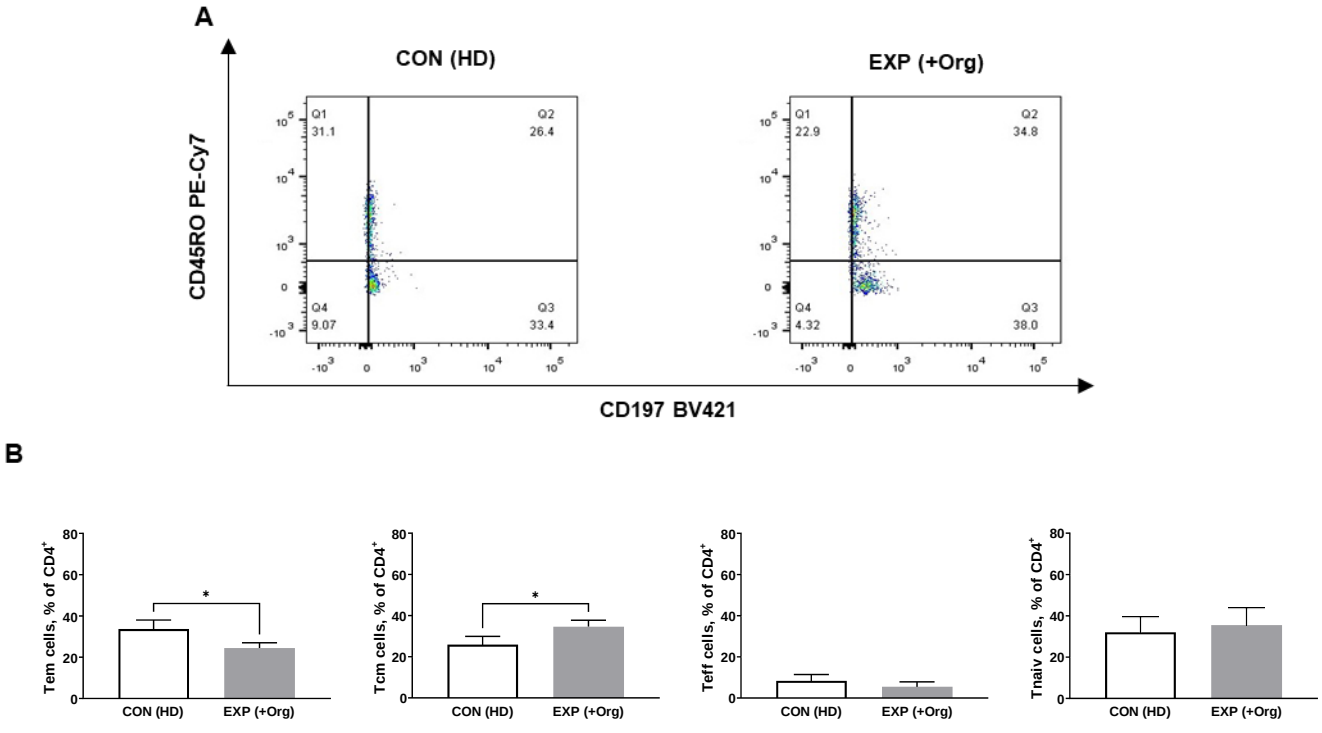

Figure 21: (A): Representative FACS plot of Memory $CD4^+$ T cell subsets in the CON (HD) and EXP (+Org) groups. (B): The population of $CD4^+$ Tcm cells was higher, while $CD4^+$ Tem cells were lower in the EXP (+Panc1) group than CON (P) group (*P<0.01, *P<0.05). However, the differences in $CD4^+$ Teff and Tnaiv populations between these two groups were not significant (P>0.05).

After analyzing the differentiation of $CD8^+$ Memory T cells, we found that the $CD8^+$ Tem population was higher, and the $CD8^+$ Tnaiv population was lower in the EXP (+Org) group (21.00% and 33.00%, respectively) than that in the CON (HD) group (10.70% and 46.70%, respectively). However, no differences were seen in $CD8^+$ Tcm and Teff population between these two groups (P>0.05, Figure 22).

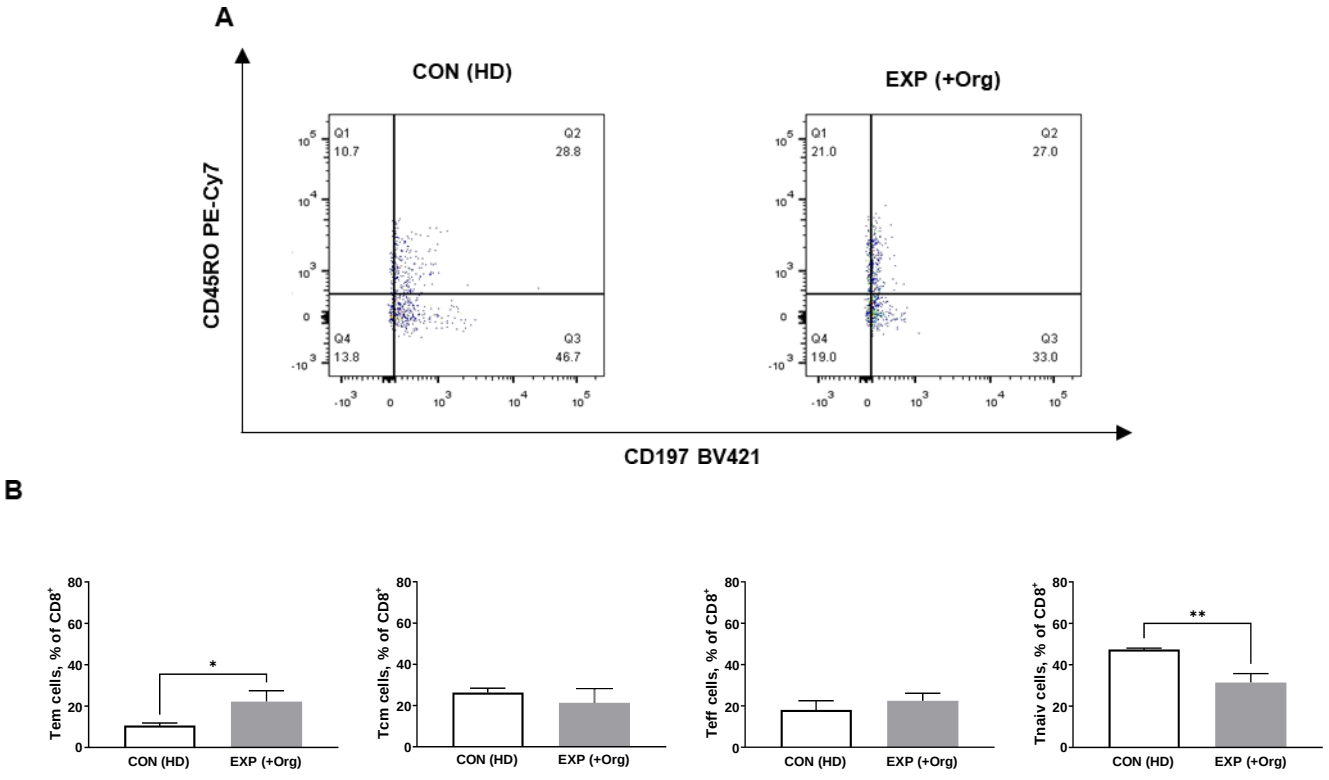

Figure 22: (A): Representative FACS plot of different Memory $CD8^+$ T cell subsets in the CON (HD) and EXP (+Org) groups. (B): The population of $CD8^+$ Tem cells was higher, and of $CD8^+$ Tnaiv cells was lower in the EXP (+Panc1) group than CON (P) group (*P<0.05, **P<0.01). However, the difference of $CD8^+$ Tcm and Teff populations between these two groups was not significant (P>0.05).

3.6.2 The population of Tregs was increased in PBMCs from HD after co-culturing with organoid lines

After co-culturing PBMCs (HD) with 3D organoids, the differentiation of Tregs from $CD4^+$ T cells was significantly increased compared to those cells cultured alone. The population of Tregs in the EXP (+Org) group was 9.45%, and in CON (HD) was 5.12% (P<0.001, Figure 23). This consequence was equal to that in the co-cultures with PBMCs (HD) and Panc1 cell lines.

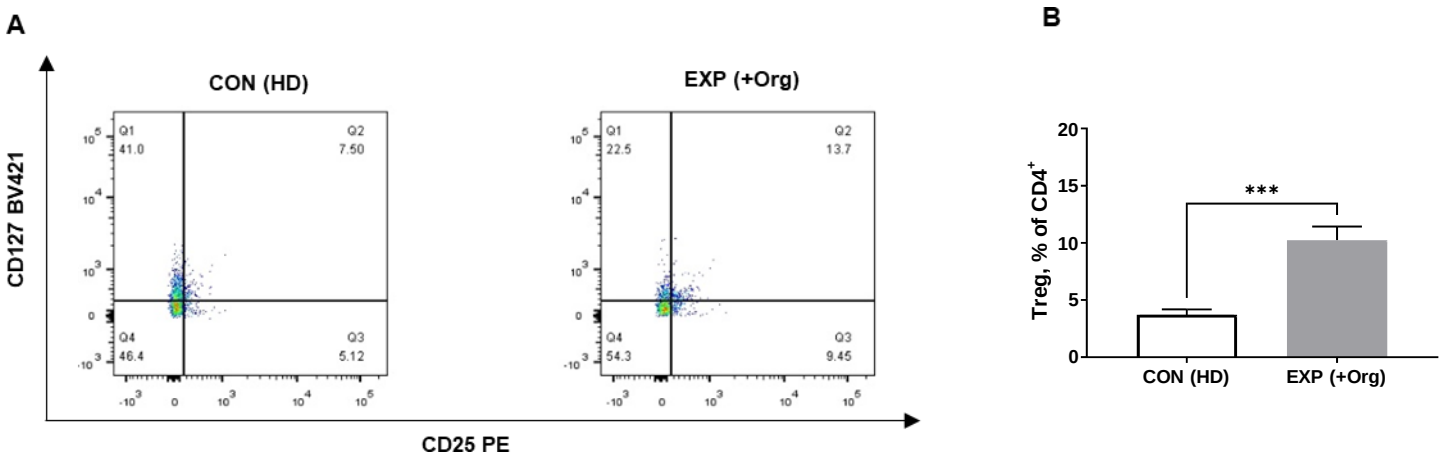

Figure 23: (A): Representative FACS plot of Tregs in the CON (HD) and EXP (+Org) groups. (B): The Treg population in the EXP (+Org) group was higher than that in the CON (HD) group (**P<0.001).

3.6.3 No effects on the production of IFN-γ in PBMCs from HD after co-culturing with organoid lines

Without additional LAC supplementation, the IFN-γ stimulation of $CD45^+$, $CD4^+$ or $CD8^+$ cells was still barely detectable in the CON (HD) and EXP (+Org) groups, while in the CON (HD) +LAC group, we observed IFN-γ production of 14.00%, 8.32% and 21.70% for $CD45^+$, $CD4^+$, and $CD8^+$ cells, respectively, and in the EXP (+Org) +LAC group, these numbers were 15.90%, 8.96%, and 30.50%, respectively. It seemed that the production of IFN-γ in $CD8^+$ T cells was increased after co-culturing PBMCs with organoid lines, but the statistical analysis showed no statistical significant differences (P>0.05, Figure 24).

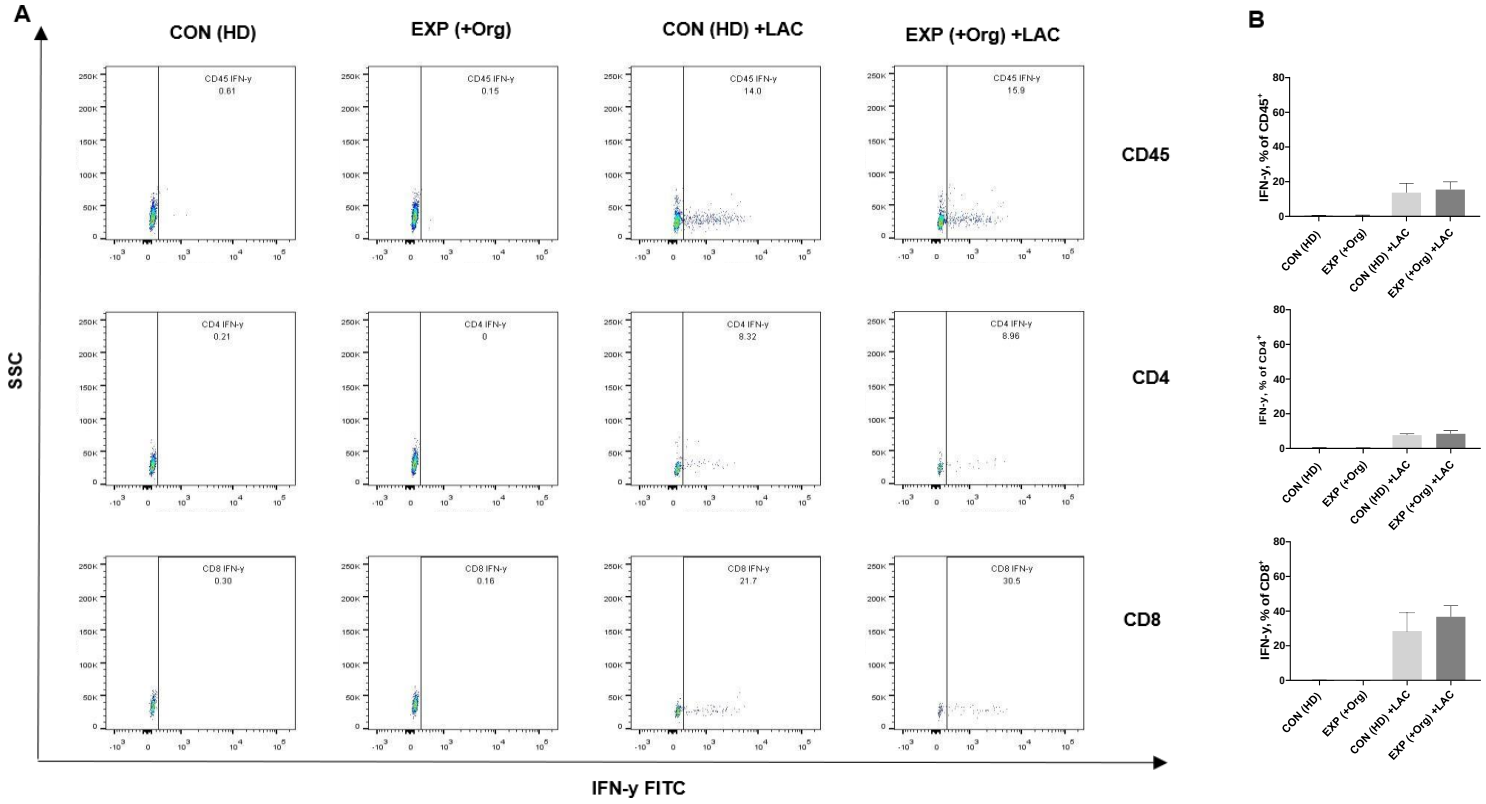

Figure 24: (A): Representative FACS plot of IFN-γ production in the CON (HD), EXP (+Org), CON (HD) +LAC, and EXP (+Org) +LAC groups. (B): The production of $CD45^+$, $CD4^+$, and $CD8^+$ IFN-γ between these two groups has no statistical significance (P>0.05).

Taken together, in co-cultures of PBMCs (HD) with patient-derived organoids, the numbers of $CD4^+$ Tcm, $CD8^+$ Tem, and Treg cells were significantly elevated, but CD4+ Tem and CD8+ Tnaiv were reduced. Intriguingly, no increase in IFN-γ production was found in this co-culture group.

3.7 Differentiation characteristics of PBMCs in each autologous co-culture model with patient-derived organoid and matched PBMCs

The co-culture model formed with PDAC patient-derived organoids and autologous PBMCs was designed to mimic the in vivo environment of tumor patients, facilitating the study of interactions between tumor cells and immune

cells in the TME.

Four organoid lines from different PDAC patients (Patient 2, 3, 7, and 9) that grew well under stable cultured conditions, had been passaged less than 5 times (Figure 25), and PBMCs were isolated from these patients before surgery. In the CON (P) group, patients' PBMCs were cultured alone in the organoid complete medium, while in the EXP (+Org) group, the PBMCs were co-cultured with organoids from the same patient. The Memory T cell and Treg differentiation, as well as IFN-γ production in both the control and experimental groups, were detected by FACS. The results were described and illustrated individually.

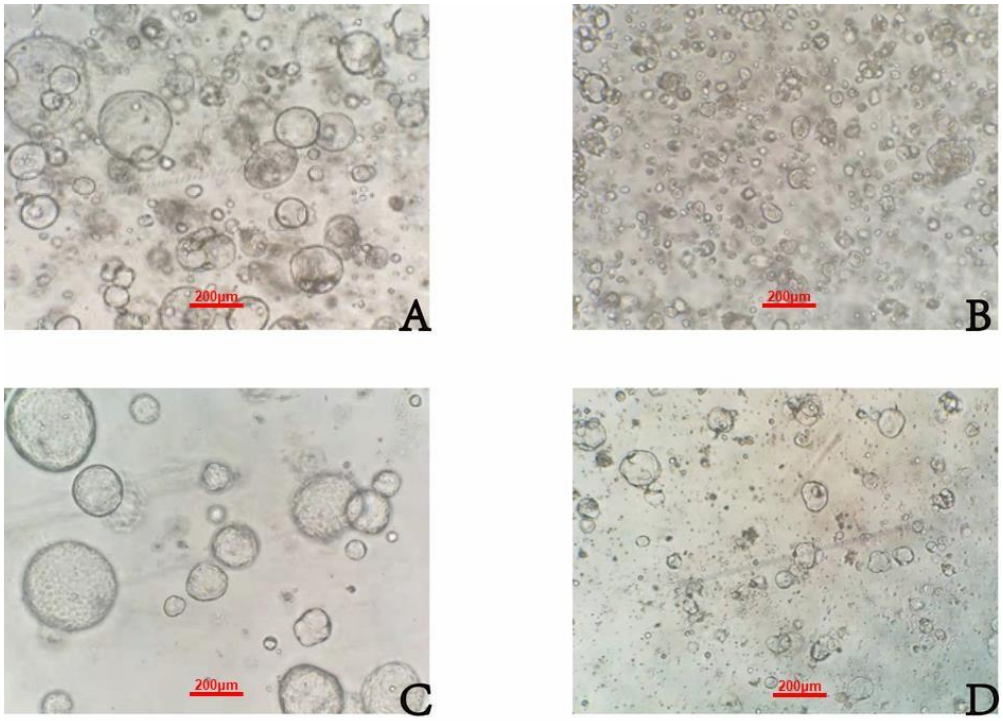

Figure 25: (A): Representative images of PDAC organoids isolated from Patient 3 before co-culture (10x), Passage 3; (B): Representative images of PDAC organoids isolated from Patient 2 before co-culture (10x), Passage 4; (C): Representative images of PDAC organoids isolated from Patient 7 before co-culture (10x), Passage 2; (D): Representative images of PDAC organoids isolated from Patient 4 before co-culture (10x), Passage 3.

3.7.1 The differentiation of Memory CD4+/CD8+ T cell differs in distinct autologous PBMC-organoid co-cultures

In the co-culture group with PBMCs (P3) and organoids (P3), the population of $CD4^+$ Tem and Teff cells was 26.60% and 5.77%, respectively, which were lower than 32.0% and 12.80% in the control group. Meanwhile, the $CD4^+$ Tcm and Tnaiv cells in the EXP (+Org3) group were detected with numbers of 18.90% and 48.70%, both higher than those in the CON (P3) group with numbers of 14.40% and 41.00%, respectively. The differentiation of these four Memory T cell subtypes in PBMCs was influenced by the tumor organoids, exhibiting similar changes as in Section 3.5.1.

Likewise, the $CD4^+$ Tem cell population decreased from 32.90% in the CON (P2) group to 25.40% in the EXP (+Org2) group, the $CD4^+$ Tcm cell slightly increased from 13.9% to 16.5%, and the $CD4^+$ Tnaiv cell improved from 41.00% to 47.20%. But the $CD4^+$ Teff cell population between these two groups showed a little discrepancy.

In contrast to that, we found no significant difference in Memory $CD4^+$ T cell subtypes population of co-culture 7 and 9 compared with their controls, probably because of the individual differences.

The FACS results of the $CD4^+$ Memory T cell differentiation in these four co-cultures and their matched controls could be seen in Figure 26.

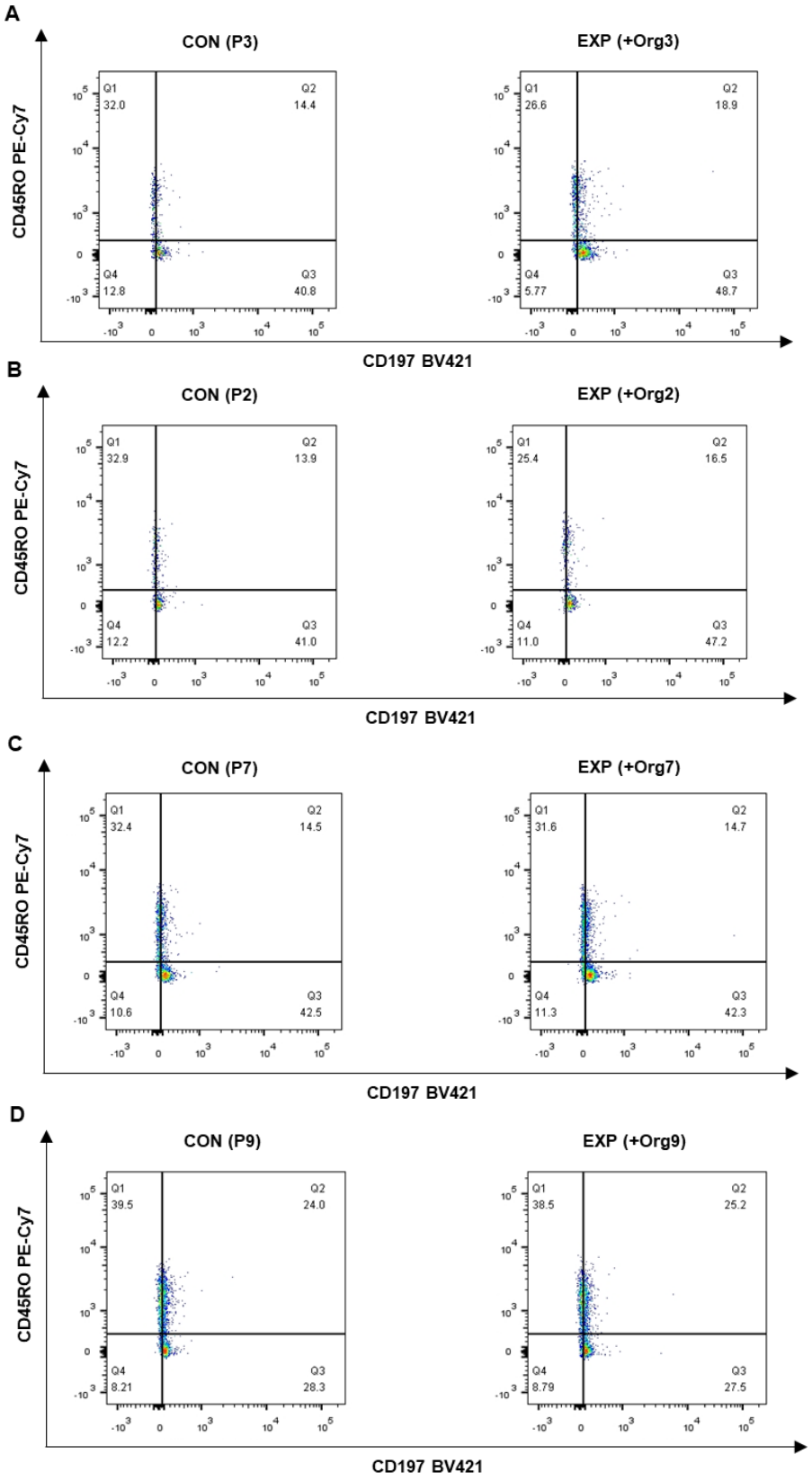

Figure 26: (A)(B)(C)(D): The differentiation of $CD4^+$ Memory T cell subsets between the CON (P) and EXP (+Org) groups of Patient 3, 2, 7, and 9 showed individual differences.

Furthermore, the Memory $CD8^+$ T cell subpopulations in Patient 3 co-culture were consistent with those in Section 3.5.1. The population of $CD8^+$ Tem in the CON (P3) group was 47.40%. This number was reduced to 26.20% in the EXP (+Org3) group. For $CD8^+$ Tcm, Teff, and Tnaiv population, the numbers of these cells gated in the co-culture group were 23.40%, 13.10%, and 37.20% respectively, higher than that in the control group with numbers of 17.80%, 18.90%, and 25.70%.

Regarding Patient 2 co-culture, we noticed a decline of $CD8^+$ Tem population from 37.30% in the CON (P2) to 27.40% in the EXP (+Org2) group, as well as a rising trend in $CD8^+$ Tcm population from 17.3% to 22.6%. These results were considered to be unanimous with the above. But the differentiation of $CD8^+$ Teff cells in the co-culture (12.40%) was a little higher than that in the control (9.73%). At the same time, the $CD8^+$ Tnaiv cell population in PBMCs of this patient demonstrated no excessive changes with co-culture.

Also, the significant variations of Memory $CD8^+$ T cells in Patient 7 and Patient 9 co-cultures could not be tracked compared to the controls.

These results were shown in Figure 27

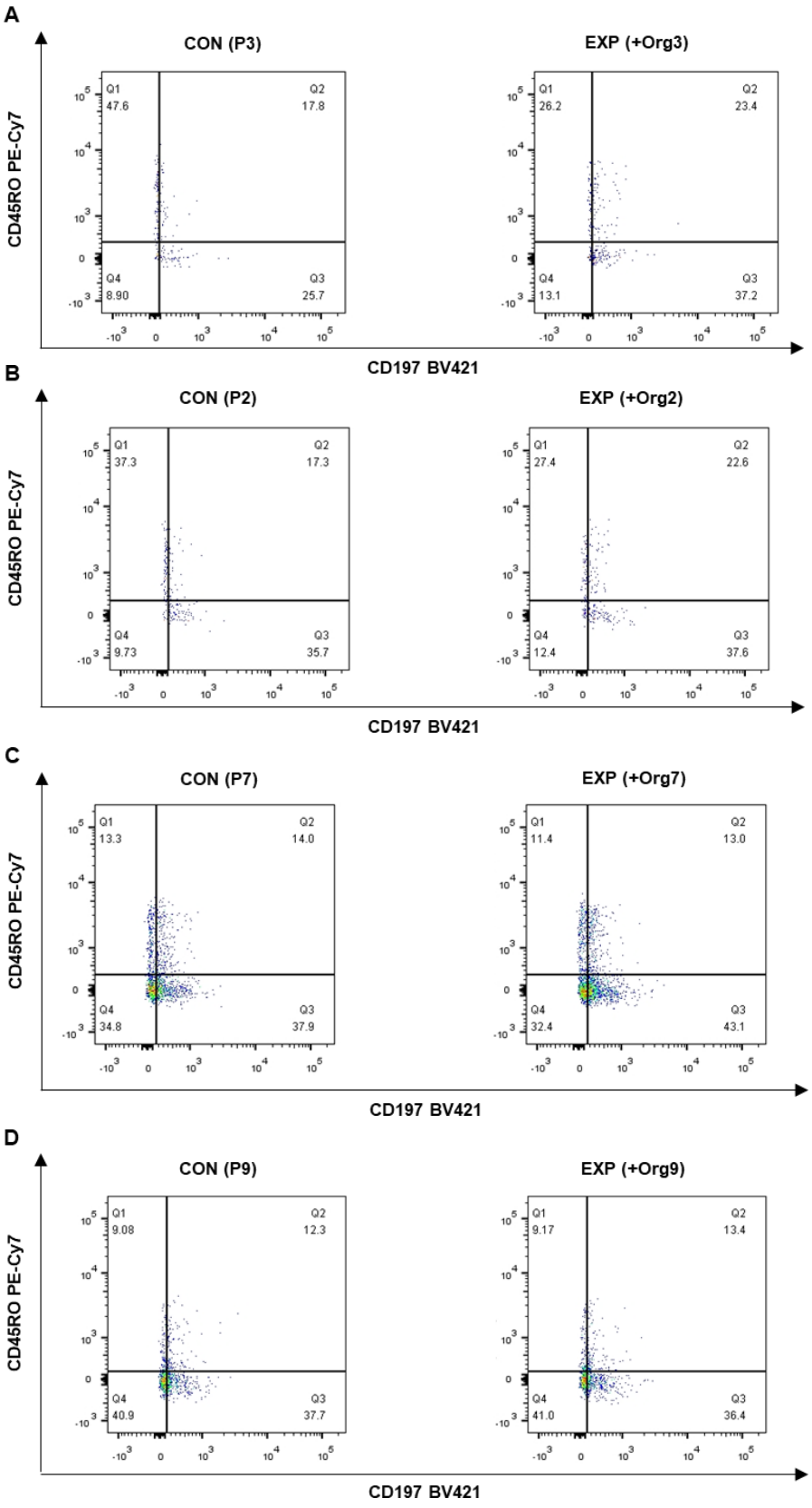

Figure 27: (A)(B)(C)(D): The population of CD4+ Memory T cell subsets between the CON (P) and EXP (+Org) groups of Patient 3, 2, 7, and 9 showed individual differences.

3.7.2 The population of Tregs increased in each co-culture model with organoids and autologous PBMCs

Our previous results in Section 3.4.2 indicated that the population of Tregs has already been increased in PBMCs of PDAC patients compared to that in healthy PBMCs. Then, the Panc1 cell line was co-cultured in direct contact with patients' PBMCs to stimulate the differentiation of Tregs, but we were unable to examine more Treg cells out of $CD4^+$ T cells from this model. However, when using the autologous organoid/PBMC co-culture, an obvious up-regulation in Treg differentiation was notable.

The population of Treg cells in PBMCs of the EXP (+Org2) and EXP (+Org3) co-culture groups was 10.70% and 8.27%, respectively, which were higher than 4.13% and 5.05% in the CON (P2) and CON (P3) groups (Figure 28 A, B).

The Memory T cell differentiation appeared to be unchanged in the EXP (+Org7) and EXP (+Org9) groups in contrast to the matched control groups. But there was a significant increase in the numbers of Treg cells between Patient 7/Patient 9 co-cultures (8.15%/13.9%) and the controls (4.08%/5.39%), displayed in Figure 28 C, D.

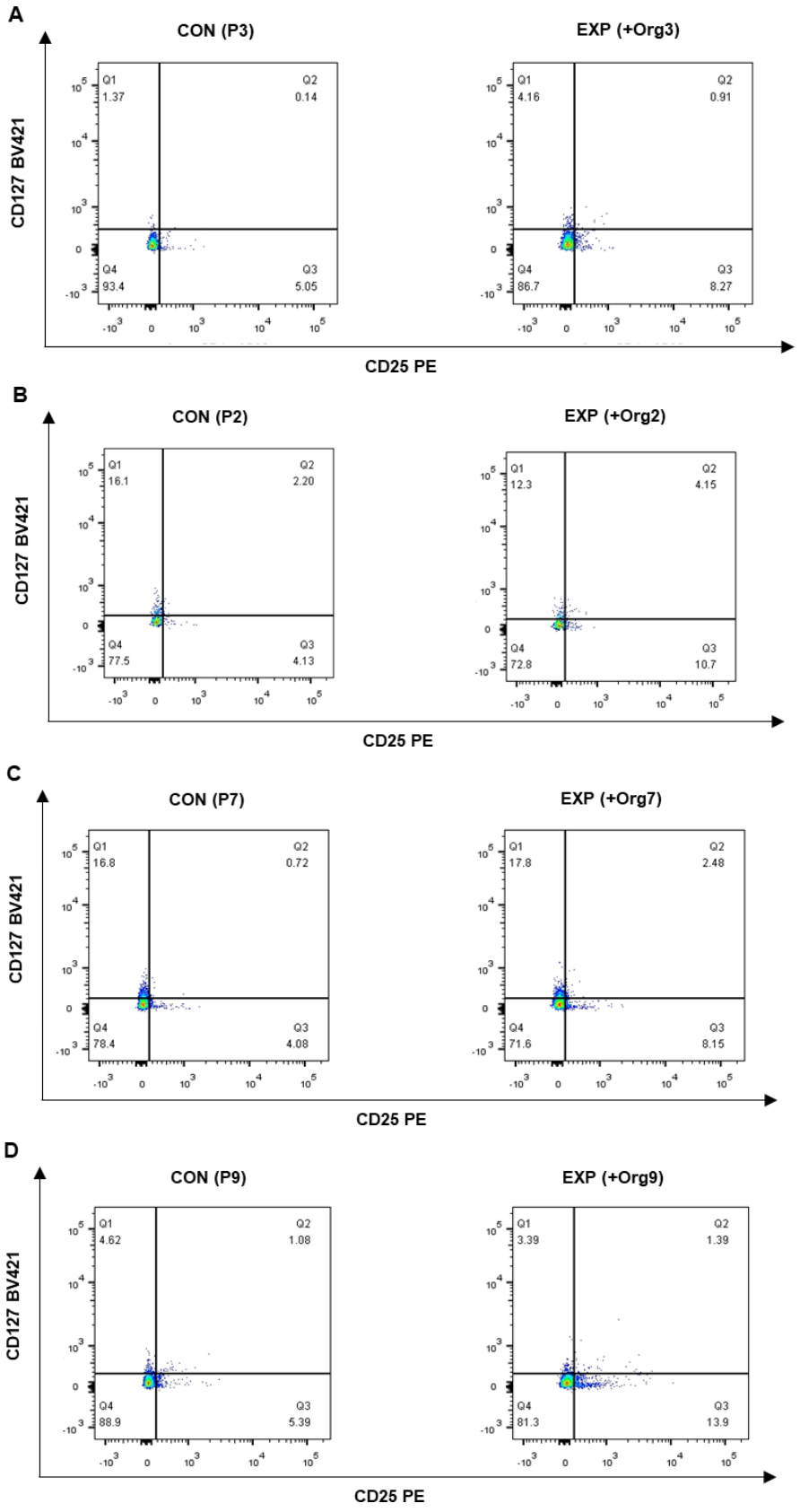

Figure 28: (A)(B)(C)(D): The numbers of Tregs were increased in the co-cultures established from Patient 3,2,7, and 9 samples, compared to that in the controls.

3.7.3 No effects on IFN-γ production in each autologous PBMC-organoid co-culture

The IFN-γ production of $CD45^+$, $CD4^+$, and $CD8^+$ cells was detected in the autologous PBMC-organoid co-cultures from Patient 3, 7, and 9, except Patient 2 due to limited blood samples.

The test groups were designed as before. The production of IFN-γ was very low in both the CON (P) and EXP (+Org) groups with no LAC supplementation, while in the CON (P) +LAC and EXP (+Org) +LAC groups, these numbers increased a lot.

For all the patients involved in this section, the comparisons of $CD45^+$, $CD4^+$, and $CD8^+$ IFN-γ production in PBMCs between positive control and experimental groups were not significant (Figure 29).

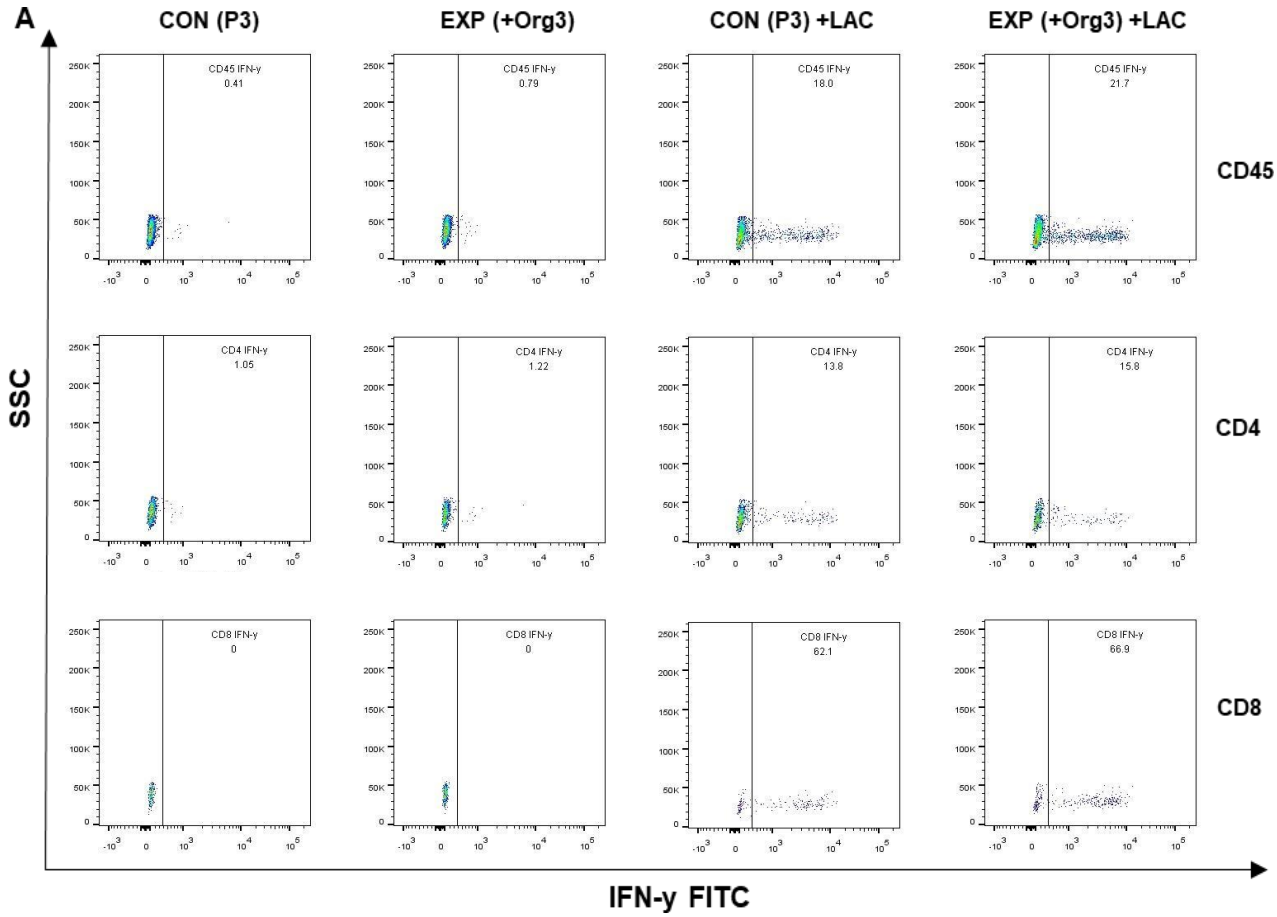

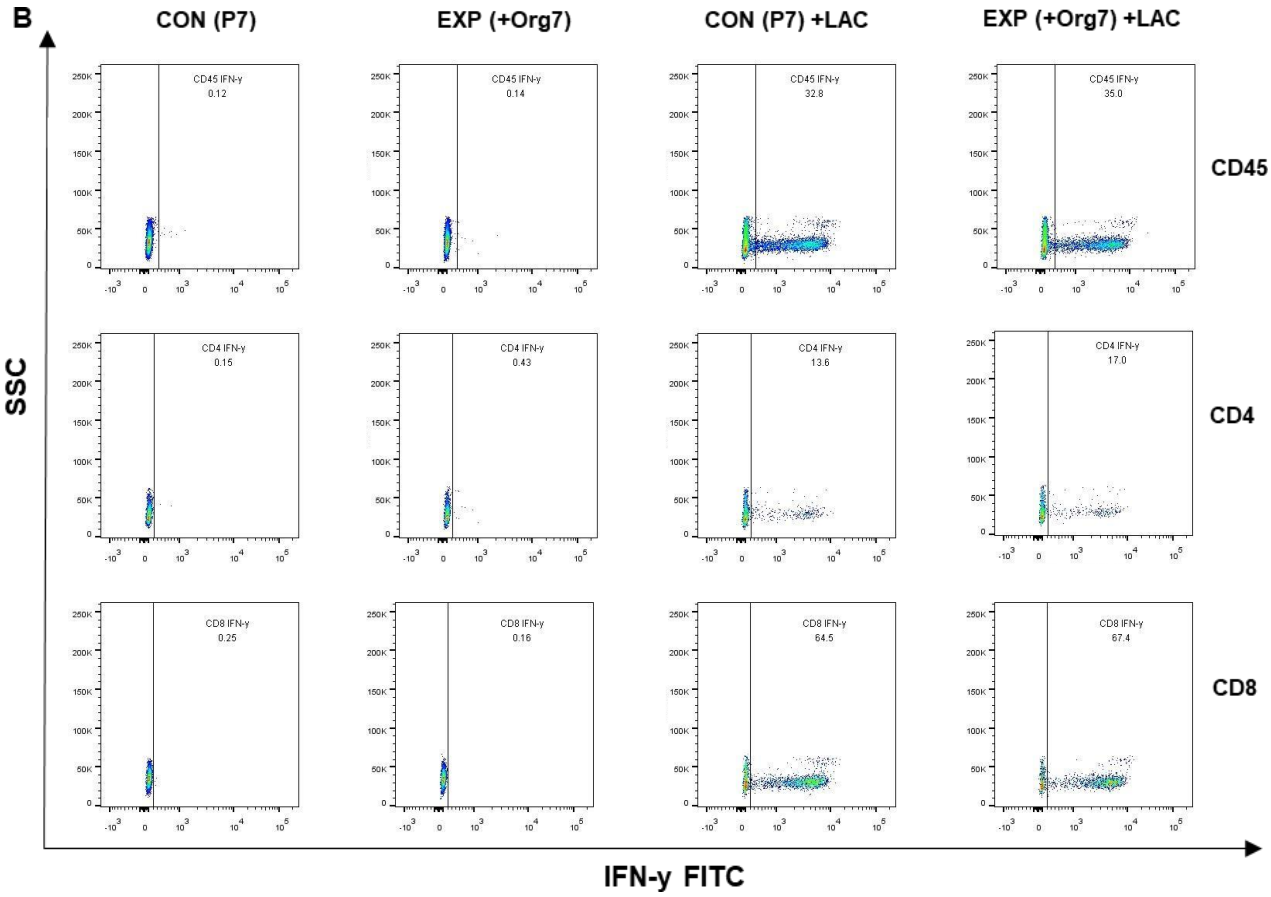
B
CON (P7)
EXP (+Org7)
CON (P7) +LAC
EXP (+Org7) +LAC
CD45 IFN-γ 0.12
CD45 IFN-γ 0.14
CD45 IFN-γ 32.8
CD45 IFN-γ 35.0
CD4 IFN-γ 0.15
CD4 IFN-γ 0.43
CD4 IFN-γ 13.6
CD4 IFN-γ 17.0
CD8 IFN-γ 0.25
CD8 IFN-γ 0.16
CD8 IFN-γ 64.5
CD8 IFN-γ 67.4
CD45
CD4
CD8
SSC
IFN-γ FITC

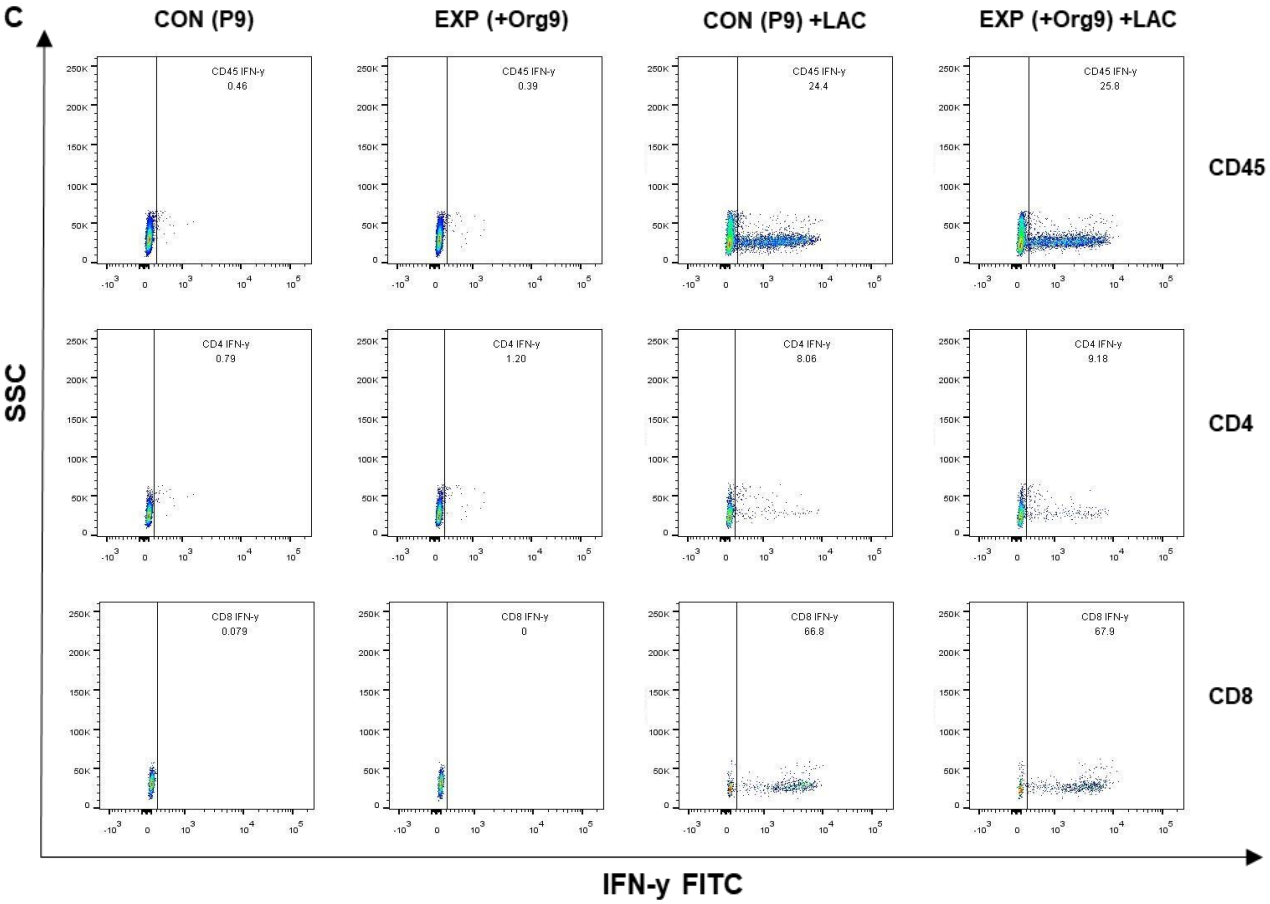
C
CON (P9)
EXP (+Org9)
CON (P9) +LAC
EXP (+Org9) +LAC
CD45 IFN-γ 0.46
CD45 IFN-γ 0.39
CD45 IFN-γ 24.4
CD45 IFN-γ 25.8
CD4 IFN-γ 0.79
CD4 IFN-γ 1.20
CD4 IFN-γ 8.06
CD4 IFN-γ 9.18
CD8 IFN-γ 0.079
CD8 IFN-γ 0
CD8 IFN-γ 66.8
CD8 IFN-γ 67.9
CD45
CD4
CD8
SSC
IFN-γ FITC

Figure 29: (A)(B)(C): The IFN-γ production of $CD45^+$. $CD4^+$ and $CD8^+$ cells in PBMCs of Patient 3, 7, and 9 were not changed in the autologous PBMC-organoid co-culture groups, compared to their matched controls.

Taken together, the differentiation of Memory T cells was not identical in autologous co-cultures established by the PBMCs and organoids isolated from 4 patients. In one patient's co-culture, the numbers of $CD4^+$ Tcm- and Tnaiv-, $CD8^+$ Tcm- and Tnaiv cells were higher, whereas of $CD4^+$ Tem- and Teff-, $CD8^+$ Tem cells were lower than those in PBMCs cultured alone group. And in another patient co-culture, the $CD4^+$ Tnaiv- and $CD8^+$ Tcm cell populations were enhanced, but the $CD4^+$ Tem- and $CD8^+$ Tem cells were declined. Besides that, the population of Treg cells in co-cultures from all these PDAC patients was higher than in their matched controls. However, the IFN-γ production was still not significantly changed in the co-culture groups.

4. Discussion

PDAC is still one of the most challenging solid tumors due to the late detection, early metastasis, and strong drug resistance, resulting in suboptimal treatment outcomes and poor prognosis [3, 150]. Currently, immunotherapy is considered to be one of the most promising clinical strategies for cancer treatment of cancer patients with long-lasting benefits and few side effects [151]. However, according to the published reports, this approach generated disappointing results in PDAC patients. The most important factor contributing to the failure of immunotherapy is the robust immunosuppressive environment within pancreatic cancer, which manipulates tumor cells to evade immune surveillance [152]. Therefore, translational research is urgently needed to elucidate the intrinsic link between immune cells and tumor cells to obtain more therapeutic strategies for these cancer patients.

Patient-derived organoid models have been widely studied as an emerging preclinical experimental model for individualized tumor response testing in various cancers [42, 153-155]. In this project, we sought to establish organoids in a multicellular co-culture model to better understand the complexity of tumor-immune cell interactions by examining the differentiation characteristics of certain T cells and hope to exploit new immunotherapeutic targets or modalities to address the practical difficulties in the clinical treatment of PDAC.

4.1 Differentiation characteristics of immune cells in the co-cultures with 2D cell lines or their secretome

Before establishing the co-cultures of patient-derived organoids and matched PBMCs, a series of models were prepared to determine the co-culture conditions, and investigate the differentiation of T cell subtypes and cytokine production in the TME.

4.1.1 The effects of CM from tumor cells on immune cell differentiation

The CM from cancer cell lines is full of numerous cytokines, enzymes, growth factors, and other soluble mediators, which plays a crucial role in regulating the growth, differentiation, and invasion of the specified cells [156]. Okada et al. [157] employed the CM from renal cell carcinoma cell line 786.O to build a platform for inducing monocytes to monocytic MDSC phenotype, acquiring the production of nitric oxide and the inhibition of T cell proliferation. Mohebbi et al. [158] also supported that the secreted cytokines from CRC cell lines could promote the monocytes in PBMCs to differentiate into inflammatory phenotypes. Bharadwaj et al. [159] indicated that the upregulation of IL-6 and G-CSF in the CM derived from a human pancreatic cancer cell line (BxPC-3) could inhibit DC differentiation and their antigen presentation function, supporting the tumor immune escape. Similarly, Du et al. [160] demonstrated that the BxPC-3-CM induced the abnormally elevated microRNA-146a in DCs, which suppressed the maturation and anti-tumor immune activation of these cells.

However, in our study, secreted proteins in the media conditioned by pancreatic cancer cell lines (Panc1 and Miapaca2) failed to stimulate the differentiation of Memory T cells and Tregs in PBMCs under FACS detection. This is likely because the cellular secretome alone is not sufficient to mimic the complexity of the immune environment in tumors, especially the lack of interactions between different cell types [156].

4.1.2 The effects of tumor cells on T cell differentiation in the co-culture models with PBMCs and cancer cell lines

In view of the results above, we further established a co-culture model in which PBMCs and 2D cell lines (Panc1 and Miapaca2) were in direct contact.

Compared with the PBMCs (HD) cultured alone in the normal medium

(RPMI1640+10%FBS+1%P/S), we found substantially increased populations of $CD4^+$ Tcm and $CD8^+$ Tem cells in PBMCs co-cultured with Panc1 cell line. This phenomenon can be explained by the fact that the Memory T cells have a lower activation threshold than Naïve T cells, which can respond to weak stimulation, and quickly respond with immune effects [161, 162]. Barski et al. [163] proved that the rapid recall ability of Memory T cells was regulated by their epigenome. The stable genes' chromatin environment and poised state in these cells can faster induce cytokine production to exert better anti-tumor efficacy.

With the co-culture of PBMCs (HD) and Panc1, we also noticed an obvious upward trend in the Treg cell population, implying that the PDAC cells drive the accumulation of Tregs within the tumors. These Treg cells can release soluble factors, and regulate or suppress other cells in the immune system, playing a principal role in monitoring immune-modulating measures [164].

Nevertheless, these results were not obtained in the Miapaca2 co-culture models. Gradiz et al. [165] identified that the Miapaca2 cell line expresses E-cadherin, but is absent of CD56; whereas the Panc1 cell line has CD56, but not E-cadherin, synaptophysin, or Neurotensin receptors (NTR)-1, so the Panc1 cells are more aggressive and easier to metastasize. Shen et al. [166] also found that the Panc1 cells exhibit higher stemness features than Miapaca2 cells due to the differentially expressed microRNAs between these two cell lines. The properties of distinct cancer cell lines might lead to the discrepancy in the immune cell differentiation in their co-cultures constructed with PBMCs.

Moreover, the PBMCs from PDAC patients were collected to characterize the differentiation of T cell subsets in the TME. When attacked by the cancer cells, the Tnaiv cells in PBMCs are activated and differentiated into Teff cells that execute the tumor-killing program. After that, the Memory T cells are generated from Teff cells through epigenetic modifications [167, 168]. Our results confirmed that the population of $CD4^+$/$CD8^+$ Tem, Tcm, and Teff cells

was larger in PBMCs from PDAC patients than in PBMCs from HD. Correspondingly, the numbers of $CD4^+$/$CD8^+$ Tnaiv cells were greatly reduced in patients' PBMCs, compared to healthy PBMCs. Similar results were found in several reports of PDAC patients [169, 170]. Besides, we also detected enhanced numbers of Tregs in patients' PBMCs. This has been proven not only in pancreatic cancers [171] but also in other solid tumors [172-175]. The differentiation of different T cell subsets in PBMCs from cancer patients was altered as cancer progressed [94, 176, 177].

Different from the healthy PBMCs, the differentiation direction of T cells in PDAC patients' PBMCs was shifted when they encounter secondary stimulation. In co-cultures of patients' PBMCs and Panc1, the numbers of $CD4^+$ Tcm cells was still higher than that of the control group, but the $CD8^+$ Tem cell population declined, and the Treg cell population was not significantly changed. In addition, we also obtained more interesting results in this co-culture model, including the downwards of $CD4^+$ Tem, $CD4^+$ Teff, and $CD8^+$ Teff population, and upwards of $CD4^+$ Tnaiv, $CD8^+$ Tcm, and $CD8^+$ Tnaiv population, in contrast with the controls. Munn et al [178] believed that tumor growth depends on the suppressive mechanisms. The more a tumor is attacked, the more counter-regulatory mechanisms may be induced. Therefore, the regulatory circuits of tumors cannot be simply summarized. More experiments should be added to verify the authenticity and accuracy of these data.

4.1.3 The activation of immune cells in response to tumor cell stimulation

IFN-γ is a pleiotropic cytokine produced by human lymphocytes, especially T cells and Natural Killer (NK) cells, with anti-tumor, immunostimulatory, and immunomodulatory functions [179]. It was reported that the high concentration of IFN-γ induced tumor apoptosis by activating JAK-STAT1 signaling [180-182]. What's more, IFN-γ is also involved in enhancing T Helper (Th) 1 cell

development, activating antigen-specific T- and B- cell responses, and inhibiting Treg generation and proliferation [183, 184]. The growing numbers of IFN-γ can reflect the activation of immune cells in the TME. Unfortunately, in this project, we were not able to observe any apparent alterations in IFN-γ production of $CD45^+$, $CD4^+$, and $CD8^+$ cells using the co-culture models with PBMCs and pancreatic cancer cell lines. However, we may not simply conclude that the production of IFN-γ in immune cells was unchanged upon the stimulation of tumor cells. One important consideration was the time point chosen [94]. In our study, the incubation time for co-culture was 48h, which might be beyond the optimal condition for detecting cytokine responses [185]. Another possible reason was that the flow cytometry can only measure the total numbers of cytokines, but not clearly define activated or functional ones [186]. Slight changes of IFN-γ production in these co-cultures detected by FACS cannot represent the actual situation of immune cells infiltrated in the TME.

In conclusion, the co-culture models established with 2D cell lines and PBMCs provided a feasible experimental scheme for our subsequent 3D modeling and introduced the differentiation characteristics of specific immune cells in the cancer setting, enhancing our understanding of intratumoral T cell populations.

4.2 Differentiation properties of PBMCs in autologous patient-derived organoids/PBMCs co-cultures

The 3D organoid culture can display cellular behavior and morphology similar to the original tumor in vivo, overcoming the limitations of the 2D cell lines and their derived CM research models [187]. We adopted the 3D organoids to establish a co-culture system in direct contact with PBMCs in the organoid complete medium, which helped to study the relationship between immune cells and tumor cells in an individual.

4.2.1 A pre-experimental co-culture model established with PBMCs (HD) and patient-derived organoids

The attempts to establish an autologous patient PBMC-organoid co-culture model were first performed using PBMCs (HD) and organoid lines from different PDAC patients. The control group was PBMCs cultured alone in certain wells of a 24-well plate with the complete organoid medium for 48h, while the experimental group consisted of matrigel-organoid mixtures covered with PBMCs under the same culture conditions as the control group so that tumor cells and immune cells could directly contact each other. Although there are several methods to achieve the co-culture of PBMCs with organoids [59, 188, 189], the existence of a basement membrane matrix and the effective contact area of the two cells were considered essential for the co-culture model establishment [190].

In the group of co-cultured PBMCs (HD) with patient-derived organoids, we identified that the populations of $CD4^+$ Tcm, $CD8^+$ Tem, and Treg cells were higher than in the PBMCs cultured alone group, which was consistent with those results from the co-cultures established by PBMCs (HD) and Panc1. Besides, the $CD4^+$ Tem and $CD8^+$ Tnaiv cell populations were significantly decreased in the co-cultures compared to the controls.

This model was thought to be more representative of the immune cell behavior in the actual setting of PDAC cancer patients and the approach could be applied to establish the co-cultures with patient-derived organoids and PBMCs to describe the immune-tumor cell interaction in individuals.

4.2.2 The autologous co-culture model establishment with organoids and PBMCs from the same patient

When co-culturing the patient-derived organoids with matched PBMCs, the differentiation of Memory T cells in one of the 4 patient co-culture models exhibited a higher population of $CD4^+$ Teff, $CD4^+$/$CD8^+$ Tcm, and $CD4^+$/$CD8^+$

Tnaiv cells, but lower of $CD4^+/CD8^+$Tem and $CD8^+$ Teff cells, which were similar to the consequences in Section 3.3. In another patient co-culture, we also found an increase in $CD4^+/CD8^+$ Tcm and a decrease in $CD4^+/CD8^+$ Tem cells, compared to the controls, followed by minor alterations in effector and naïve cells. However, for the remaining 2 patient co-cultures, no significant changes in Memory T cell differentiation were observed.

The lineage relationships between Effector, Memory, and Naive T cells, as well as between different Memory T cell subsets remain controversial [191-193]. Berard et al. [194] illustrated that IL-7 was essential for Naïve T cell survival, while the maintenance of Memory T cells was dependent on IL-12, IL-15, IL-18, and IFN-γ. In addition, some chemokines, pro-tumor factors, and adhesion molecules on the surface of the cells are also involved in supporting Memory T cell homeostasis, which helps define distinct T cell subsets [194, 195]. The microarray analysis on the variation of gene expression showed that the Memory T cells are consistently intermediate between Teff and Tnaiv cells, and closer to Teff instead of Tnaiv, clarifying why the Memory T cells can transfer to Teff cells faster than Tnaiv cells [196]. A large number of differentially expressed genes stimulate Tnaiv cells to differentiate into Teff and Tem/Tcm cells, which can be potential targets for future immunotherapy designs. Another finding demonstrated that the majority of Tcm and Tem cells were from a common naive precursor, but there was still a small part of Tem cells that can differentiate further into Tcm cells. The relatively short-lived Tem cells may randomly undergo death, transformation, or still exist as Tems [197]. Our results described the direction of T cell differentiation in the TME of each PDAC patient and reflect the inner relevance of tumor cells and immune cells, with individual differences.

Although the changes in Memory T cells varied among patients, the elevation in Treg cells was evident from our results in all autologous co-cultures. The enrichment of Tregs can suppress the anti-tumor immune responses in PDAC and result in a poor prognosis for patients [198]. The

therapies that rely on depleting Treg cells or interfering with their immunosuppressive functions are considered to be promising strategies for cancer treatment, attaining effective, reliable, and consistent clinical efficacy [199-202].

4.3 Limitations of this study

There are still some recognized restrictions associated with the approach of the patient-derived organoid-PBMC co-cultures in this study. First of all, cancer patient donors have limited blood supply, and not only that, the tumor-reactive T cells are less or dysfunctional in most patients' PBMCs [203, 204], leading to unreliable data measurements in a few FACS analyses.

Second, the successful rate of PDAC organoid isolation technology is not 100% [54, 205], probably affected by the size, quality, and freshness of the tumor tissue acquisition (no more than three hours after tissue removal), and the high cost of the culture conditions. Additionally, only resectable tissues from PDAC patients were enrolled in our study, and for those who cannot undergo surgery, the organoid establishment by means of endoscopic ultrasound (EUS)-guided fine-needle biopsy sampling at the time of diagnosis can be a better solution [206].

Third, except for immune cells and tumor cells, other cellular components, like fibroblastic, neural, and vascular cells, as well as extracellular matrix also constitute the TME of pancreatic cancer, promoting tumor growth and metastasis [64, 207]. Future work should cover these elements to more accurately simulate the in vivo microenvironment of tumor patients and solve practical problems in treatments [208].

Finally, this co-culture model is still in the laboratory research stage. It is necessary to refine the culture conditions that are suitable for different cell types and reduce the effects of some paracrine factors secreted by one cell on other components [209, 210].

4.4 Conclusion and Outlook

In summary, our study has established autologous co-cultures with patient-derived organoids and PBMCs, successfully detecting and recording the differentiation characteristics of T cell subtypes in each patient model. This pattern has great potential to be a testing model applied in both basic research and translational applications, enhancing the clinical relevance of the tumor in immunology.

Furthermore, since there is considerable cellular heterogeneity within pancreatic neoplasms [211-213], our next work will focus on investigating the heterogeneity of PBMC differentiation in co-culture with different tumor organoid lines from the same patient, with the hope of improving cancer diagnosis and therapeutic design.

Reference

1. Rahib L, Smith BD, Aizenberg R, Rosenzweig AB, Fleshman JM, Matrisian LM. Projecting cancer incidence and deaths to 2030: the unexpected burden of thyroid, liver, and pancreas cancers in the United States. Cancer research. 2014;74(11):2913-21. doi: 10.1158/0008-5472.CAN-14-0155. PubMed PMID: 24840647.

2. Quante AS, Ming C, Rottmann M, Engel J, Boeck S, Heinemann V, et al. Projections of cancer incidence and cancer-related deaths in Germany by 2020 and 2030. Cancer medicine. 2016;5(9):2649-56. doi: 10.1002/cam4.767. PubMed PMID: 27356493; PubMed Central PMCID: PMC5055190.

3. Mundry CS, Eberle KC, Singh PK, Hollingsworth MA, Mehla K. Local and systemic immunosuppression in pancreatic cancer: Targeting the stalwarts in tumor's arsenal. Biochimica et biophysica acta Reviews on cancer. 2020;1874(1):188387. doi: 10.1016/j.bbcan.2020.188387. PubMed PMID: 32579889; PubMed Central PMCID: PMC7483650.

4. Sung H, Ferlay J, Siegel RL, Laversanne M, Soerjomataram I, Jemal A, et al. Global Cancer Statistics 2020: GLOBOCAN Estimates of Incidence and Mortality Worldwide for 36 Cancers in 185 Countries. CA: a cancer journal for clinicians. 2021;71(3):209-49. doi: 10.3322/caac.21660. PubMed PMID: 33538338.

5. Takebe T, Wells JM, Helmrath MA, Zorn AM. Organoid Center Strategies for Accelerating Clinical Translation. Cell stem cell. 2018;22(6):806-9. doi: 10.1016/j.stem.2018.05.008. PubMed PMID: 29859171; PubMed Central PMCID: PMC8191130.

6. Aboulkheyr Es H, Montazeri L, Aref AR, Vosough M, Baharvand H. Personalized Cancer Medicine: An Organoid Approach. Trends in biotechnology. 2018;36(4):358-71. doi: 10.1016/j.tibtech.2017.12.005. PubMed PMID: 29366522.

7. Rauth S, Karmakar S, Batra SK, Ponnusamy MP. Recent advances in organoid development and applications in disease modeling. Biochimica et biophysica acta Reviews on cancer. 2021;1875(2):188527. doi: 10.1016/j.bbcan.2021.188527. PubMed PMID: 33640383; PubMed Central PMCID: PMC8068668.

8. McGuigan A, Kelly P, Turkington RC, Jones C, Coleman HG, McCain RS. Pancreatic cancer: A review of clinical diagnosis, epidemiology, treatment and outcomes. World journal of gastroenterology. 2018;24(43):4846-61. doi: 10.3748/wjg.v24.i43.4846. PubMed PMID: 30487695; PubMed Central PMCID: PMC6250924.

9. Hu JX, Zhao CF, Chen WB, Liu QC, Li QW, Lin YY, et al. Pancreatic cancer: A review of epidemiology, trend, and risk factors. World journal of gastroenterology. 2021;27(27):4298-321.

doi: 10.3748/wjg.v27.i27.4298. PubMed PMID: 34366606; PubMed Central PMCID: PMC8316912.

10. Carioli G, Malvezzi M, Bertuccio P, Boffetta P, Levi F, La Vecchia C, et al. European cancer mortality predictions for the year 2021 with focus on pancreatic and female lung cancer. Annals of oncology : official journal of the European Society for Medical Oncology. 2021;32(4):478-87. doi: 10.1016/j.annonc.2021.01.006. PubMed PMID: 33626377.

11. Park W, Chawla A, O'Reilly EM. Pancreatic Cancer: A Review. Jama. 2021;326(9):851-62. doi: 10.1001/jama.2021.13027. PubMed PMID: 34547082.

12. Gillen S, Schuster T, Meyer Zum Buschenfelde C, Friess H, Kleeff J. Preoperative/neoadjuvant therapy in pancreatic cancer: a systematic review and meta-analysis of response and resection percentages. PLoS medicine. 2010;7(4):e1000267. doi: 10.1371/journal.pmed.1000267. PubMed PMID: 20422030; PubMed Central PMCID: PMC2857873.

13. Conroy T, Hammel P, Hebbar M, Ben Abdelghani M, Wei AC, Raoul JL, et al. FOLFIRINOX or Gemcitabine as Adjuvant Therapy for Pancreatic Cancer. The New England journal of medicine. 2018;379(25):2395-406. doi: 10.1056/NEJMoa1809775. PubMed PMID: 30575490.

14. Abrams RA, Lowy AM, O'Reilly EM, Wolff RA, Picozzi VJ, Pisters PW. Combined modality treatment of resectable and borderline resectable pancreas cancer: expert consensus statement. Annals of surgical oncology. 2009;16(7):1751-6. doi: 10.1245/s10434-009-0413-9. PubMed PMID: 19390900.

15. Cunningham D, Chau I, Stocken DD, Valle JW, Smith D, Steward W, et al. Phase III randomized comparison of gemcitabine versus gemcitabine plus capecitabine in patients with advanced pancreatic cancer. Journal of clinical oncology : official journal of the American Society of Clinical Oncology. 2009;27(33):5513-8. doi: 10.1200/JCO.2009.24.2446. PubMed PMID: 19858379.

16. Wu Z, Li S, Zhu X. The Mechanism of Stimulating and Mobilizing the Immune System Enhancing the Anti-Tumor Immunity. Frontiers in immunology. 2021;12:682435. doi: 10.3389/fimmu.2021.682435. PubMed PMID: 34194437; PubMed Central PMCID: PMC8237941.

17. Morrison AH, Byrne KT, Vonderheide RH. Immunotherapy and Prevention of Pancreatic Cancer. Trends in cancer. 2018;4(6):418-28. doi: 10.1016/j.trecan.2018.04.001. PubMed PMID: 29860986; PubMed Central PMCID: PMC6028935.

18. Balachandran VP, Beatty GL, Dougan SK. Broadening the Impact of Immunotherapy to Pancreatic Cancer: Challenges and Opportunities. Gastroenterology. 2019;156(7):2056-72.

doi: 10.1053/j.gastro.2018.12.038. PubMed PMID: 30660727; PubMed Central PMCID: PMC6486864.

19. Schizas D, Charalampakis N, Kole C, Economopoulou P, Koustas E, Gkotsis E, et al. Immunotherapy for pancreatic cancer: A 2020 update. Cancer treatment reviews. 2020;86:102016. doi: 10.1016/j.ctrv.2020.102016. PubMed PMID: 32247999.

20. Lehtinen M, Paavonen J, Wheeler CM, Jaisamrarn U, Garland SM, Castellsague X, et al. Overall efficacy of HPV-16/18 AS04-adjuvanted vaccine against grade 3 or greater cervical intraepithelial neoplasia: 4-year end-of-study analysis of the randomised, double-blind PATRICIA trial. The Lancet Oncology. 2012;13(1):89-99. doi: 10.1016/S1470-2045(11)70286-8. PubMed PMID: 22075171.

21. Brahmer JR, Tykodi SS, Chow LQ, Hwu WJ, Topalian SL, Hwu P, et al. Safety and activity of anti-PD-L1 antibody in patients with advanced cancer. The New England journal of medicine. 2012;366(26):2455-65. doi: 10.1056/NEJMoa1200694. PubMed PMID: 22658128; PubMed Central PMCID: PMC3563263.

22. Maude SL, Frey N, Shaw PA, Aplenc R, Barrett DM, Bunin NJ, et al. Chimeric antigen receptor T cells for sustained remissions in leukemia. The New England journal of medicine. 2014;371(16):1507-17. doi: 10.1056/NEJMoa1407222. PubMed PMID: 25317870; PubMed Central PMCID: PMC4267531.

23. Wiehagen KR, Girgis NM, Yamada DH, Smith AA, Chan SR, Grewal IS, et al. Combination of CD40 Agonism and CSF-1R Blockade Reconditions Tumor-Associated Macrophages and Drives Potent Antitumor Immunity. Cancer immunology research. 2017;5(12):1109-21. doi: 10.1158/2326-6066.CIR-17-0258. PubMed PMID: 29097420.

24. Schuster SJ, Svoboda J, Chong EA, Nasta SD, Mato AR, Anak O, et al. Chimeric Antigen Receptor T Cells in Refractory B-Cell Lymphomas. The New England journal of medicine. 2017;377(26):2545-54. doi: 10.1056/NEJMoa1708566. PubMed PMID: 29226764; PubMed Central PMCID: PMC5788566.

25. Ren B, Cui M, Yang G, Wang H, Feng M, You L, et al. Tumor microenvironment participates in metastasis of pancreatic cancer. Molecular cancer. 2018;17(1):108. doi: 10.1186/s12943-018-0858-1. PubMed PMID: 30060755; PubMed Central PMCID: PMC6065152.

26. Ho WJ, Jaffee EM, Zheng L. The tumour microenvironment in pancreatic cancer - clinical challenges and opportunities. Nature reviews Clinical oncology. 2020;17(9):527-40. doi: 10.1038/s41571-020-0363-5. PubMed PMID: 32398706; PubMed Central PMCID: PMC7442729.

27. Yuki K, Cheng N, Nakano M, Kuo CJ. Organoid Models of Tumor Immunology. Trends in

immunology. 2020;41(8):652-64. doi: 10.1016/j.it.2020.06.010. PubMed PMID: 32654925; PubMed Central PMCID: PMC7416500.

28. Xu R, Zhou X, Wang S, Trinkle C. Tumor organoid models in precision medicine and investigating cancer-stromal interactions. Pharmacology & therapeutics. 2021;218:107668. doi: 10.1016/j.pharmthera.2020.107668. PubMed PMID: 32853629; PubMed Central PMCID: PMC7855432.

29. Bar-Ephraim YE, Kretzschmar K, Clevers H. Organoids in immunological research. Nature reviews Immunology. 2020;20(5):279-93. doi: 10.1038/s41577-019-0248-y. PubMed PMID: 31853049.

30. Rossi G, Manfrin A, Lutolf MP. Progress and potential in organoid research. Nature reviews Genetics. 2018;19(11):671-87. doi: 10.1038/s41576-018-0051-9. PubMed PMID: 30228295.

31. Xu H, Lyu X, Yi M, Zhao W, Song Y, Wu K. Organoid technology and applications in cancer research. Journal of hematology & oncology. 2018;11(1):116. doi: 10.1186/s13045-018-0662-9. PubMed PMID: 30219074; PubMed Central PMCID: PMC6139148.

32. Fan H, Demirci U, Chen P. Emerging organoid models: leaping forward in cancer research. Journal of hematology & oncology. 2019;12(1):142. doi: 10.1186/s13045-019-0832-4. PubMed PMID: 31884964; PubMed Central PMCID: PMC6936115.

33. Xia X, Li F, He J, Aji R, Gao D. Organoid technology in cancer precision medicine. Cancer letters. 2019;457:20-7. doi: 10.1016/j.canlet.2019.04.039. PubMed PMID: 31078736.

34. Goto T. Patient-Derived Tumor Xenograft Models: Toward the Establishment of Precision Cancer Medicine. Journal of personalized medicine. 2020;10(3). doi: 10.3390/jpm10030064. PubMed PMID: 32708458; PubMed Central PMCID: PMC7565668.

35. Huch M, Knoblich JA, Lutolf MP, Martinez-Arias A. The hope and the hype of organoid research. Development. 2017;144(6):938-41. doi: 10.1242/dev.150201. PubMed PMID: 28292837.

36. Li X, Nadauld L, Ootani A, Corney DC, Pai RK, Gevaert O, et al. Oncogenic transformation of diverse gastrointestinal tissues in primary organoid culture. Nature medicine. 2014;20(7):769-77. doi: 10.1038/nm.3585. PubMed PMID: 24859528; PubMed Central PMCID: PMC4087144.

37. De Crignis E, Hossain T, Romal S, Carofiglio F, Moulos P, Khalid MM, et al. Application of human liver organoids as a patient-derived primary model for HBV infection and related

hepatocellular carcinoma. eLife. 2021;10. doi: 10.7554/eLife.60747. PubMed PMID: 34328417; PubMed Central PMCID: PMC8384419.

38. Baktash Y, Madhav A, Coller KE, Randall G. Single Particle Imaging of Polarized Hepatoma Organoids upon Hepatitis C Virus Infection Reveals an Ordered and Sequential Entry Process. Cell host & microbe. 2018;23(3):382-94 e5. doi: 10.1016/j.chom.2018.02.005. PubMed PMID: 29544098; PubMed Central PMCID: PMC7169308.

39. Shibata W, Sue S, Tsumura S, Ishii Y, Sato T, Kameta E, et al. Helicobacter-induced gastric inflammation alters the properties of gastric tissue stem/progenitor cells. BMC gastroenterology. 2017;17(1):145. doi: 10.1186/s12876-017-0706-6. PubMed PMID: 29212456; PubMed Central PMCID: PMC5719643.

40. Pleguezuelos-Manzano C, Puschhof J, Rosendahl Huber A, van Hoeck A, Wood HM, Nomburg J, et al. Mutational signature in colorectal cancer caused by genotoxic pks(+) E. coli. Nature. 2020;580(7802):269-73. doi: 10.1038/s41586-020-2080-8. PubMed PMID: 32106218; PubMed Central PMCID: PMC8142898.

41. Matano M, Date S, Shimokawa M, Takano A, Fujii M, Ohta Y, et al. Modeling colorectal cancer using CRISPR-Cas9-mediated engineering of human intestinal organoids. Nature medicine. 2015;21(3):256-62. doi: 10.1038/nm.3802. PubMed PMID: 25706875.

42. Gao D, Vela I, Sboner A, Iaquinta PJ, Karthaus WR, Gopalan A, et al. Organoid cultures derived from patients with advanced prostate cancer. Cell. 2014;159(1):176-87. doi: 10.1016/j.cell.2014.08.016. PubMed PMID: 25201530; PubMed Central PMCID: PMC4237931.

43. Zumwalde NA, Haag JD, Sharma D, Mirrielees JA, Wilke LG, Gould MN, et al. Analysis of Immune Cells from Human Mammary Ductal Epithelial Organoids Reveals Vdelta2+ T Cells That Efficiently Target Breast Carcinoma Cells in the Presence of Bisphosphonate. Cancer prevention research. 2016;9(4):305-16. doi: 10.1158/1940-6207.CAPR-15-0370-T. PubMed PMID: 26811335; PubMed Central PMCID: PMC4818696.

44. Della Corte CM, Barra G, Ciaramella V, Di Liello R, Vicidomini G, Zappavigna S, et al. Antitumor activity of dual blockade of PD-L1 and MEK in NSCLC patients derived three-dimensional spheroid cultures. Journal of experimental & clinical cancer research : CR. 2019;38(1):253. doi: 10.1186/s13046-019-1257-1. PubMed PMID: 31196138; PubMed Central PMCID: PMC6567578.

45. Wensink GE, Elias SG, Mullenders J, Koopman M, Boj SF, Kranenburg OW, et al. Patient-derived organoids as a predictive biomarker for treatment response in cancer patients. NPJ precision oncology. 2021;5(1):30. doi: 10.1038/s41698-021-00168-1. PubMed PMID: 33846504; PubMed Central PMCID: PMC8042051.

46. Sachs N, de Ligt J, Kopper O, Gogola E, Bounova G, Weeber F, et al. A Living Biobank of Breast Cancer Organoids Captures Disease Heterogeneity. Cell. 2018;172(1-2):373-86 e10. doi: 10.1016/j.cell.2017.11.010. PubMed PMID: 29224780.

47. Li X, Pan B, Song X, Li N, Zhao D, Li M, et al. Breast cancer organoids from a patient with giant papillary carcinoma as a high-fidelity model. Cancer cell international. 2020;20:86. doi: 10.1186/s12935-020-01171-5. PubMed PMID: 32206037; PubMed Central PMCID: PMC7079375.

48. Vlachogiannis G, Hedayat S, Vatsiou A, Jamin Y, Fernandez-Mateos J, Khan K, et al. Patient-derived organoids model treatment response of metastatic gastrointestinal cancers. Science. 2018;359(6378):920-6. doi: 10.1126/science.aao2774. PubMed PMID: 29472484; PubMed Central PMCID: PMC6112415.

49. Fujii M, Shimokawa M, Date S, Takano A, Matano M, Nanki K, et al. A Colorectal Tumor Organoid Library Demonstrates Progressive Loss of Niche Factor Requirements during Tumorigenesis. Cell stem cell. 2016;18(6):827-38. doi: 10.1016/j.stem.2016.04.003. PubMed PMID: 27212702.

50. Weeber F, van de Wetering M, Hoogstraat M, Dijkstra KK, Krijgsman O, Kuilman T, et al. Preserved genetic diversity in organoids cultured from biopsies of human colorectal cancer metastases. Proceedings of the National Academy of Sciences of the United States of America. 2015;112(43):13308-11. doi: 10.1073/pnas.1516689112. PubMed PMID: 26460009; PubMed Central PMCID: PMC4629330.

51. Schutte M, Risch T, Abdavi-Azar N, Boehnke K, Schumacher D, Keil M, et al. Molecular dissection of colorectal cancer in pre-clinical models identifies biomarkers predicting sensitivity to EGFR inhibitors. Nature communications. 2017;8:14262. doi: 10.1038/ncomms14262. PubMed PMID: 28186126; PubMed Central PMCID: PMC5309787.

52. Broutier L, Mastrogiovanni G, Verstegen MM, Francies HE, Gavarro LM, Bradshaw CR, et al. Human primary liver cancer-derived organoid cultures for disease modeling and drug screening. Nature medicine. 2017;23(12):1424-35. doi: 10.1038/nm.4438. PubMed PMID: 29131160; PubMed Central PMCID: PMC5722201.

53. Fong ELS, Toh TB, Lin QXX, Liu Z, Hooi L, Mohd Abdul Rashid MB, et al. Generation of matched patient-derived xenograft in vitro-in vivo models using 3D macroporous hydrogels for the study of liver cancer. Biomaterials. 2018;159:229-40. doi: 10.1016/j.biomaterials.2017.12.026. PubMed PMID: 29353739.

54. Huang L, Holtzinger A, Jagan I, BeGora M, Lohse I, Ngai N, et al. Ductal pancreatic cancer modeling and drug screening using human pluripotent stem cell- and patient-derived tumor organoids. Nature medicine. 2015;21(11):1364-71. doi: 10.1038/nm.3973. PubMed PMID: 26501191; PubMed Central PMCID: PMC4753163.

55. Seino T, Kawasaki S, Shimokawa M, Tamagawa H, Toshimitsu K, Fujii M, et al. Human Pancreatic Tumor Organoids Reveal Loss of Stem Cell Niche Factor Dependence during Disease Progression. Cell stem cell. 2018;22(3):454-67 e6. doi: 10.1016/j.stem.2017.12.009. PubMed PMID: 29337182.

56. Linxweiler J, Hammer M, Muhs S, Kohn M, Pryalukhin A, Veith C, et al. Patient-derived, three-dimensional spheroid cultures provide a versatile translational model for the study of organ-confined prostate cancer. Journal of cancer research and clinical oncology. 2019;145(3):551-9. doi: 10.1007/s00432-018-2803-5. PubMed PMID: 30474758.

57. Lee SH, Hu W, Matulay JT, Silva MV, Owczarek TB, Kim K, et al. Tumor Evolution and Drug Response in Patient-Derived Organoid Models of Bladder Cancer. Cell. 2018;173(2):515-28 e17. doi: 10.1016/j.cell.2018.03.017. PubMed PMID: 29625057; PubMed Central PMCID: PMC5890941.

58. Tsai S, McOlash L, Palen K, Johnson B, Duris C, Yang Q, et al. Development of primary human pancreatic cancer organoids, matched stromal and immune cells and 3D tumor microenvironment models. BMC cancer. 2018;18(1):335. doi: 10.1186/s12885-018-4238-4. PubMed PMID: 29587663; PubMed Central PMCID: PMC5870823.

59. Cattaneo CM, Dijkstra KK, Fanchi LF, Kelderman S, Kaing S, van Rooij N, et al. Tumor organoid-T-cell coculture systems. Nature protocols. 2020;15(1):15-39. doi: 10.1038/s41596-019-0232-9. PubMed PMID: 31853056; PubMed Central PMCID: PMC7610702.

60. Dijkstra KK, Cattaneo CM, Weeber F, Chalabi M, van de Haar J, Fanchi LF, et al. Generation of Tumor-Reactive T Cells by Co-culture of Peripheral Blood Lymphocytes and Tumor Organoids. Cell. 2018;174(6):1586-98 e12. doi: 10.1016/j.cell.2018.07.009. PubMed PMID: 30100188; PubMed Central PMCID: PMC6558289.

61. Holokai L, Chakrabarti J, Lundy J, Croagh D, Adhikary P, Richards SS, et al. Murine- and Human-Derived Autologous Organoid/Immune Cell Co-Cultures as Pre-Clinical Models of Pancreatic Ductal Adenocarcinoma. Cancers. 2020;12(12). doi: 10.3390/cancers12123816. PubMed PMID: 33348809; PubMed Central PMCID: PMC7766822.

62. Marcon F, Zuo J, Pearce H, Nicol S, Margielewska-Davies S, Farhat M, et al. NK cells in pancreatic cancer demonstrate impaired cytotoxicity and a regulatory IL-10 phenotype. Oncoimmunology. 2020;9(1):1845424. doi: 10.1080/2162402X.2020.1845424. PubMed PMID: 33299656; PubMed Central PMCID: PMC7714501.

63. Erkan M, Hausmann S, Michalski CW, Fingerle AA, Dobritz M, Kleeff J, et al. The role of stroma in pancreatic cancer: diagnostic and therapeutic implications. Nature reviews Gastroenterology & hepatology. 2012;9(8):454-67. doi: 10.1038/nrgastro.2012.115. PubMed PMID: 22710569.

64. Feig C, Gopinathan A, Neesse A, Chan DS, Cook N, Tuveson DA. The pancreas cancer microenvironment. Clinical cancer research : an official journal of the American Association for Cancer Research. 2012;18(16):4266-76. doi: 10.1158/1078-0432.CCR-11-3114. PubMed PMID: 22896693; PubMed Central PMCID: PMC3442232.

65. Mortezaee K. Immune escape: A critical hallmark in solid tumors. Life sciences. 2020;258:118110. doi: 10.1016/j.lfs.2020.118110. PubMed PMID: 32698074.

66. Kumar BV, Connors TJ, Farber DL. Human T Cell Development, Localization, and Function throughout Life. Immunity. 2018;48(2):202-13. doi: 10.1016/j.immuni.2018.01.007. PubMed PMID: 29466753; PubMed Central PMCID: PMC5826622.

67. Golubovskaya V, Wu L. Different Subsets of T Cells, Memory, Effector Functions, and CAR-T Immunotherapy. Cancers. 2016;8(3). doi: 10.3390/cancers8030036. PubMed PMID: 26999211; PubMed Central PMCID: PMC4810120.

68. Luckheeram RV, Zhou R, Verma AD, Xia B. CD4(+)T cells: differentiation and functions. Clinical & developmental immunology. 2012;2012:925135. doi: 10.1155/2012/925135. PubMed PMID: 22474485; PubMed Central PMCID: PMC3312336.

69. Reina-Campos M, Scharping NE, Goldrath AW. CD8(+) T cell metabolism in infection and cancer. Nature reviews Immunology. 2021;21(11):718-38. doi: 10.1038/s41577-021-00537-8. PubMed PMID: 33981085; PubMed Central PMCID: PMC8806153.

70. Lugli E, Zanon V, Mavilio D, Roberto A. FACS Analysis of Memory T Lymphocytes. Methods in molecular biology. 2017;1514:31-47. doi: 10.1007/978-1-4939-6548-9_3. PubMed PMID: 27787790.

71. Lei X, Lei Y, Li JK, Du WX, Li RG, Yang J, et al. Immune cells within the tumor microenvironment: Biological functions and roles in cancer immunotherapy. Cancer letters. 2020;470:126-33. doi: 10.1016/j.canlet.2019.11.009. PubMed PMID: 31730903.

72. Farber DL, Yudanin NA, Restifo NP. Human memory T cells: generation, compartmentalization and homeostasis. Nature reviews Immunology. 2014;14(1):24-35. doi: 10.1038/nri3567. PubMed PMID: 24336101; PubMed Central PMCID: PMC4032067.

73. Sallusto F, Lenig D, Forster R, Lipp M, Lanzavecchia A. Two subsets of memory T lymphocytes with distinct homing potentials and effector functions. Nature. 1999;401(6754):708-12. doi: 10.1038/44385. PubMed PMID: 10537110.

74. Mueller SN, Gebhardt T, Carbone FR, Heath WR. Memory T cell subsets, migration patterns, and tissue residence. Annual review of immunology. 2013;31:137-61. doi: 10.1146/annurev-immunol-032712-095954. PubMed PMID: 23215646.

75. Youngblood B, Hale JS, Ahmed R. T-cell memory differentiation: insights from transcriptional signatures and epigenetics. Immunology. 2013;139(3):277-84. doi: 10.1111/imm.12074. PubMed PMID: 23347146; PubMed Central PMCID: PMC3701173.

76. Woodland DL, Kohlmeier JE. Migration, maintenance and recall of memory T cells in peripheral tissues. Nature reviews Immunology. 2009;9(3):153-61. doi: 10.1038/nri2496. PubMed PMID: 19240755.

77. Sallusto F, Geginat J, Lanzavecchia A. Central memory and effector memory T cell subsets: function, generation, and maintenance. Annual review of immunology. 2004;22:745-63. doi: 10.1146/annurev.immunol.22.012703.104702. PubMed PMID: 15032595.

78. Mueller SN, Mackay LK. Tissue-resident memory T cells: local specialists in immune defence. Nature reviews Immunology. 2016;16(2):79-89. doi: 10.1038/nri.2015.3. PubMed PMID: 26688350.

79. Lee YJ, Jameson SC, Hogquist KA. Alternative memory in the CD8 T cell lineage. Trends in immunology. 2011;32(2):50-6. doi: 10.1016/j.it.2010.12.004. PubMed PMID: 21288770; PubMed Central PMCID: PMC3039080.

80. Marusina AI, Ono Y, Merleev AA, Shimoda M, Ogawa H, Wang EA, et al. CD4(+) virtual memory: Antigen-inexperienced T cells reside in the naive, regulatory, and memory T cell compartments at similar frequencies, implications for autoimmunity. Journal of autoimmunity. 2017;77:76-88. doi: 10.1016/j.jaut.2016.11.001. PubMed PMID: 27894837; PubMed Central PMCID: PMC6066671.

81. Gattinoni L, Lugli E, Ji Y, Pos Z, Paulos CM, Quigley MF, et al. A human memory T cell subset with stem cell-like properties. Nature medicine. 2011;17(10):1290-7. doi: 10.1038/nm.2446. PubMed PMID: 21926977; PubMed Central PMCID: PMC3192229.

82. Nicholson LB. The immune system. Essays in biochemistry. 2016;60(3):275-301. doi: 10.1042/EBC20160017. PubMed PMID: 27784777; PubMed Central PMCID: PMC5091071.

83. Henning AN, Roychoudhuri R, Restifo NP. Epigenetic control of CD8(+) T cell differentiation. Nature reviews Immunology. 2018;18(5):340-56. doi: 10.1038/nri.2017.146. PubMed PMID: 29379213; PubMed Central PMCID: PMC6327307.

84. Kaech SM, Wherry EJ, Ahmed R. Effector and memory T-cell differentiation: implications for vaccine development. Nature reviews Immunology. 2002;2(4):251-62. doi: 10.1038/nri778. PubMed PMID: 12001996.

85. Togashi Y, Shitara K, Nishikawa H. Regulatory T cells in cancer immunosuppression - implications for anticancer therapy. Nature reviews Clinical oncology. 2019;16(6):356-71. doi:

10.1038/s41571-019-0175-7. PubMed PMID: 30705439.

86. Fu J, Xu D, Liu Z, Shi M, Zhao P, Fu B, et al. Increased regulatory T cells correlate with CD8 T-cell impairment and poor survival in hepatocellular carcinoma patients. Gastroenterology. 2007;132(7):2328-39. doi: 10.1053/j.gastro.2007.03.102. PubMed PMID: 17570208.

87. Petersen RP, Campa MJ, Sperlazza J, Conlon D, Joshi MB, Harpole DH, Jr., et al. Tumor infiltrating Foxp3+ regulatory T-cells are associated with recurrence in pathologic stage I NSCLC patients. Cancer. 2006;107(12):2866-72. doi: 10.1002/cncr.22282. PubMed PMID: 17099880.

88. Shen Z, Zhou S, Wang Y, Li RL, Zhong C, Liang C, et al. Higher intratumoral infiltrated Foxp3+ Treg numbers and Foxp3+/CD8+ ratio are associated with adverse prognosis in resectable gastric cancer. Journal of cancer research and clinical oncology. 2010;136(10):1585-95. doi: 10.1007/s00432-010-0816-9. PubMed PMID: 20221835.

89. Ziegler SF. FOXP3: of mice and men. Annual review of immunology. 2006;24:209-26. doi: 10.1146/annurev.immunol.24.021605.090547. PubMed PMID: 16551248.

90. Seddiki N, Santner-Nanan B, Martinson J, Zaunders J, Sasson S, Landay A, et al. Expression of interleukin (IL)-2 and IL-7 receptors discriminates between human regulatory and activated T cells. The Journal of experimental medicine. 2006;203(7):1693-700. doi: 10.1084/jem.20060468. PubMed PMID: 16818676; PubMed Central PMCID: PMC2118333.

91. Liu W, Putnam AL, Xu-Yu Z, Szot GL, Lee MR, Zhu S, et al. CD127 expression inversely correlates with FoxP3 and suppressive function of human CD4+ T reg cells. The Journal of experimental medicine. 2006;203(7):1701-11. doi: 10.1084/jem.20060772. PubMed PMID: 16818678; PubMed Central PMCID: PMC2118339.

92. Vignali DA, Collison LW, Workman CJ. How regulatory T cells work. Nature reviews Immunology. 2008;8(7):523-32. doi: 10.1038/nri2343. PubMed PMID: 18566595; PubMed Central PMCID: PMC2665249.

93. Workman CJ, Szymczak-Workman AL, Collison LW, Pillai MR, Vignali DA. The development and function of regulatory T cells. Cellular and molecular life sciences : CMLS. 2009;66(16):2603-22. doi: 10.1007/s00018-009-0026-2. PubMed PMID: 19390784; PubMed Central PMCID: PMC2715449.

94. Li C, Jiang P, Wei S, Xu X, Wang J. Regulatory T cells in tumor microenvironment: new mechanisms, potential therapeutic strategies and future prospects. Molecular cancer. 2020;19(1):116. doi: 10.1186/s12943-020-01234-1. PubMed PMID: 32680511; PubMed Central PMCID: PMC7367382.

95. Grover P, Goel PN, Greene MI. Regulatory T Cells: Regulation of Identity and Function. Frontiers in immunology. 2021;12:750542. doi: 10.3389/fimmu.2021.750542. PubMed PMID: 34675933; PubMed Central PMCID: PMC8524049.

96. Liakou CI, Kamat A, Tang DN, Chen H, Sun J, Troncoso P, et al. CTLA-4 blockade increases IFNgamma-producing CD4+ICOShi cells to shift the ratio of effector to regulatory T cells in cancer patients. Proceedings of the National Academy of Sciences of the United States of America. 2008;105(39):14987-92. doi: 10.1073/pnas.0806075105. PubMed PMID: 18818309; PubMed Central PMCID: PMC2567480.

97. Hodi FS, Butler M, Oble DA, Seiden MV, Haluska FG, Kruse A, et al. Immunologic and clinical effects of antibody blockade of cytotoxic T lymphocyte-associated antigen 4 in previously vaccinated cancer patients. Proceedings of the National Academy of Sciences of the United States of America. 2008;105(8):3005-10. doi: 10.1073/pnas.0712237105. PubMed PMID: 18287062; PubMed Central PMCID: PMC2268575.

98. Topalian SL, Hodi FS, Brahmer JR, Gettinger SN, Smith DC, McDermott DF, et al. Safety, activity, and immune correlates of anti-PD-1 antibody in cancer. The New England journal of medicine. 2012;366(26):2443-54. doi: 10.1056/NEJMoa1200690. PubMed PMID: 22658127; PubMed Central PMCID: PMC3544539.

99. Sugiyama D, Nishikawa H, Maeda Y, Nishioka M, Tanemura A, Katayama I, et al. Anti-CCR4 mAb selectively depletes effector-type FoxP3+CD4+ regulatory T cells, evoking antitumor immune responses in humans. Proceedings of the National Academy of Sciences of the United States of America. 2013;110(44):17945-50. doi: 10.1073/pnas.1316796110. PubMed PMID: 24127572; PubMed Central PMCID: PMC3816454.

100. Schaer DA, Budhu S, Liu C, Bryson C, Malandro N, Cohen A, et al. GITR pathway activation abrogates tumor immune suppression through loss of regulatory T cell lineage stability. Cancer immunology research. 2013;1(5):320-31. doi: 10.1158/2326-6066.CIR-13-0086. PubMed PMID: 24416730; PubMed Central PMCID: PMC3885345.

101. Tkachev V, Furlan SN, Watkins B, Hunt DJ, Zheng HB, Panoskaltsis-Mortari A, et al. Combined OX40L and mTOR blockade controls effector T cell activation while preserving Treg reconstitution after transplant. Science translational medicine. 2017;9(408). doi: 10.1126/scitranslmed.aan3085. PubMed PMID: 28931653; PubMed Central PMCID: PMC5681253.

102. Teng MW, Swann JB, von Scheidt B, Sharkey J, Zerafa N, McLaughlin N, et al. Multiple antitumor mechanisms downstream of prophylactic regulatory T-cell depletion. Cancer research. 2010;70(7):2665-74. doi: 10.1158/0008-5472.CAN-09-1574. PubMed PMID: 20332236.

103. Arce Vargas F, Furness AJS, Solomon I, Joshi K, Mekkaoui L, Lesko MH, et al. Fc-Optimized Anti-CD25 Depletes Tumor-Infiltrating Regulatory T Cells and Synergizes with PD-1 Blockade to Eradicate Established Tumors. Immunity. 2017;46(4):577-86. doi: 10.1016/j.immuni.2017.03.013. PubMed PMID: 28410988; PubMed Central PMCID: PMC5437702.

104. Tanaka A, Sakaguchi S. Regulatory T cells in cancer immunotherapy. Cell research. 2017;27(1):109-18. doi: 10.1038/cr.2016.151. PubMed PMID: 27995907; PubMed Central PMCID: PMC5223231.

105. LeBien TW, Tedder TF. B lymphocytes: how they develop and function. Blood. 2008;112(5):1570-80. doi: 10.1182/blood-2008-02-078071. PubMed PMID: 18725575; PubMed Central PMCID: PMC2518873.

106. Engelhard V, Conejo-Garcia JR, Ahmed R, Nelson BH, Willard-Gallo K, Bruno TC, et al. B cells and cancer. Cancer cell. 2021;39(10):1293-6. doi: 10.1016/j.ccell.2021.09.007. PubMed PMID: 34597591.

107. Wouters MCA, Nelson BH. Prognostic Significance of Tumor-Infiltrating B Cells and Plasma Cells in Human Cancer. Clinical cancer research : an official journal of the American Association for Cancer Research. 2018;24(24):6125-35. doi: 10.1158/1078-0432.CCR-18-1481. PubMed PMID: 30049748.

108. Garaud S, Buisseret L, Solinas C, Gu-Trantien C, de Wind A, Van den Eynden G, et al. Tumor infiltrating B-cells signal functional humoral immune responses in breast cancer. JCI insight. 2019;5. doi: 10.1172/jci.insight.129641. PubMed PMID: 31408436; PubMed Central PMCID: PMC6795287.

109. Kim SS, Sumner WA, Miyauchi S, Cohen EEW, Califano JA, Sharabi AB. Role of B Cells in Responses to Checkpoint Blockade Immunotherapy and Overall Survival of Cancer Patients. Clinical cancer research : an official journal of the American Association for Cancer Research. 2021;27(22):6075-82. doi: 10.1158/1078-0432.CCR-21-0697. PubMed PMID: 34230025; PubMed Central PMCID: PMC8976464.

110. Kemp TJ, Moore JM, Griffith TS. Human B cells express functional TRAIL/Apo-2 ligand after CpG-containing oligodeoxynucleotide stimulation. Journal of immunology. 2004;173(2):892-9. doi: 10.4049/jimmunol.173.2.892. PubMed PMID: 15240676.

111. Shalapour S, Font-Burgada J, Di Caro G, Zhong Z, Sanchez-Lopez E, Dhar D, et al. Immunosuppressive plasma cells impede T-cell-dependent immunogenic chemotherapy. Nature. 2015;521(7550):94-8. doi: 10.1038/nature14395. PubMed PMID: 25924065; PubMed Central PMCID: PMC4501632.

112. Vivier E, Raulet DH, Moretta A, Caligiuri MA, Zitvogel L, Lanier LL, et al. Innate or

adaptive immunity? The example of natural killer cells. Science. 2011;331(6013):44-9. doi: 10.1126/science.1198687. PubMed PMID: 21212348; PubMed Central PMCID: PMC3089969.

113. Abel AM, Yang C, Thakar MS, Malarkannan S. Natural Killer Cells: Development, Maturation, and Clinical Utilization. Frontiers in immunology. 2018;9:1869. doi: 10.3389/fimmu.2018.01869. PubMed PMID: 30150991; PubMed Central PMCID: PMC6099181.

114. Conlon KC, Lugli E, Welles HC, Rosenberg SA, Fojo AT, Morris JC, et al. Redistribution, hyperproliferation, activation of natural killer cells and CD8 T cells, and cytokine production during first-in-human clinical trial of recombinant human interleukin-15 in patients with cancer. Journal of clinical oncology : official journal of the American Society of Clinical Oncology. 2015;33(1):74-82. doi: 10.1200/JCO.2014.57.3329. PubMed PMID: 25403209; PubMed Central PMCID: PMC4268254.

115. Conlon KC, Potter EL, Pittaluga S, Lee CR, Miljkovic MD, Fleisher TA, et al. IL15 by Continuous Intravenous Infusion to Adult Patients with Solid Tumors in a Phase I Trial Induced Dramatic NK-Cell Subset Expansion. Clinical cancer research : an official journal of the American Association for Cancer Research. 2019;25(16):4945-54. doi: 10.1158/1078-0432.CCR-18-3468. PubMed PMID: 31142503; PubMed Central PMCID: PMC6697593.

116. Vivier E, Ugolini S, Blaise D, Chabannon C, Brossay L. Targeting natural killer cells and natural killer T cells in cancer. Nature reviews Immunology. 2012;12(4):239-52. doi: 10.1038/nri3174. PubMed PMID: 22437937; PubMed Central PMCID: PMC5161343.

117.Davis ZB, Felices M, Verneris MR, Miller JS. Natural Killer Cell Adoptive Transfer Therapy: Exploiting the First Line of Defense Against Cancer. Cancer journal. 2015;21(6):486-91. doi: 10.1097/PPO.0000000000000156. PubMed PMID: 26588681; PubMed Central PMCID: PMC4763946.

118. Wu SY, Fu T, Jiang YZ, Shao ZM. Natural killer cells in cancer biology and therapy. Molecular cancer. 2020;19(1):120. doi: 10.1186/s12943-020-01238-x. PubMed PMID: 32762681; PubMed Central PMCID: PMC7409673.

119. Fridlender ZG, Sun J, Kim S, Kapoor V, Cheng G, Ling L, et al. Polarization of tumor-associated neutrophil phenotype by TGF-beta: "N1" versus "N2" TAN. Cancer cell. 2009;16(3):183-94. doi: 10.1016/j.ccr.2009.06.017. PubMed PMID: 19732719; PubMed Central PMCID: PMC2754404.

120. Matlung HL, Babes L, Zhao XW, van Houdt M, Treffers LW, van Rees DJ, et al. Neutrophils Kill Antibody-Opsonized Cancer Cells by Trogoptosis. Cell reports. 2018;23(13):3946-59 e6. doi: 10.1016/j.celrep.2018.05.082. PubMed PMID: 29949776.

121. Eruslanov EB, Bhojnagarwala PS, Quatromoni JG, Stephen TL, Ranganathan A, Deshpande C, et al. Tumor-associated neutrophils stimulate T cell responses in early-stage human lung cancer. The Journal of clinical investigation. 2014;124(12):5466-80. doi: 10.1172/JCI77053. PubMed PMID: 25384214; PubMed Central PMCID: PMC4348966.

122. Singhal S, Bhojnagarwala PS, O'Brien S, Moon EK, Garfall AL, Rao AS, et al. Origin and Role of a Subset of Tumor-Associated Neutrophils with Antigen-Presenting Cell Features in Early-Stage Human Lung Cancer. Cancer cell. 2016;30(1):120-35. doi: 10.1016/j.ccell.2016.06.001. PubMed PMID: 27374224; PubMed Central PMCID: PMC4945447.

123. Shaul ME, Levy L, Sun J, Mishalian I, Singhal S, Kapoor V, et al. Tumor-associated neutrophils display a distinct N1 profile following TGFbeta modulation: A transcriptomics analysis of pro- vs. antitumor TANs. Oncoimmunology. 2016;5(11):e1232221. doi: 10.1080/2162402X.2016.1232221. PubMed PMID: 27999744; PubMed Central PMCID: PMC5139653.

124. Li TJ, Jiang YM, Hu YF, Huang L, Yu J, Zhao LY, et al. Interleukin-17-Producing Neutrophils Link Inflammatory Stimuli to Disease Progression by Promoting Angiogenesis in Gastric Cancer. Clinical cancer research : an official journal of the American Association for Cancer Research. 2017;23(6):1575-85. doi: 10.1158/1078-0432.CCR-16-0617. PubMed PMID: 27620275.

125. Coffelt SB, Kersten K, Doornebal CW, Weiden J, Vrijland K, Hau CS, et al. IL-17-producing gammadelta T cells and neutrophils conspire to promote breast cancer metastasis. Nature. 2015;522(7556):345-8. doi: 10.1038/nature14282. PubMed PMID: 25822788; PubMed Central PMCID: PMC4475637.

126. Lecot P, Sarabi M, Pereira Abrantes M, Mussard J, Koenderman L, Caux C, et al. Neutrophil Heterogeneity in Cancer: From Biology to Therapies. Frontiers in immunology. 2019;10:2155. doi: 10.3389/fimmu.2019.02155. PubMed PMID: 31616408; PubMed Central PMCID: PMC6764113.

127. Liu K, Nussenzweig MC. Origin and development of dendritic cells. Immunological reviews. 2010;234(1):45-54. doi: 10.1111/j.0105-2896.2009.00879.x. PubMed PMID: 20193011.

128. Boscardin SB, Dudziak D, Munz C, Rosa DS. Editorial: Harnessing the Participation of Dendritic Cells in Immunity and Tolerance. Frontiers in immunology. 2020;11:595841. doi: 10.3389/fimmu.2020.595841. PubMed PMID: 33117409; PubMed Central PMCID: PMC7575758.

129. Steinman RM, Banchereau J. Taking dendritic cells into medicine. Nature. 2007;449(7161):419-26. doi: 10.1038/nature06175. PubMed PMID: 17898760.

130. Eyileten C, Majchrzak K, Pilch Z, Tonecka K, Mucha J, Taciak B, et al. Immune Cells in Cancer Therapy and Drug Delivery. Mediators of inflammation. 2016;2016:5230219. doi: 10.1155/2016/5230219. PubMed PMID: 27212807; PubMed Central PMCID: PMC4860248.

131. Perez CR, De Palma M. Engineering dendritic cell vaccines to improve cancer immunotherapy. Nature communications. 2019;10(1):5408. doi: 10.1038/s41467-019-13368-y. PubMed PMID: 31776331; PubMed Central PMCID: PMC6881351.

132. Wculek SK, Cueto FJ, Mujal AM, Melero I, Krummel MF, Sancho D. Dendritic cells in cancer immunology and immunotherapy. Nature reviews Immunology. 2020;20(1):7-24. doi: 10.1038/s41577-019-0210-z. PubMed PMID: 31467405.

133. Murray PJ, Wynn TA. Protective and pathogenic functions of macrophage subsets. Nature reviews Immunology. 2011;11(11):723-37. doi: 10.1038/nri3073. PubMed PMID: 21997792; PubMed Central PMCID: PMC3422549.

134. Tanaka A, Sakaguchi S. Targeting Treg cells in cancer immunotherapy. European journal of immunology. 2019;49(8):1140-6. doi: 10.1002/eji.201847659. PubMed PMID: 31257581.

135. Chen Y, Zhang X. Pivotal regulators of tissue homeostasis and cancer: macrophages. Experimental hematology & oncology. 2017;6:23. doi: 10.1186/s40164-017-0083-4. PubMed PMID: 28804688; PubMed Central PMCID: PMC5549331.

136. Long KB, Beatty GL. Harnessing the antitumor potential of macrophages for cancer immunotherapy. Oncoimmunology. 2013;2(12):e26860. doi: 10.4161/onci.26860. PubMed PMID: 24498559; PubMed Central PMCID: PMC3902119.

137. Pathria P, Louis TL, Varner JA. Targeting Tumor-Associated Macrophages in Cancer. Trends in immunology. 2019;40(4):310-27. doi: 10.1016/j.it.2019.02.003. PubMed PMID: 30890304.

138. Pan Y, Yu Y, Wang X, Zhang T. Tumor-Associated Macrophages in Tumor Immunity. Frontiers in immunology. 2020;11:583084. doi: 10.3389/fimmu.2020.583084. PubMed PMID: 33365025; PubMed Central PMCID: PMC7751482.

139. Nakamura K, Smyth MJ. Myeloid immunosuppression and immune checkpoints in the tumor microenvironment. Cellular & molecular immunology. 2020;17(1):1-12. doi: 10.1038/s41423-019-0306-1. PubMed PMID: 31611651; PubMed Central PMCID: PMC6952382.

140. Ma T, Renz BW, Ilmer M, Koch D, Yang Y, Werner J, et al. Myeloid-Derived Suppressor Cells in Solid Tumors. Cells. 2022;11(2). doi: 10.3390/cells11020310. PubMed PMID: 35053426; PubMed Central PMCID: PMC8774531.

141. Bronte V, Brandau S, Chen SH, Colombo MP, Frey AB, Greten TF, et al. Recommendations for myeloid-derived suppressor cell nomenclature and characterization standards. Nature communications. 2016;7:12150. doi: 10.1038/ncomms12150. PubMed PMID: 27381735; PubMed Central PMCID: PMC4935811.

142. Sieminska I, Baran J. Myeloid-Derived Suppressor Cells in Colorectal Cancer. Frontiers in immunology. 2020;11:1526. doi: 10.3389/fimmu.2020.01526. PubMed PMID: 32849517; PubMed Central PMCID: PMC7426395.

143. Jiang H, Gebhardt C, Umansky L, Beckhove P, Schulze TJ, Utikal J, et al. Elevated chronic inflammatory factors and myeloid-derived suppressor cells indicate poor prognosis in advanced melanoma patients. International journal of cancer. 2015;136(10):2352-60. doi: 10.1002/ijc.29297. PubMed PMID: 25353097.

144. Gao XH, Tian L, Wu J, Ma XL, Zhang CY, Zhou Y, et al. Circulating CD14(+) HLA-DR(-/low) myeloid-derived suppressor cells predicted early recurrence of hepatocellular carcinoma after surgery. Hepatology research : the official journal of the Japan Society of Hepatology. 2017;47(10):1061-71. doi: 10.1111/hepr.12831. PubMed PMID: 27764536.

145. Xiao L, Erb U, Zhao K, Hackert T, Zoller M. Efficacy of vaccination with tumor-exosome loaded dendritic cells combined with cytotoxic drug treatment in pancreatic cancer. Oncoimmunology. 2017;6(6):e1319044. doi: 10.1080/2162402X.2017.1319044. PubMed PMID: 28680753; PubMed Central PMCID: PMC5486185.

146. Tai LH, Alkayyal AA, Leslie AL, Sahi S, Bennett S, Tanese de Souza C, et al. Phosphodiesterase-5 inhibition reduces postoperative metastatic disease by targeting surgery-induced myeloid derived suppressor cell-dependent inhibition of Natural Killer cell cytotoxicity. Oncoimmunology. 2018;7(6):e1431082. doi: 10.1080/2162402X.2018.1431082. PubMed PMID: 29872554; PubMed Central PMCID: PMC5980420.

147. Liu J, Toy R, Vantucci C, Pradhan P, Zhang Z, Kuo KM, et al. Bifunctional Janus Particles as Multivalent Synthetic Nanoparticle Antibodies (SNAbs) for Selective Depletion of Target Cells. Nano letters. 2021;21(1):875-86. doi: 10.1021/acs.nanolett.0c04833. PubMed PMID: 33395313; PubMed Central PMCID: PMC8176937.

148. Zhang Y, Zhang Z. The history and advances in cancer immunotherapy: understanding the characteristics of tumor-infiltrating immune cells and their therapeutic implications. Cellular & molecular immunology. 2020;17(8):807-21. doi: 10.1038/s41423-020-0488-6. PubMed PMID: 32612154; PubMed Central PMCID: PMC7395159.

149. Xue H, Lu B, Lai M. The cancer secretome: a reservoir of biomarkers. Journal of translational medicine. 2008;6:52. doi: 10.1186/1479-5876-6-52. PubMed PMID: 18796163; PubMed Central PMCID: PMC2562990.

150. Leinwand J, Miller G. Regulation and modulation of antitumor immunity in pancreatic cancer. Nature immunology. 2020;21(10):1152-9. doi: 10.1038/s41590-020-0761-y. PubMed PMID: 32807942.

151. Kennedy LB, Salama AKS. A review of cancer immunotherapy toxicity. CA: a cancer journal for clinicians. 2020;70(2):86-104. doi: 10.3322/caac.21596. PubMed PMID: 31944278.

152. Banerjee K, Kumar S, Ross KA, Gautam S, Poelaert B, Nasser MW, et al. Emerging trends in the immunotherapy of pancreatic cancer. Cancer letters. 2018;417:35-46. doi: 10.1016/j.canlet.2017.12.012. PubMed PMID: 29242097; PubMed Central PMCID: PMC5801196.

153. van de Wetering M, Francies HE, Francis JM, Bounova G, Iorio F, Pronk A, et al. Prospective derivation of a living organoid biobank of colorectal cancer patients. Cell. 2015;161(4):933-45. doi: 10.1016/j.cell.2015.03.053. PubMed PMID: 25957691; PubMed Central PMCID: PMC6428276.

154. Grassi L, Alfonsi R, Francescangeli F, Signore M, De Angelis ML, Addario A, et al. Organoids as a new model for improving regenerative medicine and cancer personalized therapy in renal diseases. Cell death & disease. 2019;10(3):201. doi: 10.1038/s41419-019-1453-0. PubMed PMID: 30814510; PubMed Central PMCID: PMC6393468.

155. Shi R, Radulovich N, Ng C, Liu N, Notsuda H, Cabanero M, et al. Organoid Cultures as Preclinical Models of Non-Small Cell Lung Cancer. Clinical cancer research : an official journal of the American Association for Cancer Research. 2020;26(5):1162-74. doi: 10.1158/1078-0432.CCR-19-1376. PubMed PMID: 31694835.

156. Dowling P, Clynes M. Conditioned media from cell lines: a complementary model to clinical specimens for the discovery of disease-specific biomarkers. Proteomics. 2011;11(4):794-804. doi: 10.1002/pmic.201000530. PubMed PMID: 21229588.

157. Okada SL, Simmons RM, Franke-Welch S, Nguyen TH, Korman AJ, Dillon SR, et al. Conditioned media from the renal cell carcinoma cell line 786.O drives human blood monocytes to a monocytic myeloid-derived suppressor cell phenotype. Cellular immunology. 2018;323:49-58. doi: 10.1016/j.cellimm.2017.10.014. PubMed PMID: 29103587.

158. Mohebbi B, Ashtibaghaei K, Hashemi M, Hashemi M, Asadzadeh Aghdaei H, Zali MR. Conditioned Medium from Cultured Colorectal Cancer Cells Affects Peripheral Blood Mononuclear Cells Inflammatory Phenotype in Vitro. Iranian journal of medical sciences. 2019;44(4):334-41. doi: 10.30476/IJMS.2019.44959. PubMed PMID: 31439977; PubMed Central PMCID: PMC6661523.

159. Bharadwaj U, Li M, Zhang R, Chen C, Yao Q. Elevated interleukin-6 and G-CSF in human

pancreatic cancer cell conditioned medium suppress dendritic cell differentiation and activation. Cancer research. 2007;67(11):5479-88. doi: 10.1158/0008-5472.CAN-06-3963. PubMed PMID: 17545630.

160. Du J, Wang J, Tan G, Cai Z, Zhang L, Tang B, et al. Aberrant elevated microRNA-146a in dendritic cells (DC) induced by human pancreatic cancer cell line BxPC-3-conditioned medium inhibits DC maturation and activation. Medical oncology. 2012;29(4):2814-23. doi: 10.1007/s12032-012-0175-2. PubMed PMID: 22311263.

161. MacLeod MK, Kappler JW, Marrack P. Memory CD4 T cells: generation, reactivation and re-assignment. Immunology. 2010;130(1):10-5. doi: 10.1111/j.1365-2567.2010.03260.x. PubMed PMID: 20331469; PubMed Central PMCID: PMC2855788.

162. Liu Q, Sun Z, Chen L. Memory T cells: strategies for optimizing tumor immunotherapy. Protein & cell. 2020;11(8):549-64. doi: 10.1007/s13238-020-00707-9. PubMed PMID: 32221812; PubMed Central PMCID: PMC7381543.

163. Barski A, Cuddapah S, Kartashov AV, Liu C, Imamichi H, Yang W, et al. Rapid Recall Ability of Memory T cells is Encoded in their Epigenome. Scientific reports. 2017;7:39785. doi: 10.1038/srep39785. PubMed PMID: 28054639; PubMed Central PMCID: PMC5215294 software development and provides bioinformatics support services, including installation of BioWardrobe.

164. Oleinika K, Nibbs RJ, Graham GJ, Fraser AR. Suppression, subversion and escape: the role of regulatory T cells in cancer progression. Clinical and experimental immunology. 2013;171(1):36-45. doi: 10.1111/j.1365-2249.2012.04657.x. PubMed PMID: 23199321; PubMed Central PMCID: PMC3530093.

165. Gradiz R, Silva HC, Carvalho L, Botelho MF, Mota-Pinto A. MIA PaCa-2 and PANC-1 - pancreas ductal adenocarcinoma cell lines with neuroendocrine differentiation and somatostatin receptors. Scientific reports. 2016;6:21648. doi: 10.1038/srep21648. PubMed PMID: 26884312; PubMed Central PMCID: PMC4756684.

166. Shen Y, Pu K, Zheng K, Ma X, Qin J, Jiang L, et al. Differentially Expressed microRNAs in MIA PaCa-2 and PANC-1 Pancreas Ductal Adenocarcinoma Cell Lines are Involved in Cancer Stem Cell Regulation. International journal of molecular sciences. 2019;20(18). doi: 10.3390/ijms20184473. PubMed PMID: 31510100; PubMed Central PMCID: PMC6770012.

167. Akondy RS, Fitch M, Edupuganti S, Yang S, Kissick HT, Li KW, et al. Origin and differentiation of human memory CD8 T cells after vaccination. Nature. 2017;552(7685):362-7. doi: 10.1038/nature24633. PubMed PMID: 29236685; PubMed Central PMCID: PMC6037316.

168. Youngblood B, Hale JS, Kissick HT, Ahn E, Xu X, Wieland A, et al. Effector CD8 T cells dedifferentiate into long-lived memory cells. Nature. 2017;552(7685):404-9. doi:

10.1038/nature25144. PubMed PMID: 29236683; PubMed Central PMCID: PMC5965677.

169. Liu HL, Guan CJ, Wu YJ, Hu MG, Zhao ZM, Liu R. Clinical Significance of Preoperative CD8+ Central Memory T Cells for Operable Pancreatic Adenocarcinoma. Digestive surgery. 2015;32(6):433-8. doi: 10.1159/000440681. PubMed PMID: 26402444.

170. Hang J, Huang J, Zhou S, Wu L, Zhu Y, Zhu L, et al. The clinical implication of CD45RA(+) naive T cells and CD45RO(+) memory T cells in advanced pancreatic cancer: a proxy for tumor biology and outcome prediction. Cancer medicine. 2019;8(3):1326-35. doi: 10.1002/cam4.1988. PubMed PMID: 30767430; PubMed Central PMCID: PMC6434335.

171. Hiraoka N, Onozato K, Kosuge T, Hirohashi S. Prevalence of FOXP3+ regulatory T cells increases during the progression of pancreatic ductal adenocarcinoma and its premalignant lesions. Clinical cancer research : an official journal of the American Association for Cancer Research. 2006;12(18):5423-34. doi: 10.1158/1078-0432.CCR-06-0369. PubMed PMID: 17000676.

172. Curiel TJ, Coukos G, Zou L, Alvarez X, Cheng P, Mottram P, et al. Specific recruitment of regulatory T cells in ovarian carcinoma fosters immune privilege and predicts reduced survival. Nature medicine. 2004;10(9):942-9. doi: 10.1038/nm1093. PubMed PMID: 15322536.

173. Bates GJ, Fox SB, Han C, Leek RD, Garcia JF, Harris AL, et al. Quantification of regulatory T cells enables the identification of high-risk breast cancer patients and those at risk of late relapse. Journal of clinical oncology : official journal of the American Society of Clinical Oncology. 2006;24(34):5373-80. doi: 10.1200/JCO.2006.05.9584. PubMed PMID: 17135638.

174. Griffiths RW, Elkord E, Gilham DE, Ramani V, Clarke N, Stern PL, et al. Frequency of regulatory T cells in renal cell carcinoma patients and investigation of correlation with survival. Cancer immunology, immunotherapy : CII. 2007;56(11):1743-53. doi: 10.1007/s00262-007-0318-z. PubMed PMID: 17487490.

175. Jordanova ES, Gorter A, Ayachi O, Prins F, Durrant LG, Kenter GG, et al. Human leukocyte antigen class I, MHC class I chain-related molecule A, and CD8+/regulatory T-cell ratio: which variable determines survival of cervical cancer patients? Clinical cancer research : an official journal of the American Association for Cancer Research. 2008;14(7):2028-35. doi: 10.1158/1078-0432.CCR-07-4554. PubMed PMID: 18381941.

176. Bae J, Samur M, Munshi A, Hideshima T, Keskin D, Kimmelman A, et al. Heteroclitic XBP1 peptides evoke tumor-specific memory cytotoxic T lymphocytes against breast cancer, colon cancer, and pancreatic cancer cells. Oncoimmunology. 2014;3(12):e970914. doi: 10.4161/21624011.2014.970914. PubMed PMID: 25941601; PubMed Central PMCID: PMC4356023.

177. Sakaguchi S, Mikami N, Wing JB, Tanaka A, Ichiyama K, Ohkura N. Regulatory T Cells

and Human Disease. Annual review of immunology. 2020;38:541-66. doi: 10.1146/annurev-immunol-042718-041717. PubMed PMID: 32017635.

178. Munn DH, Bronte V. Immune suppressive mechanisms in the tumor microenvironment. Current opinion in immunology. 2016;39:1-6. doi: 10.1016/j.coi.2015.10.009. PubMed PMID: 26609943; PubMed Central PMCID: PMC5627973.

179. Ivashkiv LB. IFNgamma: signalling, epigenetics and roles in immunity, metabolism, disease and cancer immunotherapy. Nature reviews Immunology. 2018;18(9):545-58. doi: 10.1038/s41577-018-0029-z. PubMed PMID: 29921905; PubMed Central PMCID: PMC6340644.

180. Ni C, Wu P, Zhu X, Ye J, Zhang Z, Chen Z, et al. IFN-gamma selectively exerts pro-apoptotic effects on tumor-initiating label-retaining colon cancer cells. Cancer letters. 2013;336(1):174-84. doi: 10.1016/j.canlet.2013.04.029. PubMed PMID: 23643941.

181. Hao Q, Tang H. Interferon-gamma and Smac mimetics synergize to induce apoptosis of lung cancer cells in a TNFalpha-independent manner. Cancer cell international. 2018;18:84. doi: 10.1186/s12935-018-0579-y. PubMed PMID: 29946223; PubMed Central PMCID: PMC6001173.

182. Song M, Ping Y, Zhang K, Yang L, Li F, Zhang C, et al. Low-Dose IFNgamma Induces Tumor Cell Stemness in Tumor Microenvironment of Non-Small Cell Lung Cancer. Cancer research. 2019;79(14):3737-48. doi: 10.1158/0008-5472.CAN-19-0596. PubMed PMID: 31085700.

183. Martynova E, Rizvanov A, Urbanowicz RA, Khaiboullina S. Inflammasome Contribution to the Activation of Th1, Th2, and Th17 Immune Responses. Frontiers in microbiology. 2022;13:851835. doi: 10.3389/fmicb.2022.851835. PubMed PMID: 35369454; PubMed Central PMCID: PMC8969514.

184. Gocher AM, Workman CJ, Vignali DAA. Interferon-gamma: teammate or opponent in the tumour microenvironment? Nature reviews Immunology. 2022;22(3):158-72. doi: 10.1038/s41577-021-00566-3. PubMed PMID: 34155388; PubMed Central PMCID: PMC8688586.

185. Waldrop SL, Davis KA, Maino VC, Picker LJ. Normal human CD4+ memory T cells display broad heterogeneity in their activation threshold for cytokine synthesis. Journal of immunology. 1998;161(10):5284-95. PubMed PMID: 9820501.

186. Foster B, Prussin C, Liu F, Whitmire JK, Whitton JL. Detection of intracellular cytokines by flow cytometry. Current protocols in immunology. 2007;Chapter 6:Unit 6 24. doi: 10.1002/0471142735.im0624s78. PubMed PMID: 18432993.

187. Drost J, Clevers H. Organoids in cancer research. Nature reviews Cancer. 2018;18(7):407-18. doi: 10.1038/s41568-018-0007-6. PubMed PMID: 29692415.

188. Staab JF, Lemme-Dumit JM, Latanich R, Pasetti MF, Zachos NC. Co-Culture System of Human Enteroids/Colonoids with Innate Immune Cells. Current protocols in immunology. 2020;131(1):e113. doi: 10.1002/cpim.113. PubMed PMID: 33166041; PubMed Central PMCID: PMC8363138.

189. Meng Q, Xie S, Gray GK, Dezfulian MH, Li W, Huang L, et al. Empirical identification and validation of tumor-targeting T cell receptors from circulation using autologous pancreatic tumor organoids. Journal for immunotherapy of cancer. 2021;9(11). doi: 10.1136/jitc-2021-003213. PubMed PMID: 34789550; PubMed Central PMCID: PMC8601084.

190. Zhou G, Lieshout R, van Tienderen GS, de Ruiter V, van Royen ME, Boor PPC, et al. Modelling immune cytotoxicity for cholangiocarcinoma with tumour-derived organoids and effector T cells. British journal of cancer. 2022. doi: 10.1038/s41416-022-01839-x. PubMed PMID: 35597867.

191. Restifo NP, Gattinoni L. Lineage relationship of effector and memory T cells. Current opinion in immunology. 2013;25(5):556-63. doi: 10.1016/j.coi.2013.09.003. PubMed PMID: 24148236; PubMed Central PMCID: PMC3858177.

192. Pepper M, Jenkins MK. Origins of CD4(+) effector and central memory T cells. Nature immunology. 2011;12(6):467-71. doi: 10.1038/ni.2038. PubMed PMID: 21739668; PubMed Central PMCID: PMC4212218.

193. Miron M, Meng W, Rosenfeld AM, Dvorkin S, Poon MML, Lam N, et al. Maintenance of the human memory T cell repertoire by subset and tissue site. Genome medicine. 2021;13(1):100. doi: 10.1186/s13073-021-00918-7. PubMed PMID: 34127056; PubMed Central PMCID: PMC8204429.

194. Berard M, Tough DF. Qualitative differences between naive and memory T cells. Immunology. 2002;106(2):127-38. doi: 10.1046/j.1365-2567.2002.01447.x. PubMed PMID: 12047742; PubMed Central PMCID: PMC1782715.

195. Tanel A, Fonseca SG, Yassine-Diab B, Bordi R, Zeidan J, Shi Y, et al. Cellular and molecular mechanisms of memory T-cell survival. Expert review of vaccines. 2009;8(3):299-312. doi: 10.1586/14760584.8.3.299. PubMed PMID: 19249972; PubMed Central PMCID: PMC2680212.

196. Holmes S, He M, Xu T, Lee PP. Memory T cells have gene expression patterns intermediate between naive and effector. Proceedings of the National Academy of Sciences of the United States of America. 2005;102(15):5519-23. doi: 10.1073/pnas.0501437102. PubMed PMID: 15809420; PubMed Central PMCID: PMC556264.

197. Bouneaud C, Garcia Z, Kourilsky P, Pannetier C. Lineage relationships, homeostasis, and recall capacities of central- and effector-memory CD8 T cells in vivo. The Journal of experimental medicine. 2005;201(4):579-90. doi: 10.1084/jem.20040876. PubMed PMID: 15710650; PubMed Central PMCID: PMC2213051.

198. Yamamoto T, Yanagimoto H, Satoi S, Toyokawa H, Hirooka S, Yamaki S, et al. Circulating CD4+CD25+ regulatory T cells in patients with pancreatic cancer. Pancreas. 2012;41(3):409-15. doi: 10.1097/MPA.0b013e3182373a66. PubMed PMID: 22158072.

199. Zhou W, Zhou Y, Chen X, Ning T, Chen H, Guo Q, et al. Pancreatic cancer-targeting exosomes for enhancing immunotherapy and reprogramming tumor microenvironment. Biomaterials. 2021;268:120546. doi: 10.1016/j.biomaterials.2020.120546. PubMed PMID: 33253966.

200. Zhang Y, Lazarus J, Steele NG, Yan W, Lee HJ, Nwosu ZC, et al. Regulatory T-cell Depletion Alters the Tumor Microenvironment and Accelerates Pancreatic Carcinogenesis. Cancer discovery. 2020;10(3):422-39. doi: 10.1158/2159-8290.CD-19-0958. PubMed PMID: 31911451; PubMed Central PMCID: PMC7224338.

201. Zhang X, Lao M, Xu J, Duan Y, Yang H, Li M, et al. Combination cancer immunotherapy targeting TNFR2 and PD-1/PD-L1 signaling reduces immunosuppressive effects in the microenvironment of pancreatic tumors. Journal for immunotherapy of cancer. 2022;10(3). doi: 10.1136/jitc-2021-003982. PubMed PMID: 35260434; PubMed Central PMCID: PMC8906048.

202. Shafiekhani S, Dehghanbanadaki H, Fatemi AS, Rahbar S, Hadjati J, Jafari AH. Prediction of anti-CD25 and 5-FU treatments efficacy for pancreatic cancer using a mathematical model. BMC cancer. 2021;21(1):1226. doi: 10.1186/s12885-021-08770-z. PubMed PMID: 34781899; PubMed Central PMCID: PMC8594222.

203. Vodnala SK, Eil R, Kishton RJ, Sukumar M, Yamamoto TN, Ha NH, et al. T cell stemness and dysfunction in tumors are triggered by a common mechanism. Science. 2019;363(6434). doi: 10.1126/science.aau0135. PubMed PMID: 30923193; PubMed Central PMCID: PMC8194369.

204. Neesse A, Bauer CA, Ohlund D, Lauth M, Buchholz M, Michl P, et al. Stromal biology and therapy in pancreatic cancer: ready for clinical translation? Gut. 2019;68(1):159-71. doi: 10.1136/gutjnl-2018-316451. PubMed PMID: 30177543.

205. Beato F, Reveron D, Dezsi KB, Ortiz A, Johnson JO, Chen DT, et al. Establishing a living biobank of patient-derived organoids of intraductal papillary mucinous neoplasms of the pancreas. Laboratory investigation; a journal of technical methods and pathology. 2021;101(2):204-17. doi: 10.1038/s41374-020-00494-1. PubMed PMID: 33037322; PubMed Central PMCID: PMC7855435.

206. Tiriac H, Bucobo JC, Tzimas D, Grewel S, Lacomb JF, Rowehl LM, et al. Successful creation of pancreatic cancer organoids by means of EUS-guided fine-needle biopsy sampling for personalized cancer treatment. Gastrointestinal endoscopy. 2018;87(6):1474-80. doi: 10.1016/j.gie.2017.12.032. PubMed PMID: 29325707; PubMed Central PMCID: PMC6143289.

207. Zahmatkesh E, Khoshdel-Rad N, Mirzaei H, Shpichka A, Timashev P, Mahmoudi T, et al. Evolution of organoid technology: Lessons learnt in Co-Culture systems from developmental biology. Developmental biology. 2021;475:37-53. doi: 10.1016/j.ydbio.2021.03.001. PubMed PMID: 33684433.

208. Gronholm M, Feodoroff M, Antignani G, Martins B, Hamdan F, Cerullo V. Patient-Derived Organoids for Precision Cancer Immunotherapy. Cancer research. 2021;81(12):3149-55. doi: 10.1158/0008-5472.CAN-20-4026. PubMed PMID: 33687948.

209. Kook YM, Jeong Y, Lee K, Koh WG. Design of biomimetic cellular scaffolds for co-culture system and their application. Journal of tissue engineering. 2017;8:2041731417724640. doi: 10.1177/2041731417724640. PubMed PMID: 29081966; PubMed Central PMCID: PMC5564857.

210. Frohlich E. Comparison of conventional and advanced in vitro models in the toxicity testing of nanoparticles. Artificial cells, nanomedicine, and biotechnology. 2018;46(sup2):1091-107. doi: 10.1080/21691401.2018.1479709. PubMed PMID: 29956556; PubMed Central PMCID: PMC6214528.

211. Campbell PJ, Yachida S, Mudie LJ, Stephens PJ, Pleasance ED, Stebbings LA, et al. The patterns and dynamics of genomic instability in metastatic pancreatic cancer. Nature. 2010;467(7319):1109-13. doi: 10.1038/nature09460. PubMed PMID: 20981101; PubMed Central PMCID: PMC3137369.

212. Almendro V, Marusyk A, Polyak K. Cellular heterogeneity and molecular evolution in cancer. Annual review of pathology. 2013;8:277-302. doi: 10.1146/annurev-pathol-020712-163923. PubMed PMID: 23092187.

213. Verbeke C. Morphological heterogeneity in ductal adenocarcinoma of the pancreas - Does it matter? Pancreatology : official journal of the International Association of Pancreatology. 2016;16(3):295-301. doi: 10.1016/j.pan.2016.02.004. PubMed PMID: 26924665.

Acknowledgment

During the period of my living and working in Germany, I have received a lot of great help and support. At the end of my thesis, please allow me to express my gratitude to all those who have offered me tremendous assistance in these three years.

First, I would like to express my heartfelt thanks to my first supervisor, PD Dr. Bernhard Renz from the Department of General, Visceral and Transplant Surgery, Klinikum Grossharden, Munich, who provided me with this precious chance to conduct research at Ludwig-Maximilians-Universität (LMU), and helped me a lot while studying here. He is always happy to share his experiences and gives many valuable suggestions for my project selection and improvement. Without his careful supervision, this project cannot have been completed successfully.

Second, I want to acknowledge my second supervisor, Prof. Dr. Alexandr Bazhin who always proposed feasible and useful advice when I encountered problems, and contributed a lot to my graduation thesis and the published paper. His excellent professional knowledge, rigorous logical thinking, and nice personality have set a wonderful example for me in my future work and scientific research.

I am also very grateful to Prof. Dr. med. Dr. med. Univ. Jens H.L. Neumann becomes my third supervisor, who is always supportive and kind, showing a great sense of responsibility.

Furthermore, I want to thank all the friendly and professional researchers in our laboratory and biobank. My dear colleagues, Anna Christina Schmidt, Xiaochun Cao (Ehlker), Maresa Demmel, Dennis Nothdurft, Saskia Doerbecker, and Peter Iffelsberger, who helped me to collect many tumor tissues from surgical resection and blood from PDAC patients, making my project go smoothly; Michaela Svihla, Johanna Knallinger, Nicole Strobl, Nadine Gesse, who taught me important experimental skills and helped to

solve problems in my lab work with standard scientific instructions; and my lovely friends Xinyu Li, Xiaokang Li, Yongsheng Han, Zhiqiang Li, Zixin Wang, Haochen Yu, Shristee Mudusetti, Natalja Ring and Beirith Iris, who recommended me with interesting ideas and assisted me a lot in this project, as well as accompanied with me through a pleasant time.

In addition, my deepest gratefulness to my parents Hongwen Ma and Lixia Sun, who always gave me great support and trust, and encouraged me in times of frustration. Their unfailing love has always surrounded me wherever I go.

During my M.D., I was fortunate to harvest a wealth of scientific knowledge, meet many kind people, and gain insight into different cultures. The good memories turned into pictures that were imprinted in my mind. I will miss everything here.